AD-A087 676 GARD INC NILES ILL F/G 20/4
ADEQUACY OF WIND VENTILATION IN UPGRADED SHELTERS.(U)
MAY 80 R H HENNINGER, R J TSAL DCPA01-78-C-0319
UNCLASSIFIED GARD-A1-11 (1713) NL

1 of 2

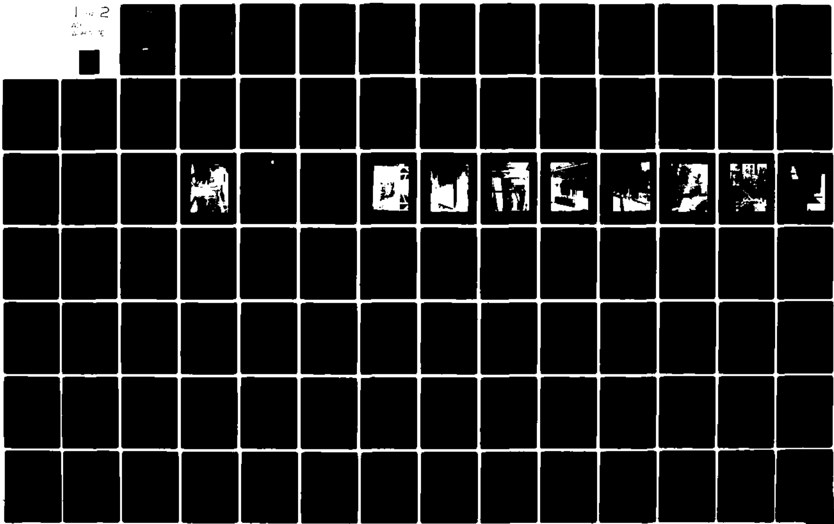

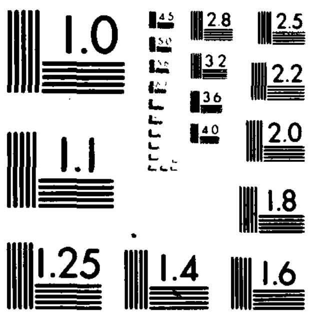

MICROCOPY RESOLUTION TEST CHART
NATIONAL BUREAU OF STANDARDS 1963 A

LEVEL II

(12)

ADA087676

DTIC
ELECTE
AUG 7 1980
D

GATX GARD, INC.

7449 NORTH NATCHEZ AVE.
NILES, IL60648

DDC FILE COPY

80 8 6 024

GARD, INC.
SUBSIDIARY OF GATX CORPORATION
7449 North Natchez Avenue
Niles, Illinois 60648

(12)

FEMA Review Notice

This report has been reviewed in the Federal Emergency Management Agency and approved for publication. Approval does not signify that the contents necessarily reflect the views and policies of the Federal Emergency Management Agency.

ADEQUACY OF WIND VENTILATION IN UPGRADED SHELTERS

GARD FINAL REPORT A1-11 (1713)

June, 1980

FEMA Work Unit 1214B

by

R. Henninger
C. Krishnakumar
R. Tsal

For

Donald A. Bettge
FEDERAL EMERGENCY MANAGEMENT AGENCY
Washington, D. C. 20472

under Contract No. DCPA01-78-C-0319

Approved for Public Release; Distribution Unlimited

UNCLASSIFIED

SECURITY CLASSIFICATION OF THIS PAGE (When Data Entered)

REPORT DOCUMENTATION PAGE

READ INSTRUCTIONS BEFORE COMPLETING FORM

1. REPORT NUMBER
(14) GARD - A1-11 (1713)

2. GOVT ACCESSION NO.
AD-A087676

3. RECIPIENT'S CATALOG NUMBER

4. TITLE (and Subtitle)
(6) Adequacy of [redacted] Wind Ventilation in Upgraded Shelters.

5. TYPE OF REPORT & PERIOD COVERED
(9) Final Report, Oct 78 — May 80,

6. PERFORMING ORG. REPORT NUMBER

7. AUTHOR(s)
(10) R. J. / Henninger, [redacted] / Tsai, R. J., C. K. / Krishnakumar, C. K.

8. CONTRACT OR GRANT NUMBER(s)
(15) FEMA Contract No. 0319 new DCPA01-78-027 C-0319

9. PERFORMING ORGANIZATION NAME AND ADDRESS
GARD, INC.
7449 N. Natchez Avenue
Niles, IL 60648

10. PROGRAM ELEMENT, PROJECT, TASK AREA & WORK UNIT NUMBERS
FEMA Work Unit 1214B

11. CONTROLLING OFFICE NAME AND ADDRESS
Federal Emergency Management Agency
Washington, D.C. 20472

12. REPORT DATE
(11) May [redacted] 80

13. NUMBER OF PAGES

14. MONITORING AGENCY NAME & ADDRESS (if different from Controlling Office)
N/A (12) 117

15. SECURITY CLASS. (of this report)
Unclassified

15a. DECLASSIFICATION/DOWNGRADING SCHEDULE

16. DISTRIBUTION STATEMENT (of this Report)
Approved for public release;
Distribution unlimited.

17. DISTRIBUTION STATEMENT (of the abstract entered in Block 20, if different from Report)

18. SUPPLEMENTARY NOTES

19. KEY WORDS (Continue on reverse side if necessary and identify by block number)
VENTILATION
FALLOUT SHELTERS
MODEL TESTING
WIND TUNNEL

20. ABSTRACT (Continue on reverse side if necessary and identify by block number)

Experimental and analytical investigations were conducted for the purpose of evaluating the adequacy of natural ventilation in upgraded shelters. A unique low-speed wind tunnel which uses photographic measurement techniques for flow tracing of neutrally buoyant bubbles through openings was utilized to conduct scaled model tests of three shelter models to determine the ventilation air throughput CFM as a function of wind speed, relative wind approach angle and opening pattern.

DD FORM 1 JAN 73 1473 EDITION OF 1 NOV 65 IS OBSOLETE

UNCLASSIFIED 40 76

SECURITY CLASSIFICATION OF THIS PAGE (When Data Entered)

The results indicate that sizeable ventilation rates are achieveable at low wind speeds and based upon data reported by ASHRAE would result in adequate ventilation rates to meet the 82°F effective temperature and 90% adequacy criteria for but all the southeast portion of the U.S. Further research is required however, to determine the effects of internal flow reisitances, air stratification, areas and locations of openings, etc., before the ventilation throughput characteristics of upgraded shelters are understood.

PREFACE

GARD, INC. the research and development subsidiary of GATX, has prepared this report for the Federal Emergency Management Agency (FEMA) in Washington, D.C. Originally, the study was contracted for by the Defense Civil Preparedness Agency (DCPA), which has since become part of FEMA. Mr. Donald Bettge of FEMA served as Project Monitor during the entire program.

This report describes the results of the experimental and analytical studies that were conducted to aid in the preparation of a methodology to determine the potential of natural ventilation to ventilate upgraded shelters. Scale model experimental tests were conducted using a unique low speed wind tunnel that was designed and built especially for this program. Experimental data was then incorporated into a mathematical model which can be used to assess the adequacy of natural ventilation to limit the internal environment of certain simple upgraded shelter configurations to acceptable limits.

Individuals at GARD which participated in this program include:

R. H. Henninger - Project Engineer
Dr. R. J. Tsal - Technology Review and Mathematical Modeling
Dr. S. F. Fields - Experimental Modeling
Dr. C. K. Krishnakumar - Experimental Modeling
J. B. Koh - Data Reduction
R. J. Honegger - Wind Tunnel Design

GARD wishes to thank Mr. Bettge and FEMA for the opportunity to have undertaken this study.

Respectfully submitted,
R. H. Henninger
R. H. Henninger
Project Engineer

Approved by:
P. A. Saigh
P. A. Saigh
Director, Contract Programs

ABSTRACT

Experimental and analytical investigations were conducted during this study for the purpose of evaluating the adequacy of natural ventilation in upgraded shelters. A unique low-speed wind tunnel which uses photographic measurement techniques for flow tracing of neutrally buoyant bubbles through openings was utilized to conduct scaled model tests of three shelter models to determine the ventilation air throughput CFM as a function of wind speed, relative wind approach angle and opening pattern. The results, as summarized below, indicate that sizeable ventilation rates are achieveable at low wind speeds and based upon data reported by FEMA* would result in adequate ventilation rates to meet the 82^{o}F effective temperature and 90% adequacy criteria for all but the southeast portion of the U.S. Further research is required however, to determine the effects of internal flow resistances provided by partition walls and occupants, air stratification, areas and locations of openings, etc. before these results can be accepted with confidence.

ESTIMATED VENTILATION FLOWS RATES ACHIEVABLE WITH NATURAL VENTILATION BASED ON SCALED MODEL TESTS FOR WIND SPEEDS IN EXCESS OF 5 mph AND OCCUPANT DENSITY OF 10 SQ. FT. PER PERSON

SHELTER	FLOOR AREA (SQ.FT)	OPENING CONFIGURATION	TOTAL OPENING AREA (SQ.FT)	VENTILATION RATE (CFM/OCC)		
				0^{o}	45^{o}	90^{o}
I	2120	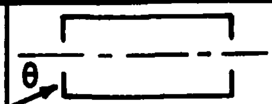	84	41	44	0
II	2120	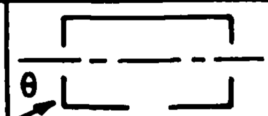	146	46	52	75
III	2120	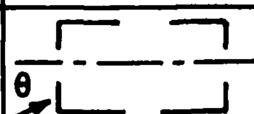	208	50	103	102

* FEMA indicates that 7.5 to 40 CFM per person is adequate to maintain 82^{o}F effective temperature and 90% adequacy (Ref: ASHRAE Applications Handbook, 1978, Chapter 12, Figure 13)

Section		Page
	PREFACE	iv
	ABSTRACT	v
1	INTRODUCTION	1-1
	1.1 Background	1-1
	1.2 Study Objective and Scope	1-2
	1.3 Study Approach	1-2
	1.4 Study Plan	1-3
	References for Section 1	1-4
2	TECHNOLOGY REVIEW	2-1
	2.1 ASHRAE Natural Ventilation Model and Application to Above-Ground Fallout Shelters	2-1
	2.2 Other Natural Ventilation and Building Infiltration Flow Models	2-3
	References for Section 2	2-7
3	SCALED MODEL TESTING PROGRAM AND RESULTS	3-1
	3.1 Approach	3-1
	3.2 Scaling Considerations	3-1
	3.3 Description of Low Speed Wind Tunnel	3-2
	3.4 Calibration and Tune-up of the Wind Tunnel	3-16
	3.5 Description of Scaled Models	3-20
	3.6 Test Procedure	3-27
	3.7 Description of Results	3-28
	3.8 Discussion of Results	3-36
	References for Section 3	3-47
4	NATURAL VENTILATION ADEQUACY ASSESSMENT TECHNIQUE	4-1
	4.1 Adequacy and Effective Temperature	4-1
	4.2 Occupant Metabolic Heat	4-6
	4.3 Shelter Heat Balance	4-8
	4.4 Ventilation Air Throughput	4-10
	4.5 Adequacy Assessment Technique	4-12
	References for Section 4	4-20

LIST OF FIGURES

LIST OF FIGURES (CONTINUED)

LIST OF TABLES

Section 1

INTRODUCTION

1.1 Background

The survival of the occupants of a shelter is dependent upon the following environmental factors:

1) the nuclear radiation level in the shelter,
2) the chemical composition of the air in the shelter, and
3) the thermal level in the shelter.

Among these three requirements, the second and the third are related to the ventilation rate of the shelter. Previous studies by the Defense Civil Preparedness Agency (now part of the Federal Emergency Management Agency) indicated that a ventilation rate of approximately 3 CFM per occupant would suffice for chemical balance. Since this ventilation rate is easily attainable, the chemical composition of the shelter air is adequately provided for. Thus, the main environmental control problem in a shelter is *the provision of sufficient* ventilation to protect the occupants against excessive thermal levels within the shelter.

Ventilating a shelter with ambient air to control the thermal level within the shelter might be accomplished in two ways:

1) Natural Ventilation - ventilation through open windows, doors stairwells, etc. caused by atmospheric winds or thermal effects
2) Forced Ventilation - ventilation by artifical means using mechanical devices.

If natural ventilation can be shown to be reliable, one approach might be to utilize Pedal Ventilator Kits (PVK) and Kearny Pump Kits (KPK) (Ref. 1.1) only in those locations and shelters where natural ventilation would not be adequate. The need arose therefore, for an accurate assessment technique to be developed which could determine the adequacy or non-adequacy of natural ventilation for upgraded shelters, shelters whose ventilation characteristics had not been previously studied.

1.2 Study Objective and Scope

Previous studies concerning natural ventilation effects of fallout shelters have dealt with typical above and/or below-ground fallout shelters in existing structures; this study deals with upgraded shelters, i.e. shelters having full earth berms with at least 6 inches of earth overhead. It is questionable if previous field test data (Section 2) obtained for sharp-edged structures are applicable to the sloped-sided configuration of upgraded shelters. The objective of this study was therefore to experimentally and analytically assess the potential of natural ventilation in upgraded shelters.

1.3 Study Approach

The wind induced ventilation air flow rate through a building is a complex function of several geometric and flow variables. Important among these variables are wind speed, wind direction, boundary layer velocity profile of approaching wind, building geometry, areas and locations of windows and doors, internal obstacles within the building and the nature and proximity of neighboring buildings and obstructions. Where the building is situated in open country, the problem simplifies to some extent. In that case, reasonable assumptions can be made for the boundary layer profile of the approaching wind. Further, if the building is sharp edged, the flow separation points are well defined. This is not true of flows over buildings with curved exteriors like the bermed buildings of the present study. Even for buildings of relatively simple geometries, however, the velocity and pressure profiles in and around these buildings are so complex as to render a complete analytical or numerical solution impractical.

A common approach used to study problems of this nature is to construct a theoretical model and complement it with data from carefully conducted experiments. Data acquisition from experiments of full size buildings alone is prohibitively expensive and time consuming. The solution therefore lies in conducting tests on properly designed scaled model systems, feeding the data into a theoretical model and finally testing the results with representative field data. Often, feed back between model and field tests may be necessary to correct inaccuracies in the model system or to interpret field data. Such an approach has been adapted here where a series of tests were designed to yield a clear understanding of the effects of the important variables individually, and in groups, on ventilation air flow rates. The building geometry was kept relatively simple and internal flow resistances were excluded. Natural ventilation due to thermal effects are also being ignored for the present. Information gained from these studies together with data from future tests on building models with internal resistances should enable reasonably accurate predictions to be made of ventilation air flow rates through full size buildings of the types considered.

1.4 Study Plan

The study plan employed for this project was structured around the experimental and analytical approach described in the previous section and included the following work tasks:

- Task 1 - Technology review
- Task 2 - Identify applicable analytical flow models, flow parameters and shelter configurations
- Task 3 - Scaled model testing
  - 3A - Formulate test plan
  - 3B - Investigate scaling effects
  - 3C - Design and build test stand and models
  - 3D - Calibrate wind tunnel
  - 3E - Conduct tests
  - 3F - Reduce data and interpret results
- Task 4 - Analytical model testing
  - 4A - Develop analytical natural ventilation assessment model
  - 4B - Incorporate experimental data into model
- Task 5 - Assess adequacy of natural ventilation based on results
- Task 6 - Prepare final report and recommendations.

References For Section 1

1.1 Buday, J. M., et. al., "Development of Two Types Of Ventilators", GARD Report 1703, GARD, INC., Niles, Illinois, April, 1979.

Section 2

TECHNOLOGY REVIEW

Natural ventilation as applied to buildings (Refs. 2.6 through 2.14) found widespread application back in the 1920-40 era where ventilation due to wind and thermal effects were routinely incorporated into building designs. The acceptance and general use of air conditioning since that period however, has limited its use to only industrial buildings. Presently, there seems to be a resurgence of interest in natural ventilation as a building energy conservation technique.

The state of the art of natural ventilation calculation techniques is described in the 1977 ASHRAE Handbook of Fundamentals. These procedures have their roots in data and experience gained from the 1920's and 30's and have changed little since that time. Research in the last decade has concentrated in an area directly related to natural ventilation, that being building infiltration. Both are wind induced and both deal with ambient air movement through aperatures. Natural ventilation is generally controllable and desireable, whereas infiltration cannot be effectively controlled and is undesireable. A survey was made of infiltration studies to determine the applicability of results and mathematical models to this present study. Mathematical models developed as part of these studies are varied and generally can be applied to only certain building types. This section summarizes those models which have been developed for treating both natural ventilation and infiltration in buildings and structures.

2.1 ASHRAE Natural Ventilation Model And Application to Above-Ground Fallout Shelters

Extensive experimental and analytical studies of natural ventilation for above-ground fallout shelters were conducted by the Defense Civil Preparedness Agency back in the 1960's. These studies utilized a relationship obtained from the continuity equation to determine wind-induced air flow through ventilation openings. This relation, based upon the presentation in the 1965 ASHRAE Guide and Data Book, is given below and still represents the state of the art as is witnessed in the 1977 ASHRAE Handbook of Fundamentals (Ref. 2.1).

$$Q = (1 + \beta) EAV$$

where Q = volume flow rate (ft^3/min/occupant)

β = fractional multiplying factor which arises from unequal inlet and outlet areas

E = effectiveness factor

A = A_{tot}/N

A_{tot} = smaller of the air inlet area or air outlet area (ft^2)

N = number of occupants

V = atmospheric wind speed (ft/min).

The value of β is dependent upon the ratio of inlet area to outlet area, or vice versa, whichever is greater that one. This dependence is not linear, but is as indicated in Figure 2.1. Increasing inlet area over outlet area, or vice versa, will increase the induced ventilation, but not in proportion to the added area.

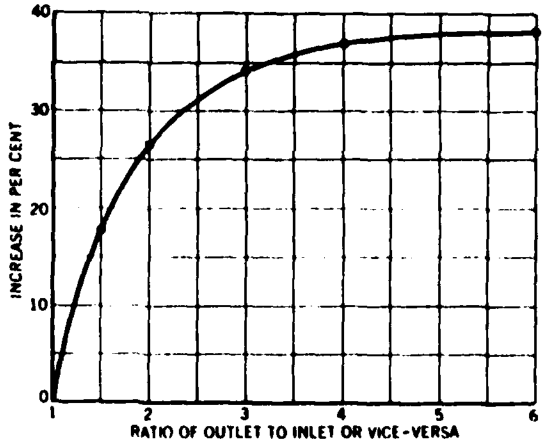

Figure 2.1 INCREASE IN FLOW CAUSED BY INEQUALITY OF INLET AND OUTLET AREAS

The E-factor in the above equation represents the effectiveness of openings and ASHRAE indicates that E should be taken as 0.50 to 0.60 for winds perpendicular to the openings, and 0.25 to 0.35 for diagonal winds. Experimental tests conducted by DCPA for 4 different shelters (Refs. 2.2 through 2.5) indicated that as atmospheric wind speed increased, the air flow induced by the atmospheric wind did not follow the expected linear relationship. This can be seen, for example, by examining Figure 2.2 which presents the results for the Evanston, Illinois test (Ref 2.4). In this rectangularly-shaped aboveground shelter, all windows had the same openable area. In Test 1, four windows were open (one on each wall) and in Tests 2 and 3, two windows were open (one on each opposite wall with different opposite walls in Tests 2 and 3). The test results show a scattered distribution and departure from linearity, especially at higher atmospheric wind speeds. This behavior is probably due to several other effects that are present but not accounted for in the ASHRAE equation, e.g.,

1) the effect of the atmospheric wind direction,
2) the type of window openings,
3) the interior structural elements,
4) the exterior structures that disturb the surface wind velocity field, and
5) the variation in height between the shelter location and the location at which the atmospheric wind speed and direction are determined.

2.2 Other Natural Ventilation And Building Infiltration Flow Models

Some 100 or more technical papers relating to natural ventilation and infiltration of buildings and structures were reviewed to determine the scope of knowledge related to these subjects. A compilation of the more pertinent papers are presented in the reference list found at the end of this section. Appendix A summarizes the mathematical flow models that were gleaned from this review.

Since the 1960's, little work has been carried on in the specific area of natural ventilation of buildings except for the four DCPA studies previously referenced. Recent studies have concentrated rather in the related area of infiltration of ambient air into residential and commercial buildings through their exterior envelopes. Ross and Grimsrud (Ref. 2.53) compiled a thorough summary of past and recent works conducted in this area and should be consulted for a more complete discussion. Many of the infiltration models developed as part of those studies were specific to a particular building or building

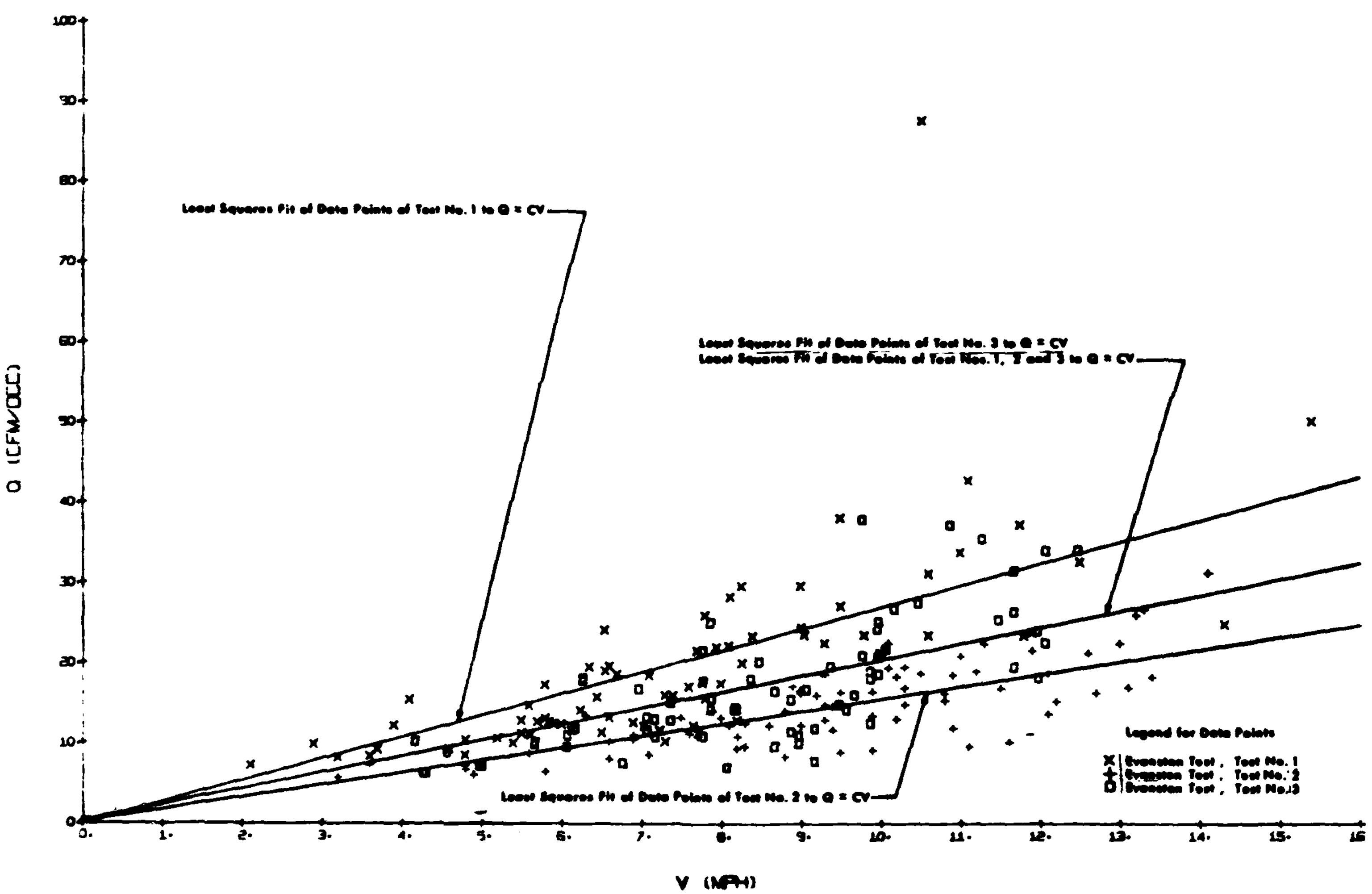

Figure 2.2 EXPERIMENTAL RESULTS OF EVANSTON SHELTER TEST AND LEAST SQUARES FIT OF DATA POINTS TO Q = CV, C = CONSTANT (REF. 2.4)

classification and as such are not applicable to our study.

The ASHRAE linear model discussed previously represents the simplest of the flow models in existence. It assumes that the air flow through a building is a linear function of wind speed only, leaving all other effects, such as wind direction, type of opening, ratio of opening area to wall area, etc., to be accounted for by the Effectiveness Factor (E).

In 1955, G. A. Macksimov (Ref. 2.13) formulated an equation for air flow through buildings as a function of static pressure difference between the windward and leeward sides of the building. This was developed through application of Bernoulli's Law and resulted in a non-linear function of air flow to wind speed.

Many authors have attempted to develop specific non-linear equations by using results of experimental field tests (Refs. 2.7, 2.13, 2.19, 2.20, 2.38, 2.46, 2.47, 2.50, 2.51, 2.54, 2.56, 2.57). Usually the dynamic flow coefficients obtained were for specific building configurations and characteristics and could not be generalized to other types of buildings and conditions.

Although most authors recognize that air flow through a building is a function of wind direction, few have included this effect directly as an independent variable. Some (Refs. 2.6, 2.21, 2.25, 2.46, 2.50, 2.56) have included the relative angle between the wind direction and the normal to the wall in linear or non-linear equations but have developed pressure coefficients for only one reference direction. Pressure coefficients are of course a function also of building configuration, placement of openings, ratio of wall and opening areas, etc. These have usually been neglected.

More general equations for residential application have been developed recently to account for such other effects as frequency of dooring opening, presence of fireplaces and chimneys, operation of ventilators and exhaust fans, furnace operation, etc. (Refs 2.10, 2.19, 2.20, 2.21, 2.28, 2.38, 2.46, 2.48, 2.50, 2.51). A good example of this approach was that done by Ohio State University (Ref. 2.46) for residential application. As is true for this work as well as the others, the coefficients determined by field tests for insertion into the polynomial expressions are specific to the structures studied and especially to the quality of construction.

Computerized models developed by Konstantinova (Ref. 2.20) and Sander and Tamura (Ref. 2.37 and 2.38) using numerical methods allowed for a more detailed solution to the problem by being able to handle more complex structures where a series of equations must be solved simultaneously. But still these models required that pressure coefficients be determined independently as a function of wind speed and direction. Computerized models also gave the opportunity to utilize recorded hourly weather data and to study the independent effects of certain variables as they are varied over their range of occurrence.

As will be seen in Section 3, the type of structure under study in this program, i.e., bermed one-story buildings, are not like the sharp-edged structures studied to date but rather have curved or sloped sides which give them flow characteristics different from typical buildings. Dynamic pressure coefficients and coefficients determined for polynomial expressions previously discussed therefore made application of these data to our problem questionable.

Reference for Section 2

2.1 ASHRAE Handbook of Fundamentals, Chapter 21,"Infiltration and Ventilation", 1977.

2.2 Madsen, C. A., et. al., "Natural Ventilation Test of an Aboveground Fallout Shelter in Bozeman, Montana", November, 1964, DDC No. 453070.

2.3 Madsen, C. A., et. al., "Natural Ventilation Test of an Aboveground Fallout Shelter in Baton Rouge, Louisiana", January, 1965, DDC No. 456893.

2.4 Meier, H. A., et. al., "Natural Ventilation Test of an Aboveground Fallout Shelter in Evanston, Illinois", January, 1966.

2.5 Henninger, R. H., et. al., "Natural Ventilation Test of an Aboveground Fallout Shelter in Chicago, Illinois", August, 1966, DDC No. 641701.

2.6 Randal, W. C.,"Aeration of Industrial Buildings",ASHVE Trans., Vol. 34, 1928.

2.7 Emsiler, J. E., Arbor, A., Randall, W. C., "Pressure Difference Across Windows in Relation to Wind Velocity", 36th Annual Meeting of ASHVE, Philadelphia, January, 1930.

2.8 Bailey. V., "Wind Pressure on Buildings Including Effects of Adjacent Buildings",England Institute of Civil Engineering, 1943.

2.9 Dick, J. B., "The Fundamentals of Natural Ventilation of Houses", Building Research Station, June, 1950.

2.10 Dick, J. D., Thomas, D. A., "Ventilation Research in Occupied Houses", Journal of the Institute of Heating and Ventilating Engineers, October, 1957.

2.11 Candill, W. W., Srites, S. E., Smith, E. G., "Some General Considerations in the Natural Ventilation of Buildings",Research Report No. 22, College Station, Texas, February, 1951.

2.12 White, R. F., "Effects of Landscape Development of the Natural Ventilation of Buildings and their Adjacent Areas", Research Report 45, College Station, Texas, March, 1957.

2.13 Macksimov, G. A., "Heating and Ventilation", Part II, Stroysdat, Moscow, 1955.

2.14 Evans, E., "Natural Air Flow Around Buildings", Research Report No. 59, College Station, Texas, March 1957.

2.15 Bahnfleth, R. D., Mosley, T. D., Harris, W. S., "Measurement of Infiltration in two Residences", Semi-Annual Meeting of the ASHRAE, Murray Bay, Canada, June, 1957.

2.16 Jensen, M., "The Model-Law for Phenomena in Natural Wind", Engineering International Edition, Vol. 2, No. 4, 1958.

2.17 Haddon, J. D., "The Use of Wind-Tunnel Model for Determining the Wind Pressure on Buildings", Civil Engineering, Vol. 55, No. 645, April, 1960.

2.18 Dalgliesh, W. H., Boyd, D. W., "Wind on Buildings", National Research Council of Canada, 1962.

2.19 Tamura, G. T., Wilson, A. G., "Air Leakage and Pressure Measurements on Two Occupied Houses", *ASHRAE Journal*, *Vol*. 5, No. 12, 1963.

2.20 Konstantinova, V. E., "Air Change Calculation in Residential and Commercial Buildings", Stroysdat, Moscow, 1964.

2.21 Laschober, R. B., Healy, J. H., "Statistical Analysis of Air Leakage in Split-Level Residences", 71st ASHRAE Annual Meeting, Cleveland, Ohio, June, 1964.

2.22 Svaeri, O. W., Dembo, M. M., "Simulated Occupany Tests and Air Distribution in a 480-Person Community Fallout Shelter", Civil Defense Support Group, 1965.

2.23 "Air Distribution in a Multi-Room Shelter Using a Package Ventilation Kit", Technical Report for Joint Civil Defense Support Group, University of Florida, July, 1965.

2.24 King, J. C., "Gravity Ventilation of Underground Shelters", Technical Report R-307, U. S. Naval Civil Engineering Laboratory, March, 1965.

2.25 Baturin, V. V., "Fundamentals of Industrial Ventilation Technique", Profysdat, Moscow, 1965.

2.26 Ratter, A. E., Streshenov, S. E., "Aerodynamics of Buildings", Stroysdat, Moscow, 1968.

2.27 Isenberg, M. W., McLaughlin, E. R., et. al., "Natural Ventilation for Fallout Shelters, Pennsylvania State University", Interim Report, January, 1966.

2.28 Howard, J. S., "Ventilation Measurements in Houses and the Influence of Wall Ventilators", Buildings Science, Vol. 1, Pergamon Press, 1966.

2.29 Rathmann, C. E., Baschiere, R. J., "Shelter Environmental Prediction Computer Code", GARD Report 1423, 1968.

2.30 Svaeri, O. W., Stein, N. I., "Air Distribution in Multi-Room Shelters," Office of Civil Defense, April, 1968.

2.31 Baschiere, R. J., Rathman, C. E., Lokmanhekim, M., "Adequacy of Evaporative Cooling and Shelter Environmental Prediction", GARD Final Report 1423, June 1968.

2.32 Baschiere, R. J., Rathmann, C. E., Rouse, R. V., "Control of Fallout Shelter Environments", Survival Shelter Problems, Symposium, San Francisco, 1970.

2.33 Everetts, J., McLaughlin, E. R., Witte, E. R., "Conditioned Air for Improving Shelter Habitability", Survival Shelter Problems, Symposium, San Fransisco, 1970.

2.34 Torrance, V. B., "Wind Profiles Over a Suburban Site and Wind Effects on a Half Full-Scale Model Building", Building Science, Vol. 7 Pergamon Press, 1972.

2.35 Elkins and Wensman, "Natural Ventilation of Modern Tightly Constructed Houses", AGA Conference on Natural Gas Research and Technology, Chicago, February, 1979.

2.36 Barber, E. M., Kusuda, T., Reynolds, P. J., Powell, F. J., "A Study of Air Distribution in Survival Shelter Using a Small-Scale Modeling Techniques", National Bureau of Standards Report, 1972.

2.37 Sander, D. M., Tamura, G. T., "A FORTRAN IV Program to Simulate Air Movement in Multi-Story Buildings", National Research Council of Canada, Ottawa, 1973.

2.38 Sander, D. M., "FORTRAN IV Program to Calculate Air Infiltration in Buildings", National Research Council of Canada, Ottawa, Canada, 1974.

2.39 "Subroutine Algorithms for Heating and Cooling Loads to Determine Building Energy Requirement", ASHRAE, Copyright 1975.

2.40 Hittman Associates, "Technology Assessment of Residential Energy Conservation Innovations", May, 1975.

2.41 Idelchick, I. E. "Handbook of Hydraulic Resistances", Mashin Building, Moscow, 1975.

2.42 Larsen, B. T., "Digital Simulation of Energy Consumption in Residential Buildings", International Symposium of Energy Consumption in the Built Environment, Building Research Station, Garston, England, 1976.

2.43 Cockroft, J. P., Robertson, P., "Ventilation of an Enclosure Through a Single Opening", Building and Environment, Vol. 11, 1976.

2.44 Staroverov, I. G., "Ventilation and Air Conditioning", Stroysdat, Moscow, 1977.

2.45 Dillington, D. P., Gould, P. L., Schnobrich, W. C., "Reinforced Concrete Cooling Tower Shells- Practice and Commentary", American Concrete Institute Journal, 1977.

2.46 Sepsy, Jones, McBride, Blancett, "Air Infiltration Study for Residential Application", Ohio State University, Unpublished report, 1977.

2.47 Shaw, C. Y., Tamura, G. T., "The Calculation of Air Infiltration Rates Caused by Wind and Stack Action for Tall Buildings", ASHRAE Trans., 1977.

2.48 Malik, N., "Field Studies of Dependence of Air Infiltration on Outside Temperature and Wind", Energy and Buildings, 1, 1977/1978.

2.49 Sinder, F. W., "Wind, Temperature and Natural Ventilation - Theoretical Considerations", Energy and Buildings, 1, 1977/1978.

2.50 Konrad, A., Larsen, B. T., and Shaw, C. Y., "Programmed Computer Model of Air Infiltration in Small Residential Buildings with Oil Furnaces", Third International Symposium on The Use of Computers for Environmental Engineering Related to Buildings, Banff, Canada, 1978.

2.51 Hayakawa, S., Togari, S., Hioki, M., "Air Flow Rate Variation of HVAC Caused by Window Opening and Stack Effect", Third Symposium, Banff, Canada, 1978.

2.52 Cockroft, J. P., "Some Aspects of Design of Air-Conditioning Systems for Critical Areas", Third Symposium, Banff, Canada, 1978.

2.53 Ross, H. D., Grimsrud, D. T., "Air Infiltration in Buildings: Literature Survey and Proposed Research Agenda", Report for International Energy Agency, February, 1978.

2.54 Reeves, G., McBride, M., Sepsy, S. F., "Air Infiltration Model for Residences", Preprint for Inclusion in ASHRAE Trans., 1979, Vol. 85, Part 1.

2.55 Peterson "Estimating Air Infiltration into Houses", ASHRAE Journal, January, 1979.

2.56 Shaw, C. Y., "A Method for Predicting Air Infiltration Rates for a Tall Building Surrounded by Lower Structures of Uniform Height", Preprint for Inclusion in ASHRAE Trans., 1979, Vol, 85, Part 1.

2.57 Tamura, G. T., "The Calculation of House Infiltration Rates", Preprint for Inclusion in ASHRAE Trans., 1979, Vol. 85, Part 1.

Section 3

SCALED MODEL TESTING PROGRAM AND RESULTS

3.1 Approach

The model tests in this study were designed with the object of gaining insight into the phenomena of wind flow through and around bermed shelter buildings and formulating relationships between ventilation flow rate and major parameters affecting it. It was realized at the outset that measurement of volume flow rates through the model openings would be difficult. Flow patterns in the vicinity of the openings are very complex, flow areas are not well defined, and conventional probes are not desirable. In view of these problems, the goal for this initial study was to develop a viable measurement technique and apply it to simple models. This has been successfully achieved in this study.

The technique developed by GARD consists of tracing the flow of neutrally buoyant bubbles through models and recording their path lines using motion photography. These recordings can be analyzed using a variable speed projector to yield valuable quantitative and qualitative data.

3.2 Scaling Considerations

The basic requirement in model testing is dynamic similarity between the full-scale and model systems. Dynamic similarity, which implies similarity of geometries and flow fields, is a prerequisite for translating model data to the full-scale. In most cases, perfect similarity is impractical. However, it often suffices to ensure similarities only with regard to the dominant characteristics of the two flow systems. A dimensional analysis of the problem shows that dynamic similarity can be achieved by ensuring that 1) the model and full-scale systems are geometrically similar, 2) values of Reynolds numbers based on building height, width and length are the same for the model and full-scale systems, 3) velocity profiles of the approach wind boundary layers are similar (which means that the exponent of the power-law distribution is the same for the two systems), and 4) ratios of building height to wind boundary layer thickness are the same in the two systems. (In open terrain or bush country, the wind boundary layer is about 60 to 80 feet thick, which is 4 to 5 times the height of a typical single-story building.) Equality of Reynolds numbers is crucial only in the laminar and transitional regimes of flow. In these regimes, the flow structure behind edges and corners is very sensitive to Reynolds number. Sharp-edged buildings offer a simplification in that the flow separation points are well defined. This is not true of bodies with curved edges like the bermed shelters of the present study. The strong influence of Reynolds number on wake flow patterns and separation points associated with curved surfaces is well illustrated in the experimental plots of drag coefficient versus Reynolds number for cylinders (Ref. 3.1 and 3.2). When the approach stream is in the fully turbulent regime, the drag coefficient is nearly independent of Reynolds number, (Ref 3.2). This is because the major component of drag - the contribution from wake flow - approaches an asymptotic value at those Reynolds numbers. Since, the earth's boundary layer is always turbulent, it suffices in the present study, to ensure that model Reynolds numbers are large enough to guarantee good turbulent mixing in the boundary layers, thereby negating the possibility of regular vortex shedding of the Karman vortex street type (Karman vortex street behind cylinders are observed only at Reynolds numbers of 5,000 or less).

Two different model systems - a wind tunnel (or air model) and a water tunnel - were considered as possible choices. Each system has some advantages and disadvantages with respect to the other. For example, pressure and velocity measurements can be made more accurately in a water tunnel. Flow visualization is also very effective in water. However, major considerations like tunnel blockage, wall boundary layer interference effects, problems of handling large-flow-rate hydraulic circuits and generating thick boundary layers, favored the selection of a wind tunnel over a water tunnel.

3.3 Description of Low Speed Wind Tunnel

GARD's wind tunnel was designed specially to suit air flow studies involving simulation of wind velocity profiles. The following considerations strongly influenced its design.

1) Tunnel width and height must be large enough to accommodate large models without creating significant blockage or boundary layer interference effects (large models are necessary to permit reasonably accurate and meaningful measurements). If the blockage of the flow area caused by the model is more that about 5% of the

tunnel's cross-section, velocities significantly greater than the approach wind free stream velocity will be generated in the test section (Ref. 3.3). Interaction of the stream lines deflected off the edges of the model with the tunnel wall boundary layers could also lead to errors.

2) Thick boundary layers simulating the earth's wind boundary layer should be obtainable in the tunnel's test section (typical values for the thickness of the earth's wind boundary layer in open terrain or bush country range from 60 feet to 80 feet).

3) The tunnel should be readily adaptable to visualization techniques.

GARD's low speed wind tunnel is situated in a very large room which forms the return circuit between the inlet and the exhaust. A photograph and a schematic of the wind tunnel are shown in Figures 3.1 and 3.2, respectively. The tunnel consists of a convergent intake section, 4 rectangular sections (60" width x 30" height x 96" length), a transition section at the exhaust end, and a 33" diameter centrifugal blower which operates in the suction mode and exhausts the air through a 90° elbow. Free stream velocities of up to 20 fps can be generated in the test section with the present blower.
The convergent intake includes a honey-comb entrance panel followed by a fine mesh screen. This arrangement straightens the flow and makes the turbulence intensity uniform. A short distance downstream of the intake section is a manifold that blows small jets of air counter to the main stream at a downward angle. The succeeding sections have square bars laid on the floor at regular intervals spanning the entire width. The counter jets, together with the lateral bars, have been found to efficiently generate and sustain thick boundary layers of the magnitude required in the present study for wind velocity profile simulation. This system, also called the Momentum Defect Generating System, was instituted after a careful analysis of several techniques that have been tried in the past for the same purpose (Ref. 3.4, 3.5 and 3.6). The test section is fabricated from clear Plexiglas sheets and has an access door located on the side wall. Sections 1 and 4 are clear on the sides and Section 2 is clear on the top and the sides. The transition section, following Section 4, consists of a diffuser, a vibration isolator, a large area chamber with a honey-comb panel and an adapter leading to the blower.

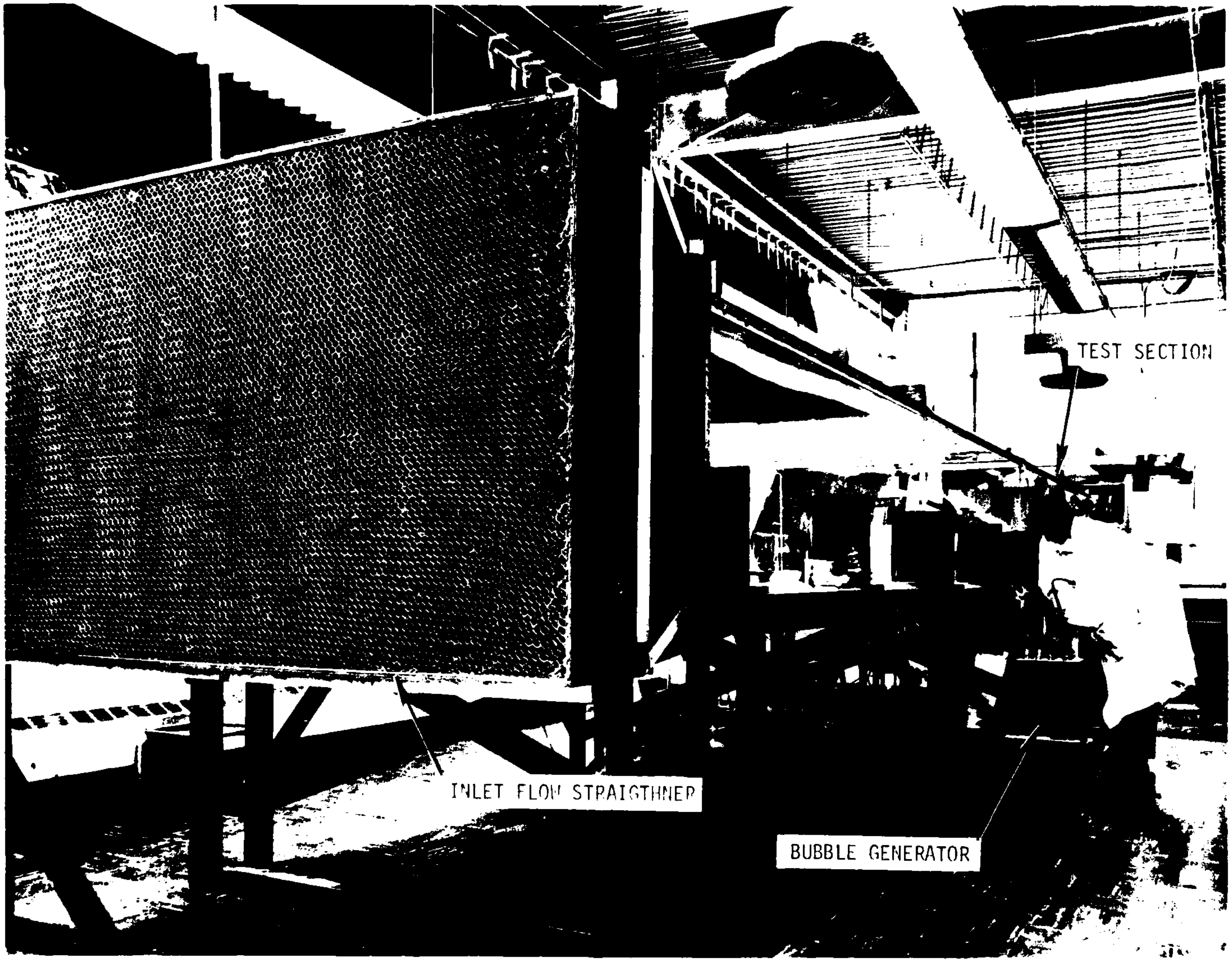

Figure 3.1 LOW SPEED WIND TUNNEL LOCATED IN GARD LABORATORY BUILDING, NILES, ILLINOIS

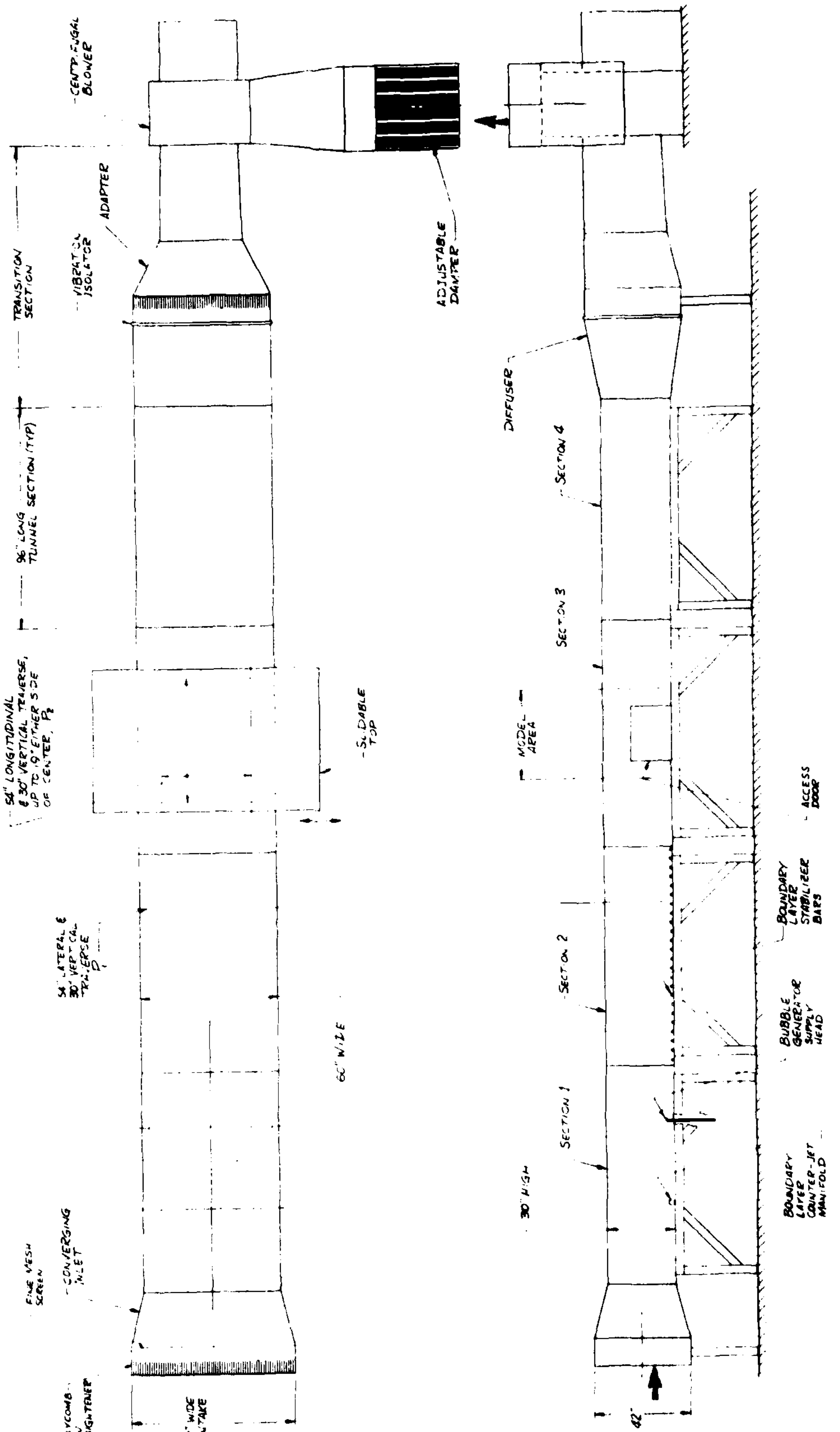

Figure 3.2 SCHEMATIC OF WIND TUNNEL

A damper fixed to the elbow on the blower exhaust regulates the tunnel throughput flow rate. Figures 3.3 through 3.10 provide a walk-through of the wind tunnel and its instrumentation.

Instrumentation of the tunnel consists of the following :

1) Pitot-static tubes P_1 and P_2 (Figures 3.2 and 3.7). These probes determine the pressure and velocity profiles in the tunnel's cross-section upstream of the model and in its vicinity. They are connected to a precision manometer that can accurately read pressure differentials to 0.002 inches of water. Probe P_1 can traverse the entire width and height of the tunnel's cross-section while probe P_2 can additionally traverse a distance of 4½ feet in the longitudinal direction.

2) Bubble generator unit (Figures 3.8, 3.9 and 3.11). This unit delivers neutrally buoyant bubbles of high stability through two bubble release tubes located about 30 inches upstream of the model. The unit consists of high pressure cylinders of helium and air, a 3-channel bubble generator console, two bubble heads, vortex chambers and bubble release tubes. Within each bubble head, helium passes through a central hypodermic tube. Helium also forces a bubble film solution stored in the console through an annulus surrounding the hypodermic tube to form helium-filled bubbles. The bubbles are blown off the tip by compressed air passing through the outermost annular passage in the head. By properly metering the helium, bubble film solution and compressed air flow rates, and setting the helium and air supply pressures, neutrally buoyant bubbles of nearly uniform size, from 1/16 to 1/4 inches in diameter, can be continuously generated from each head. Lighter and heavier bubbles are filtered off by the vortex chambers, so that only nearly neutrally buoyant bubbles reach the release tubes. These bubbles are much more stable than normal soap bubbles. Although, some of the bubbles do burst on contacting solid boundaries, a good many of them successfully trace the flow completely through and around the model. The bubbles have good reflectivity, so that with proper lighting they can be photographically recorded.

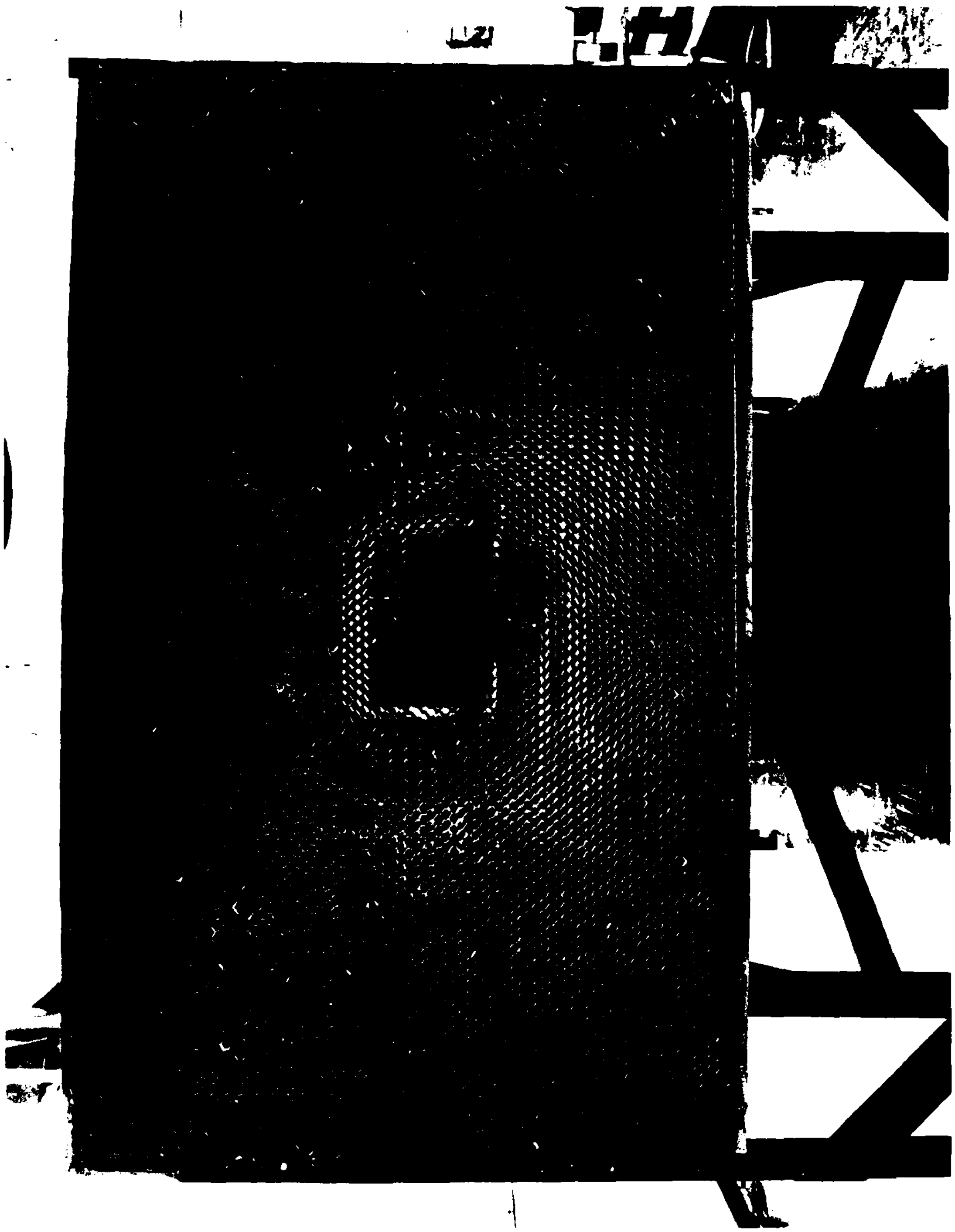

Figure 3.3 HONEY-COMB FLOW STRAIGHTENER

Figure 3.4 CONVERGENT INTAKE CONE

Figure 3.5 COUNTER-JET MANIFOLD AND BOUNDARY LAYER STABILIZERS

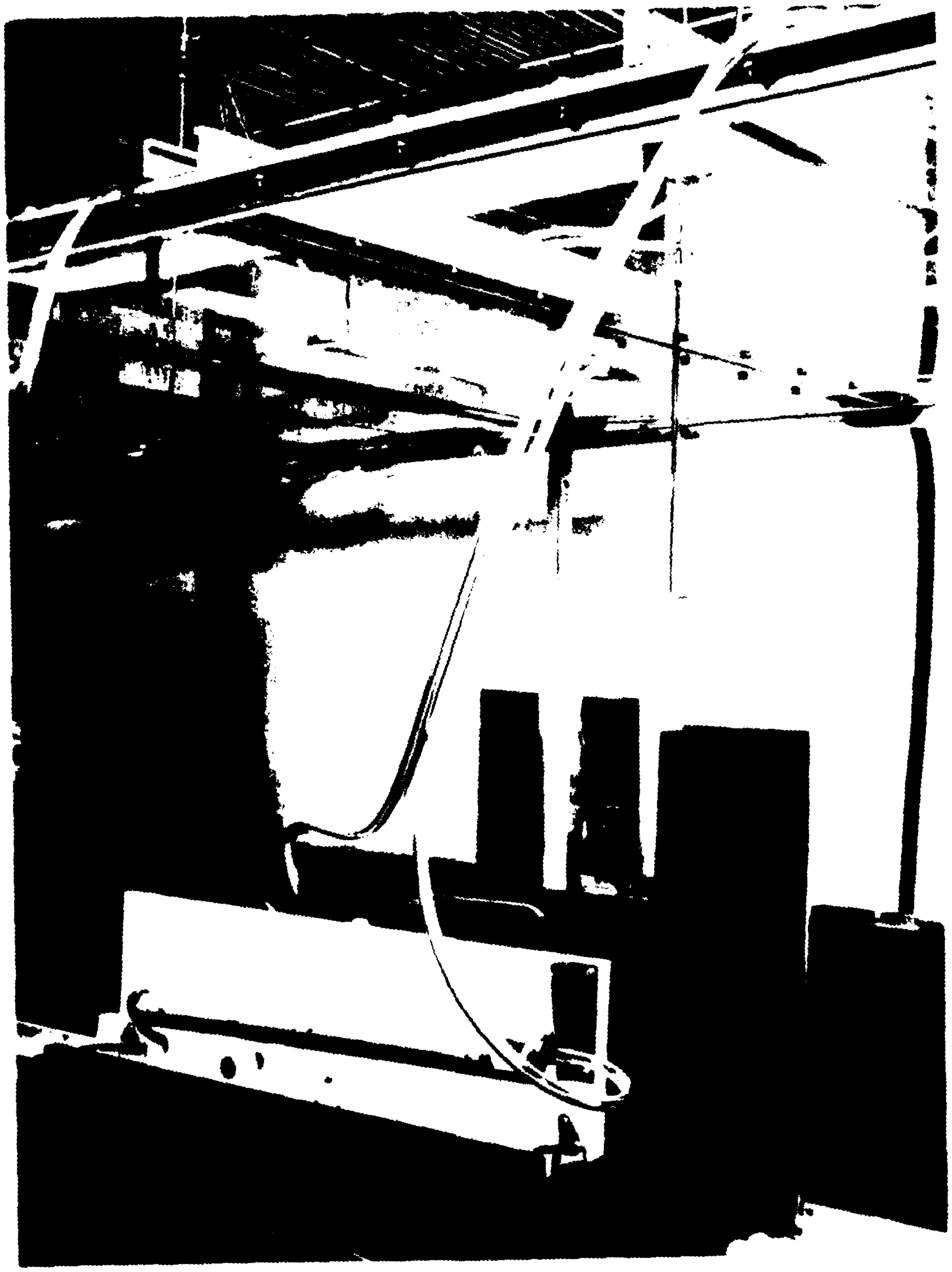

Figure 3.6 PRECISION MANOMETER

GARD, INC.

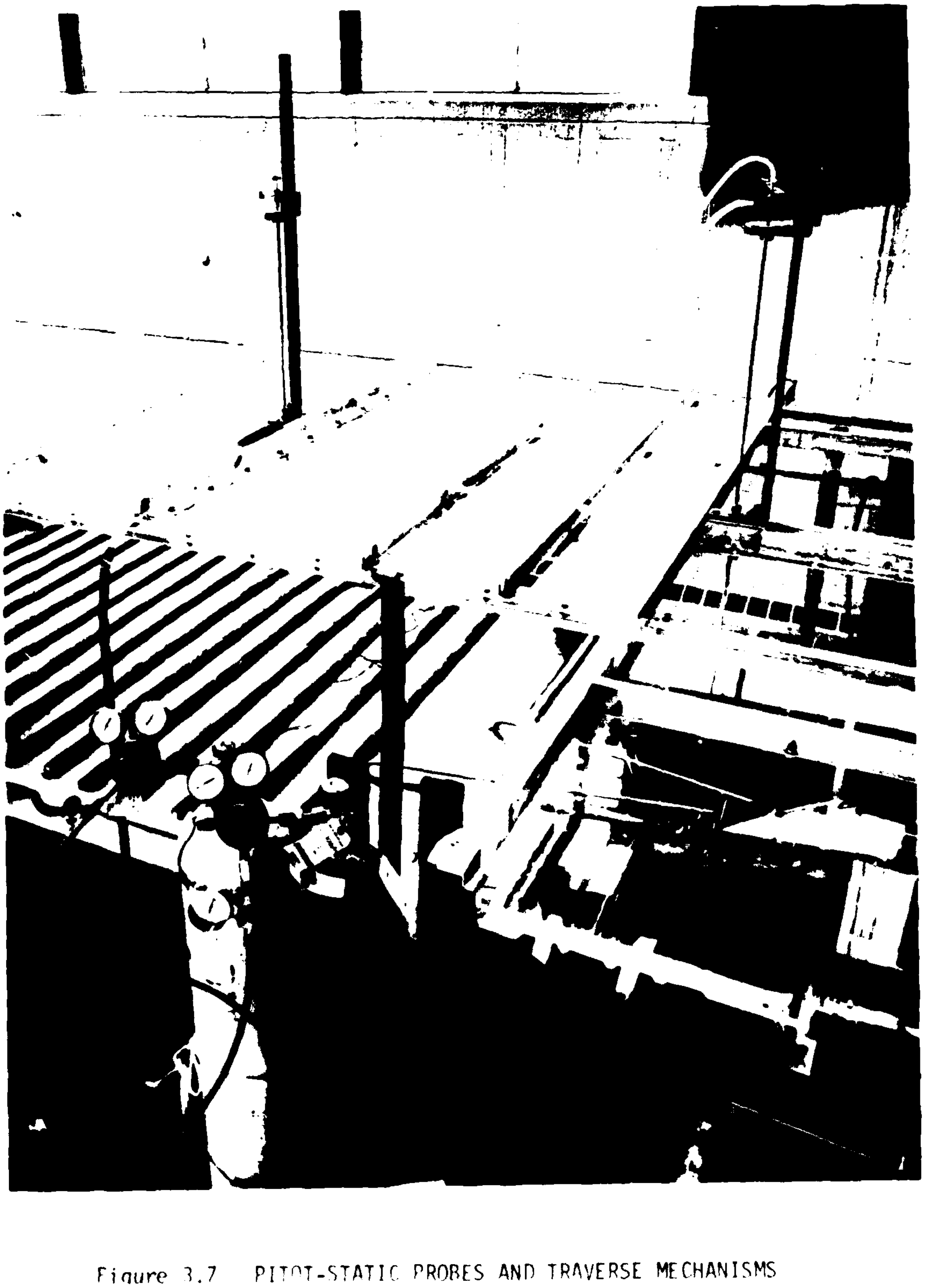

Figure 3.7 PITOT-STATIC PROBES AND TRAVERSE MECHANISMS

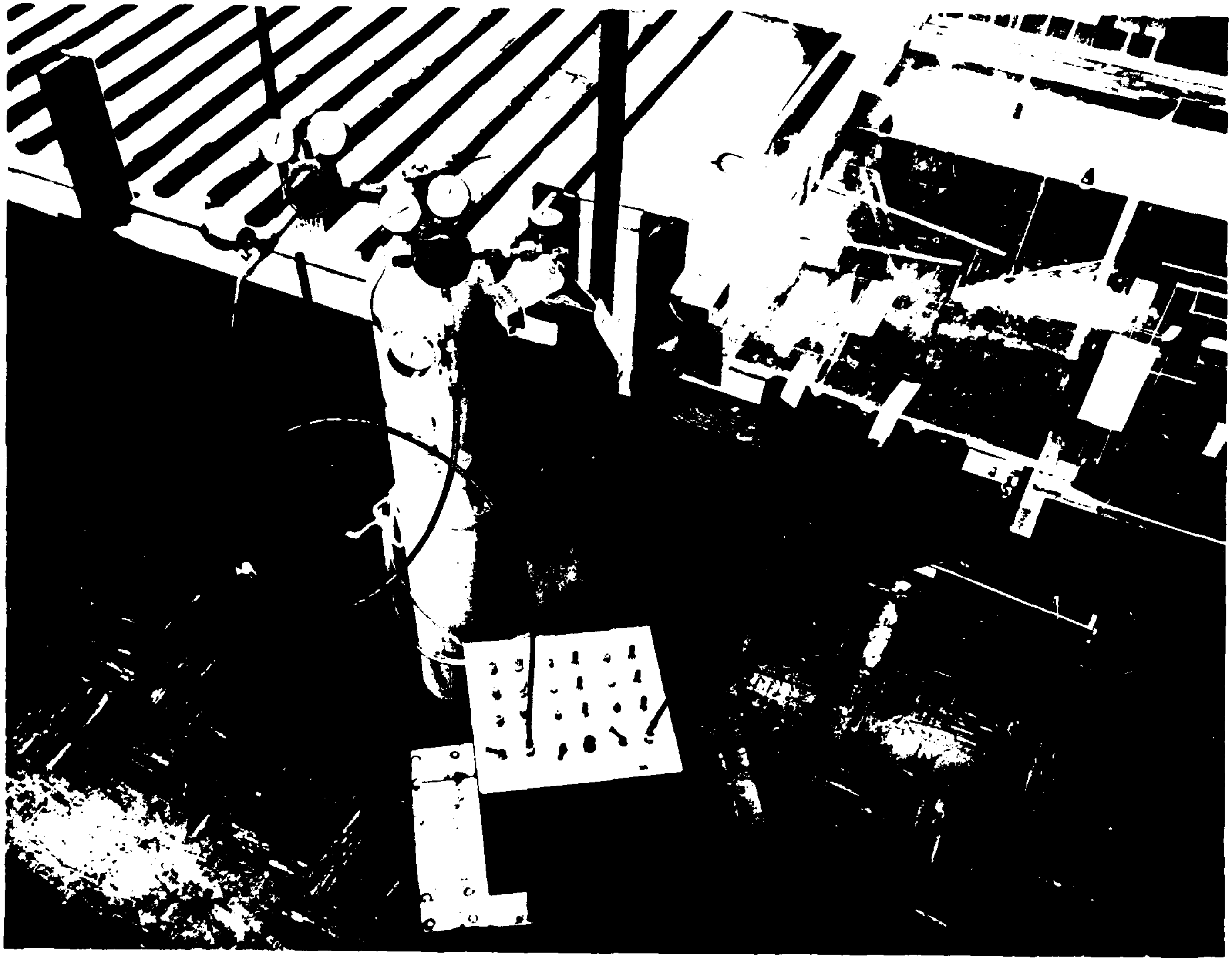

Figure 3.8 THE BUBBLE GENERATOR SYSTEM

Figure 3.9 A TYPICAL TEST SET-UP

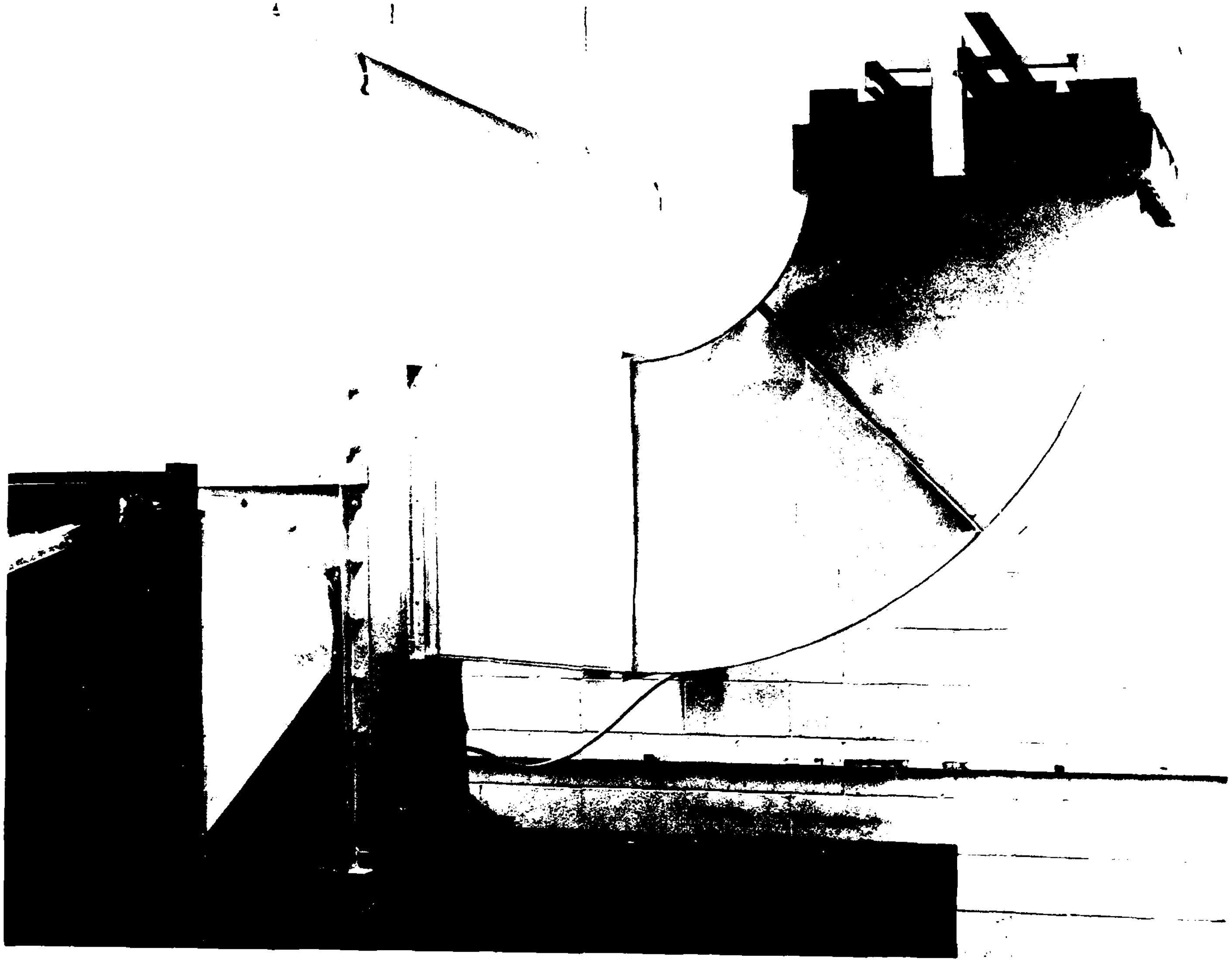

Figure 3.10 DISCHARGE ELBOW AND DAMPER

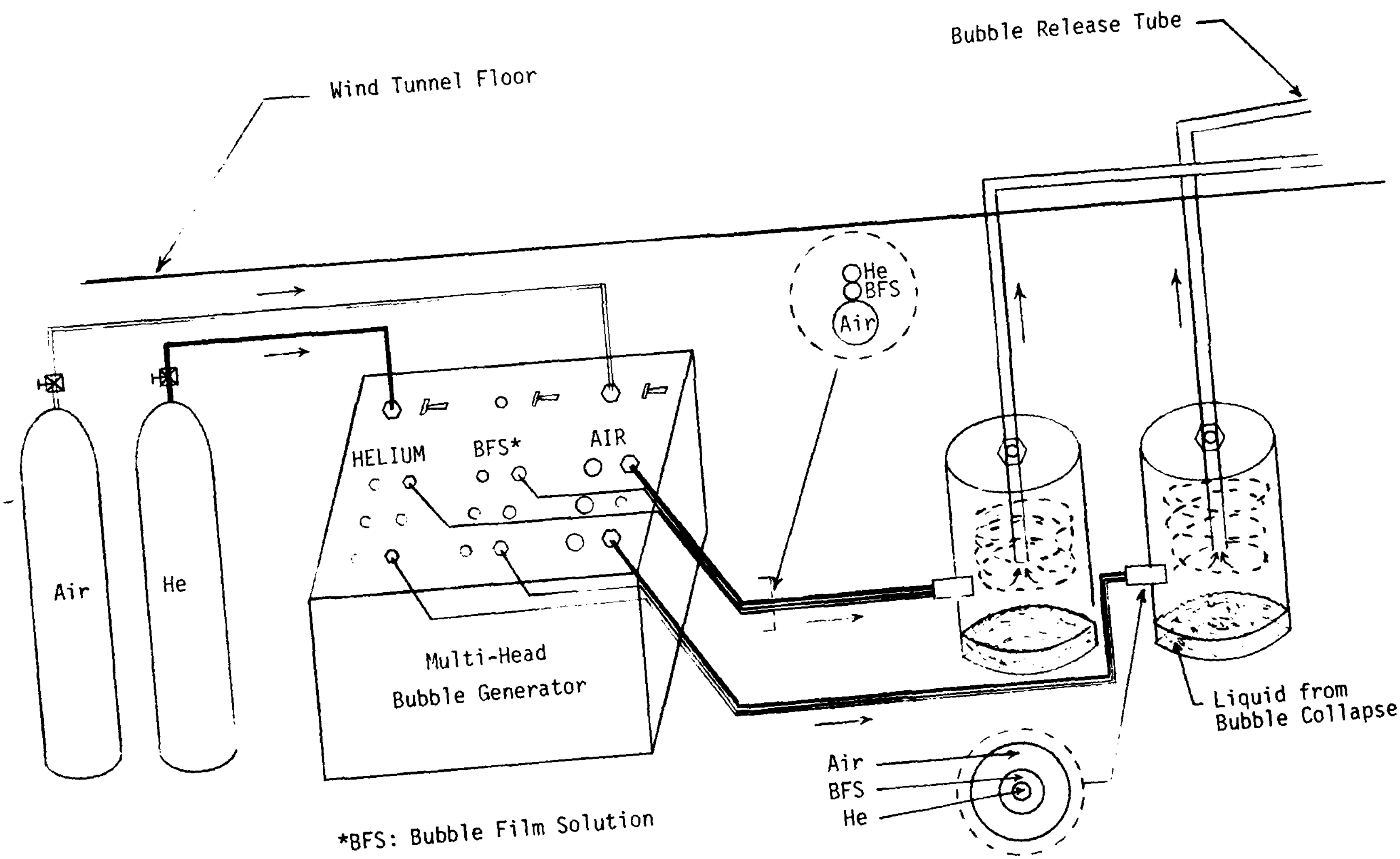

Figure 3.11 BUBBLE GENERATOR SYSTEM SCHEMATIC

3.4 Calibration and Tune-up of the Wind Tunnel

Before making the final test models, a trial plywood model was fabricated and several exploratory runs were made in the wind tunnel to ensure that

1) the required approach wind boundary layer velocity profiles are obtainable on the floor of the test section,

2) boundary layers on the walls and ceiling of the tunnel are not too thick,

3) with the selected linear scale of 1:50, blockage effects due to the model are insignificant, and

4) clearances between model and tunnel walls and ceiling are large enough to render errors from boundary layer interference effects insignificant.

First, with no model in the test section, vertical traverses were made with the pitot-static probe P_1 (see Figures 3.2 and 3.7) at span-wise locations from wall to wall to determine velocity profiles. The wall boundary layer thicknesses of the tunnel were observed to be not more than about 3 inches. Probe P_2 was then moved along the tunnel axis to its most forward position and vertical traverses made with it. The velocity profiles were identical to those obtained from readings of probe P_1 in planes near to the tunnel axis. Typical profiles obtained from readings of probe P_2 at a counter-jet manifold pressure of 4 inches of water are shown in Figures 3.12, 3.13, and 3.14 (for all the test runs, counter-jet manifold pressure was maintained at 4 inches of water). It can be seen that the distribution fits very closely a power law with an exponent of 1/4.5. (Recommended values of the exponent for a bush country vary between 1/6 and 1/3.5, Ref. 3.7). The boundary layer thickness is about 18 inches, giving a model height to boundary layer thickness ratio of 1:4.5. This translates to a wind boundary layer thickness of 72 feet approaching a single story building 16 feet tall (this falls well within the range of 60 to 80 feet recommended for open terrain or bush country). Reynolds numbers based on tunnel floor boundary layer thickness range from 0.7×10^5 to 1.7×10^5, granting good turbulent mixing in these layers (the value of critical Reynolds number based on boundary layer thickness for flow over a flat plate is only about 3×10^3).

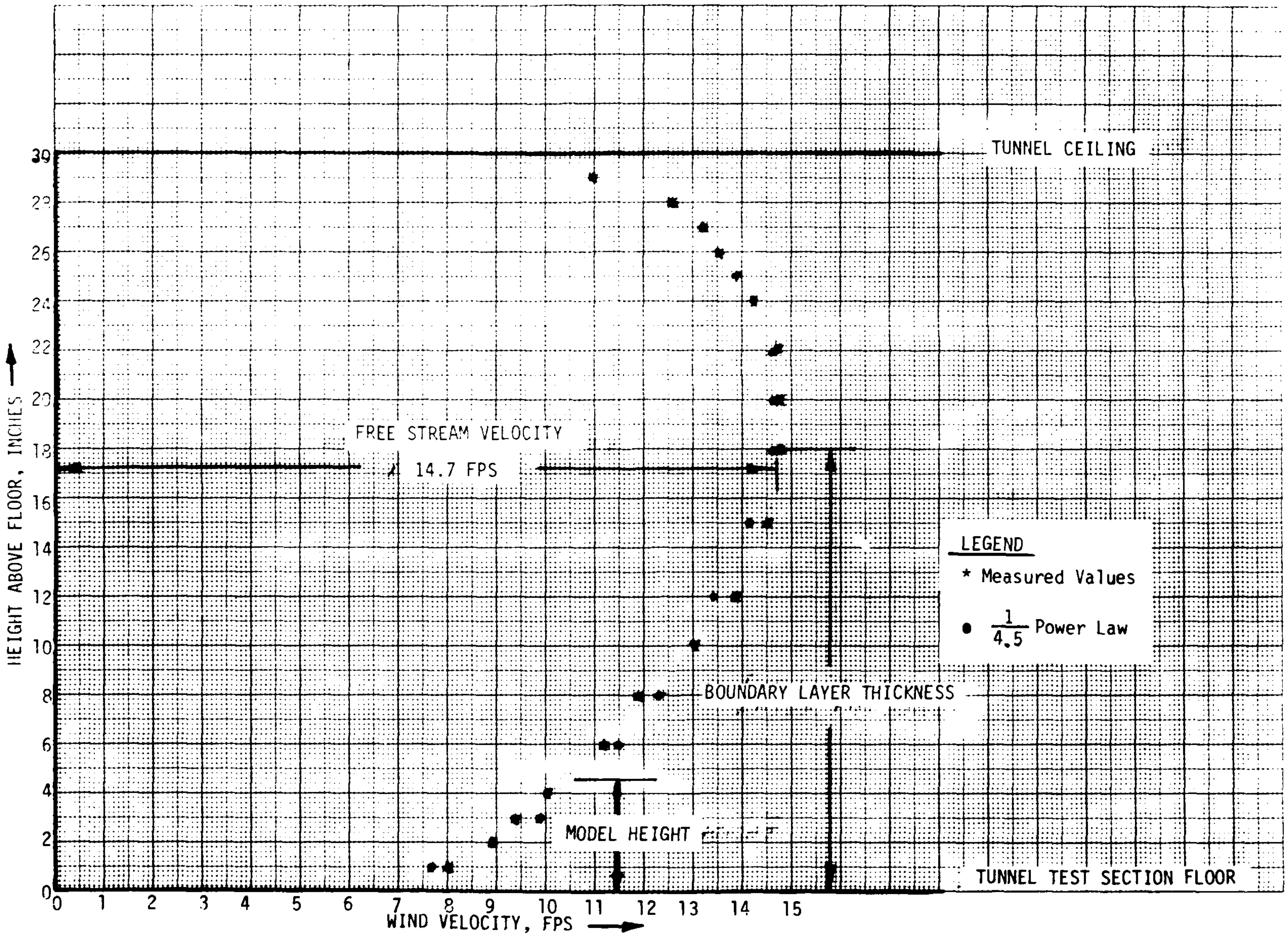

Figure 3.12 BOUNDARY LAYER VELOCITY PROFILE AT 14.7 FPS

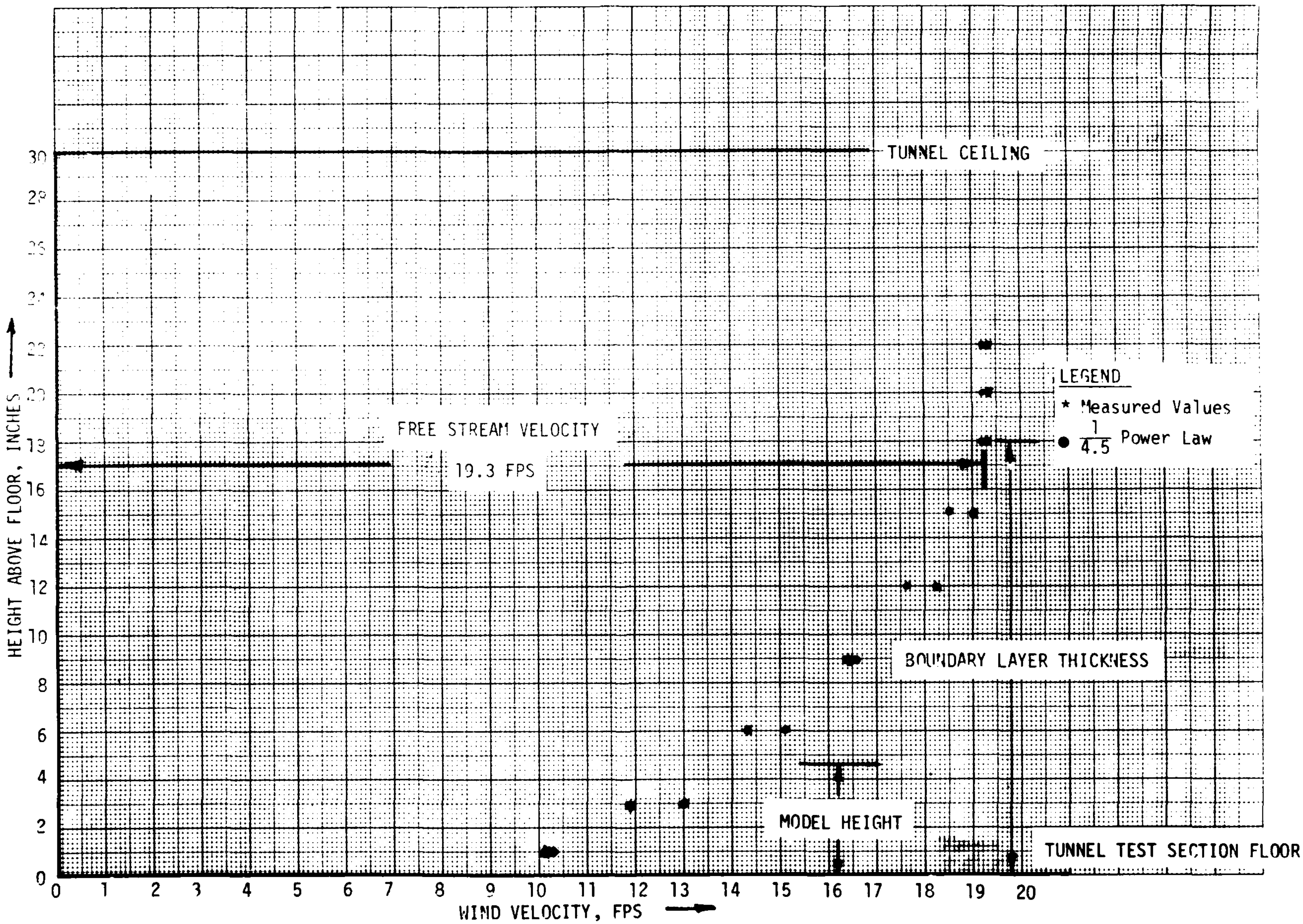

Figure 3.13 BOUNDARY LAYER VELOCITY PROFILE AT 19.3 FPS

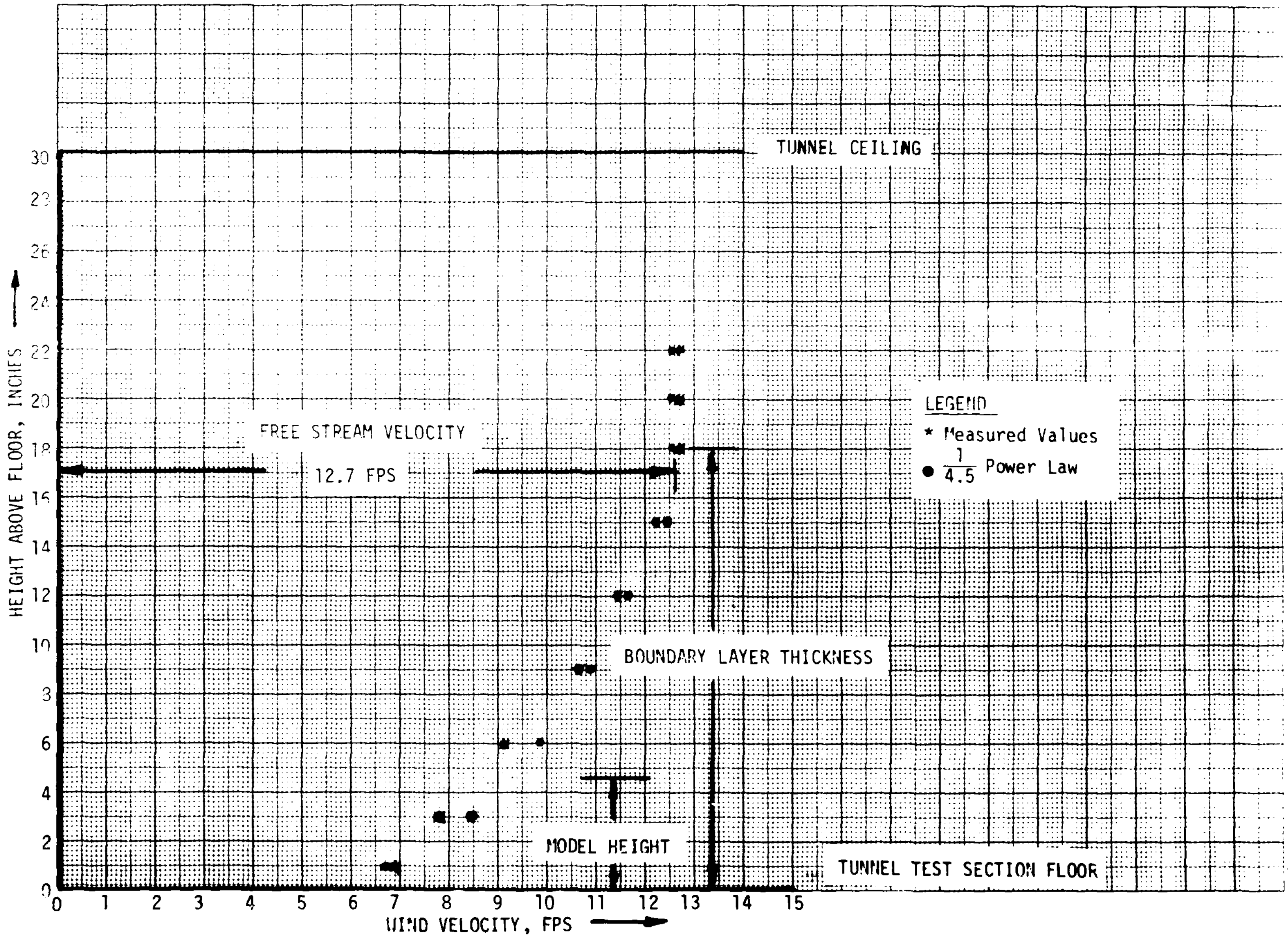

Figure 3.14 BOUNDARY LAYER VELOCITY PROFILE AT 12.7 FPS

Next, the damper opening on the discharge elbow of the blower was calibrated against free stream velocity. As a result, a single reading of either probe P_1 or P_2 (at a height more than 18 inches above the tunnel floor) was sufficient to check the accuracy of the damper setting.

The trial model was then placed inside the test section, about 20 inches downstream of probe P_2. The overall dimensions of this model equalled those of the proposed test models (Section 3.5), which were designed to a linear scale of 1:50. The blockage ratio based on projected frontal area was less than 4%. The model height was 4 inches giving a clearance of 26 inches between its roof and the tunnel ceiling. On the sides, the clearance between the foot of the berms and the tunnel walls was 20 inches for zero-degree wind angle.

With the trial model located as described, a vertical traverse was made using probe P_2 which was 20 inches upstream of the model. The velocity profiles closely approximated those obtained without the model. Probe P_2 was moved downstream to locations directly above the model and both lateral and vertical traverses were made. Maximum velocities directly above the model were within 5% of free stream values showing that the clearance between model and tunnel ceiling was large enough to yield accurate test results. Lateral traverses revealed that approach wind boundary layer velocity profiles obtained without the model were approximated at locations between the model and tunnel walls. This proved that the side clearances were also large enough to yield accurate test results with models of the size selected.

Several trial runs were also made to determine optimum settings of pressure regulator and metering valves of the bubble generator unit, locations and maneuverability of bubble release tubes, lighting and background settings, and camera location and film speed. Extended trial runs were necessary before a satisfactory system could be put together that is easy to operate and yields acceptable data (a typical set-up is shown in Figure 3.9).

3.5 Description of Scaled Models

At the time of our investigations, it was not known what the average upgraded fallout shelter would look like as they had not been located and surveyed. The shelters surveyed as part of the National Fallout Shelter Survey several years ago did not necessarily represent the shelters now being considered. DCPA indicated that the upgraded shelter would probably be single-story, residential and small commercial type structures that could support full earth berms.

Since the full scope of these type structures could not be completely investigated as part of this study, it was mutually decided to keep the shelter configurations simple to ensure good accuracy and reliability of the data taken during the scaled model testing. The general configuration of a bermed shelter is shown in Figure 3.15. The rectangular structure is typical of a small commercial building, one story high with slab-on-grade construction. Openings can be either windows or doors with a variation in opening patterns possible. The slope of the bermed sides depends on the type of soil used, varying from 30^{o} to 45^{o}. For the scale models, an angle of 36^{o} was used. Floor to ceiling wall partitions with doorways offer the main internal impedance to airflow through the building.

As per mutual agreement it was decided that the shelter configurations to be studied should represent extreme conditions, i.e.,

1) above and below grade shelters
2) high and low internal impedance to airflow
3) simple and complex opening patterns
4) high and low occupant densities

Figure 3.16 presents the structures that contain this range of characteristics and are summarized in Table 3.1. Applying the principles of fluid mechanics, it is possible to imagine the airflow patterns that might result within each shelter configuration for various opening patterns. These are depicted in Figure 3.17. For this phase of the study, investigations were limited to simple configurations with no internal partitions and with scaled dimensions adjusted to ensure no tunnel blockage effects as model was rotated to simulate various wind angles.

Figure 3.18 shows shelter geometries modeled in the present study. Shelter type I has a door in the front and rear, type II additionally has a window on one of the sides and type III has windows on both sides. Models are assembled from triangular pine-wood prisms representing the earth berms, a plexiglas sheet for the floor and a plywood sheet for the ceiling. Changing from one model type

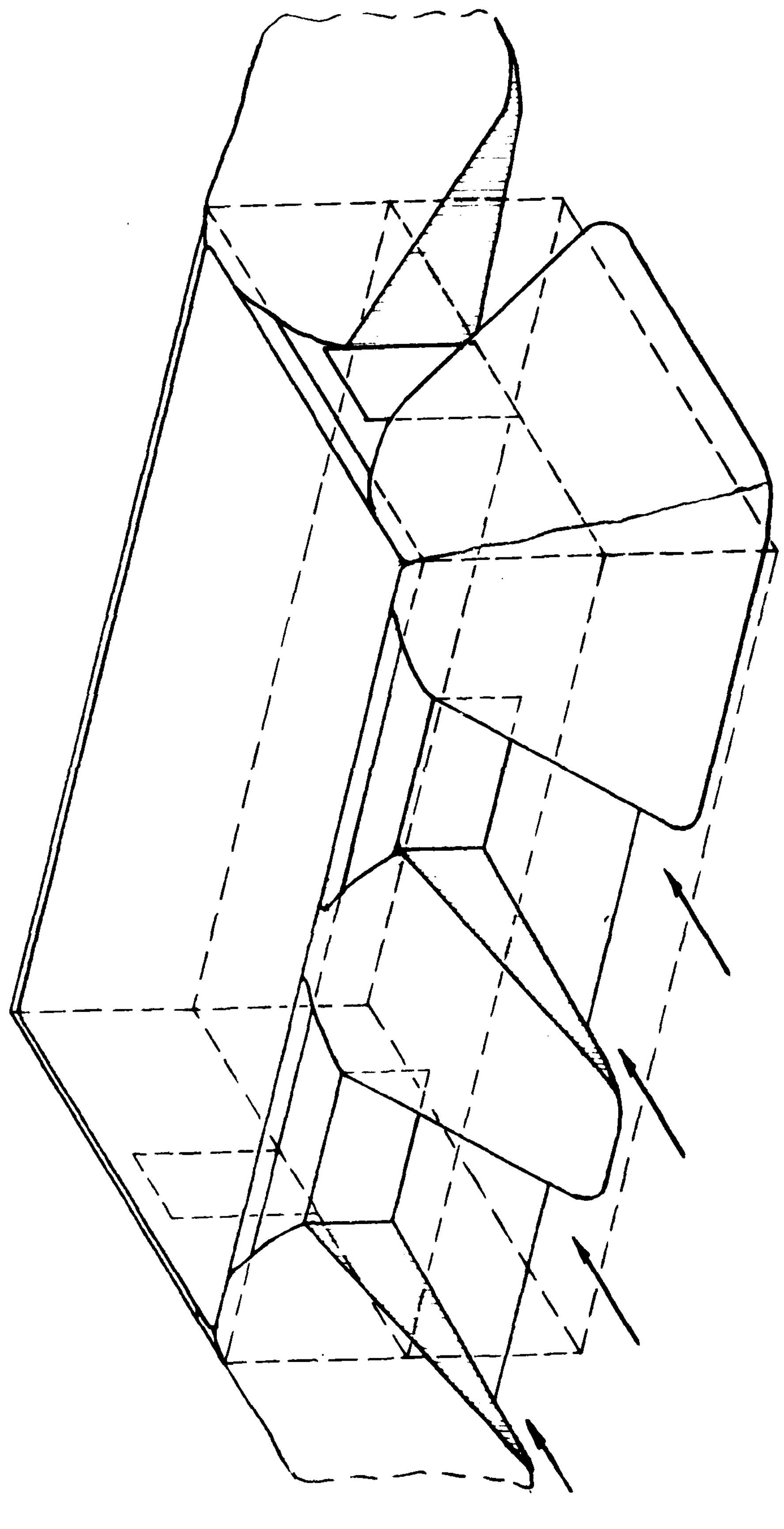

Figure 3.15 ILLUSTRATION OF A TYPICAL EARTH BERMED SHELTER

GARD, INC.

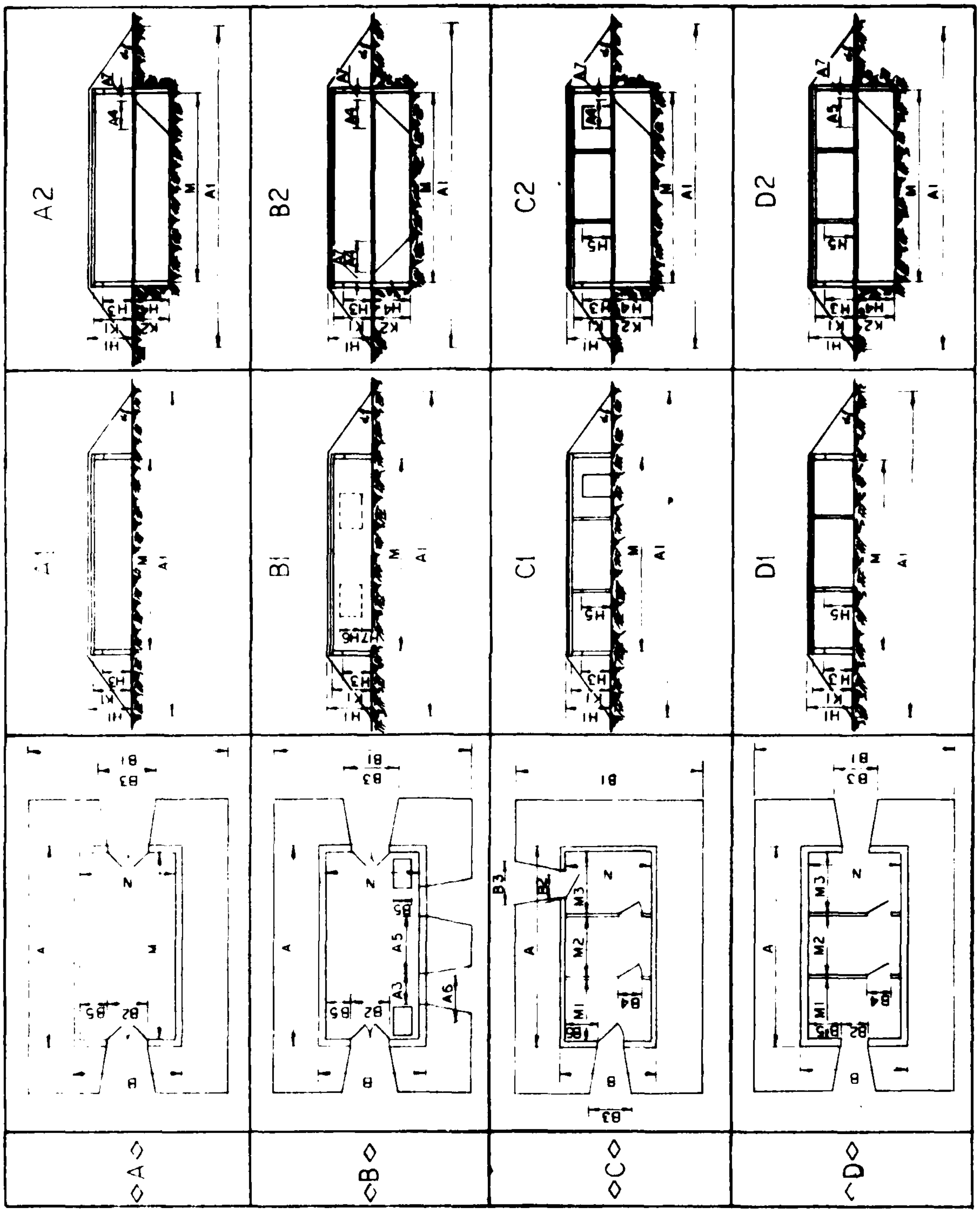

Figure 3.16 TYPICAL SHELTER CONFIGURATIONS

Table 3.1

Summary of Shelter Model Characteristics

Shelter Configuration	Internal Impedance		Opening Pattern		Grade Location	
	Low	High	Simple	Complex	Above	Below
A1	✓		✓		✓	
A2	✓		✓			✓
B1	✓			✓	✓	
B2	✓			✓		✓
C1		✓		✓	✓	
C2		✓		✓		✓
D1		✓	✓		✓	
D2		✓	✓			✓

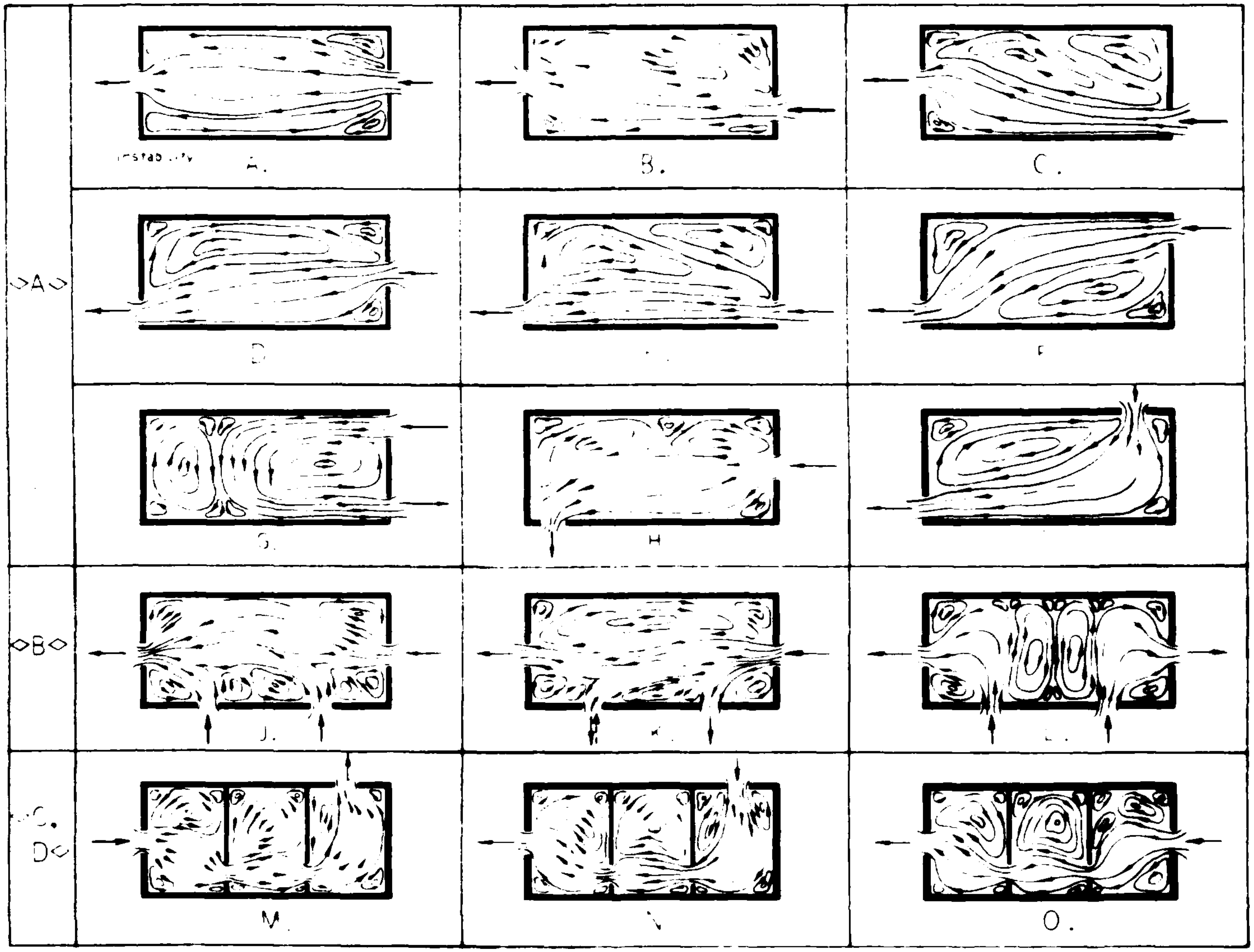

Figure 3.17 AIRFLOW PATTERNS FOR VARIOUS SHELTER CONFIGURATIONS

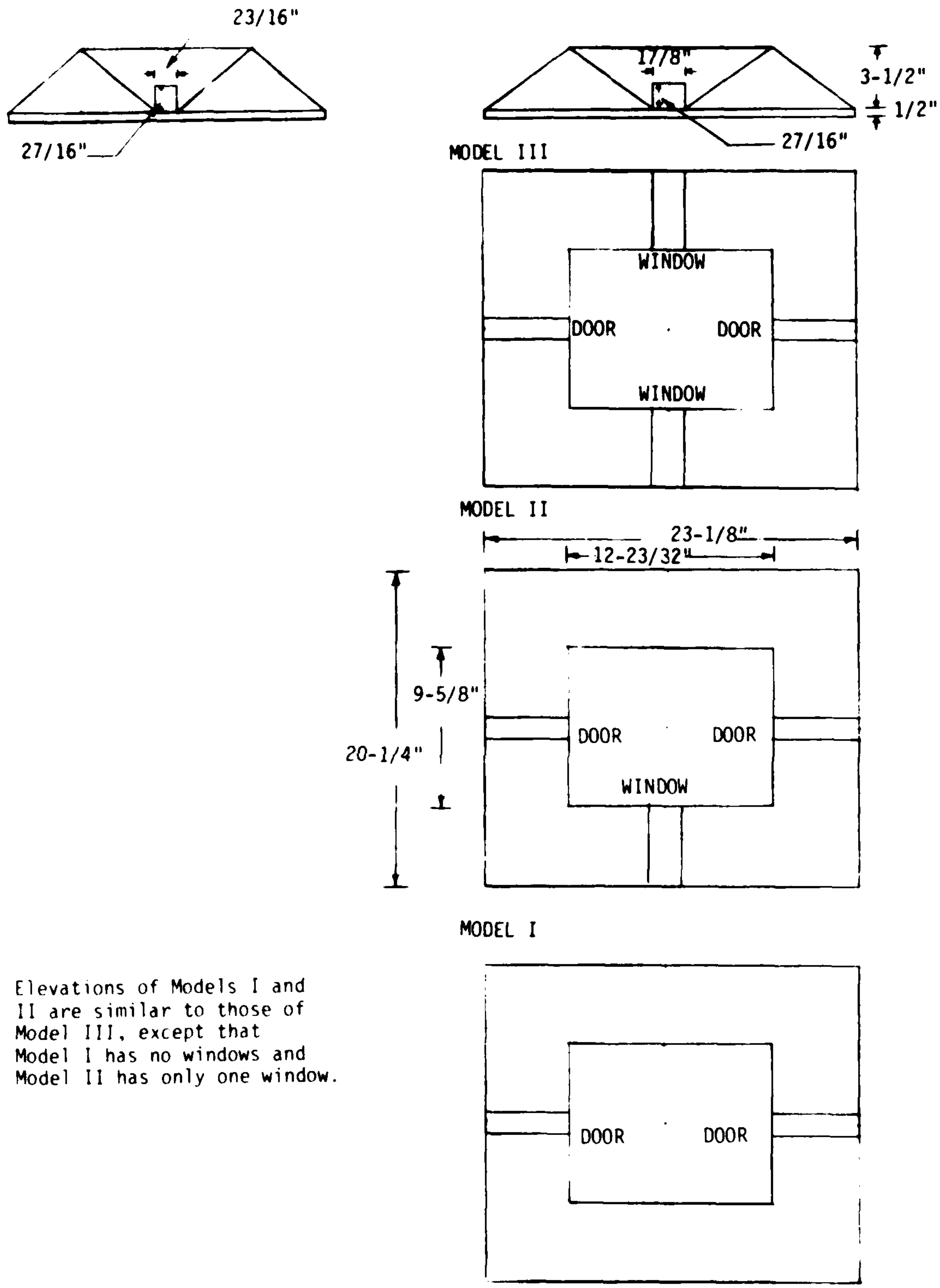

NOTE: Elevations of Models I and II are similar to those of Model III, except that Model I has no windows and Model II has only one window.

Figure 3.18 SHELTER GEOMETRIES TESTED

to another can be easily accomplished with this setup. The prisms and the plywood sheet are painted black on all sides to eliminate undesired light reflections.

Models were made to a linear scale of 1:50. A full-size shelter 53 feet long x 40 feet wide x 16.5 feet tall scaled to a model 12-23/32 inches x 9-5/8 inches x 4 inches. The smallest of the model dimensions - namely the height of 4 inches - gives a Reynolds number of about 10^4 at the lowest free-stream wind velocity tested (7.5 feet per sec.). This value is well above the upper bound of 5,000 quoted in reference 3.1 for shedding of vortices of the Karman vortex street type.

3.6 Test Procedure

Model I was placed in the test section so that it faced the approaching flow at a prescribed angle. Probes P_1 and P_2 were set at 20" above the tunnel floor. Two 250-watt lights (effective diameter about 2") were used to illuminate the bubble paths. One of the lights was placed 18" behind the rear door, the other 30" upstream of the front door opening. The light beams were directed through the doors to illuminate the door-to-door pathway. The damper opening was set for a particular free-stream wind velocity and the blower was turned on. After conditions became steady, probe P_2 was read to obtain the free-stream wind velocity. (Probes P_1 and P_2 read the same ensuring that blockage effects were insignificant.) Thin white lines were marked at 1/4" intervals for a total length of 2 inches across each opening to serve as distance markers.

A fine quality mirror (3' x 2') mounted on an adjustable frame was positioned beneath the tunnel test section at 45° to the floor. The movie camera was stationed at a distance of about 4 feet from the center of the mirror, and focused on the mirror image of the model's interior. Helium and compressed air supplies to the bubble generator were opened and the control knobs of the console adjusted to release neutrally buoyant bubbles (~ 1/8-inch diameter) through the release tubes at the desired rate. The lights illuminating the doorways were turned on. Positions of the bubble release tubes were adjusted for optimal frequency of bubble flow through the model. The camera was turned on for about 30-40 seconds at a nominal speed of 64 frames per second. Thereafter, the lights and the bubble generator were turned off and the damper opening adjusted for a different free-stream wind velocity. The test was repeated for the new wind velocity after conditions became steady. For each orientation of the building, bubble flow was filmed for 5 different free-stream wind velocities. Once this was completed, the test section access door was opened and the model rotated to a new angle for a different orientation. With each model, filming was done for 5 different relative wind angles (0° to 90°).

When all the measurements with model I were completed, model II was placed in the test section. An additional light source was installed and the beam from it directed through the side window opening. Filming of this series was done following the same procedure as in the previous series. After completing tests on model II, model III was placed in the test section and similar tests were performed. For accurate determination of film speed, the movement of the seconds needle of a precision stop watch was also periodically photographed for five seconds. The correct film speed was found to be 73 frames per second.

When the planes of the side openings were at acute angles to the wind direction, it was difficult to discern whether bubbles were entering or leaving through the side openings. This was due to the complex vortex motion just outside of these openings. In such cases, additional runs were made with the bubble release tubes turned sideways. This increased the external bubble flow rate past the side openings considerably and reduced the number of bubbles entering through the front opening to practically zero. From these runs one could determine the proper bubble flow direction through the side openings without ambiguity.

3.7 Description of Results

The processed films were projected on a screen frame by frame and the bubble movement distance through an opening per frame was noted. Knowing the film speed (73 frames per second) and the distance moved per frame, the bubble velocity through the opening could be calculated. The mean air flow velocity through an opening was obtained by averaging the velocities of 15-20 bubbles.

Let,

χ = bubble movement distance in inches through an opening in one frame,

a = cross-sectional area of the model opening in square inches,

n = number of bubbles whose velocity is averaged.

Then, the average air flow velocity ($\bar{v}$) in feet per second through the model opening is,

$$\bar{v} = \sum_{i=1}^{n} \left(\frac{\chi_i}{12}\right) \times \frac{1}{(1/73)} \times \frac{1}{n}$$

$$= 6.083 \times \bar{\chi}$$

where $\bar{\chi} = \dfrac{\sum_{i=1}^{n} \chi_i}{n}$.

The volume flow rate (q) in cubic feet per minute through the model opening is,

$$q = 6.083 \times \bar{\chi} \times \frac{a}{144} \times 60$$

$$= 2.535 \times \bar{\chi} \times a$$

With a linear scale of 1:50, flow rate through the full size shelter opening can be calculated as,

$$Q = q \times 50 \times 50$$

$$= 6336.8 \times \bar{\chi} \times a$$

When there are more than one inlet or exit openings, the throughput flow rate is taken as the sum of the flow rates through all the inlet or exit openings. The variation of ventilation throughput with the free stream wind velocity (V_∞) is shown in graphical form in Figures 3.19, 3.20, and 3.21. The same data is shown in tabular form in Tables 3.2, 3.3 and 3.4.

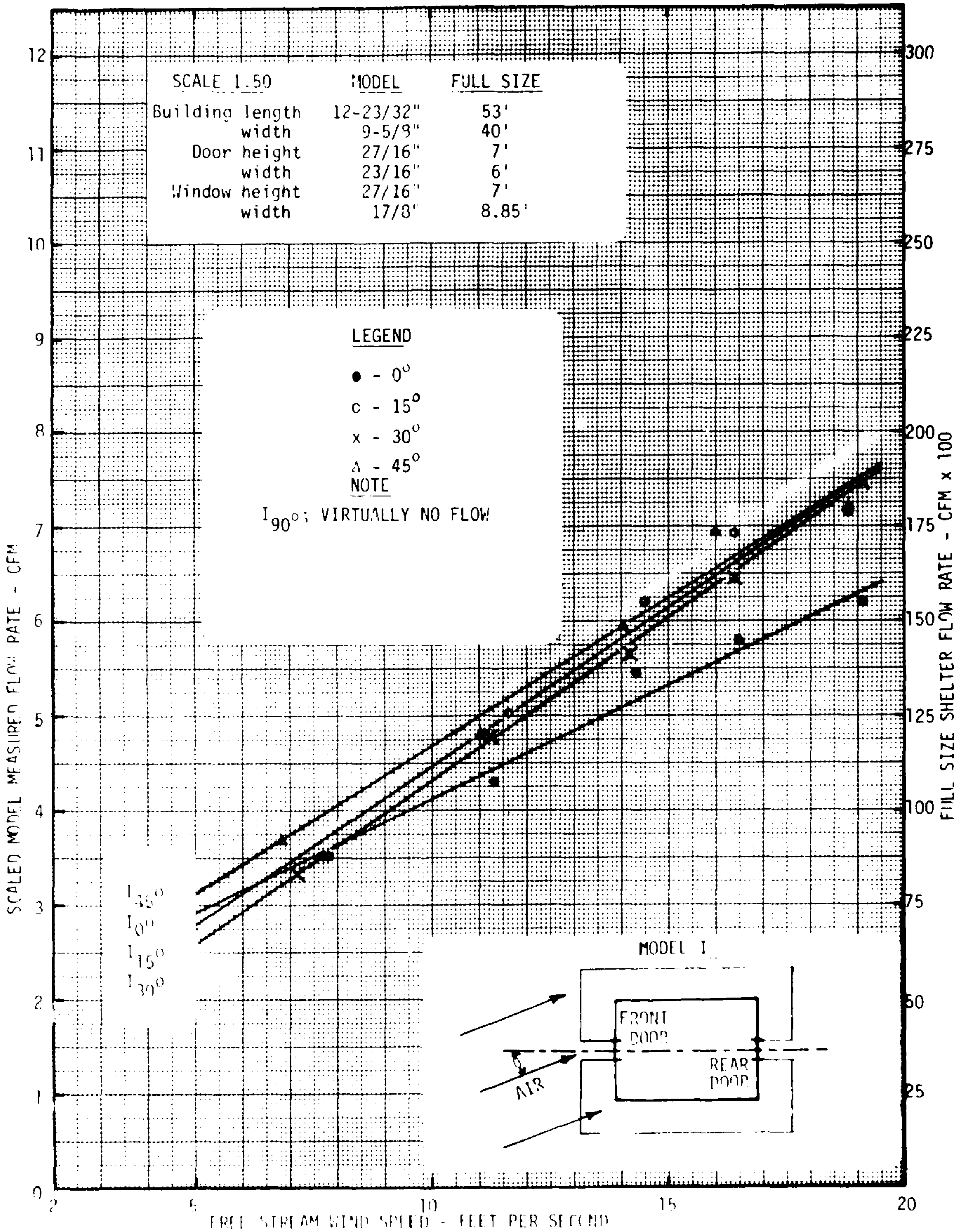

Figure 3.19 VENTILATION THROUGHPUT CFM VS. V. FOR MODEL I

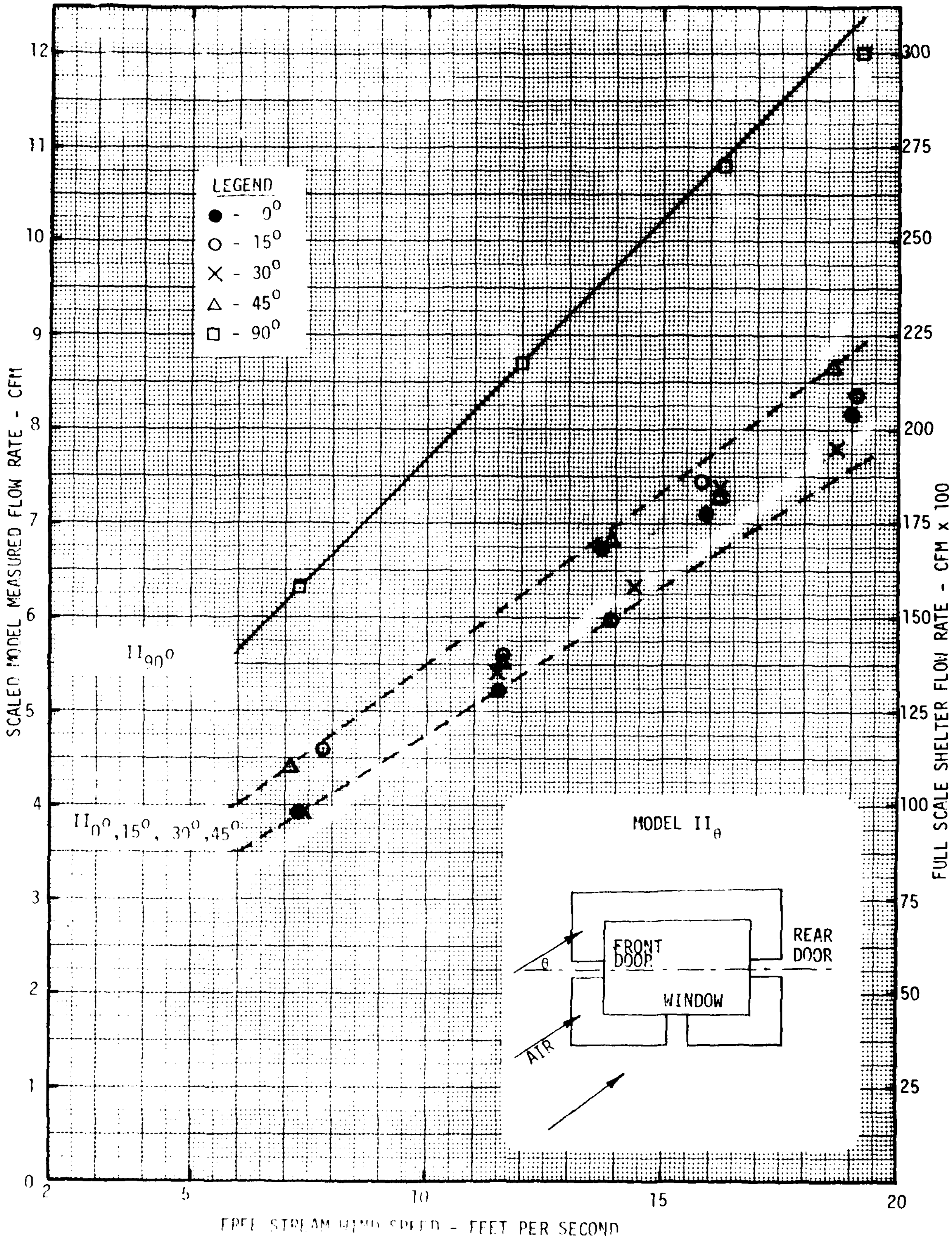

Figure 3.20 VENTILATION THROUGHPUT CFM VS. V_∞ FOR MODEL II

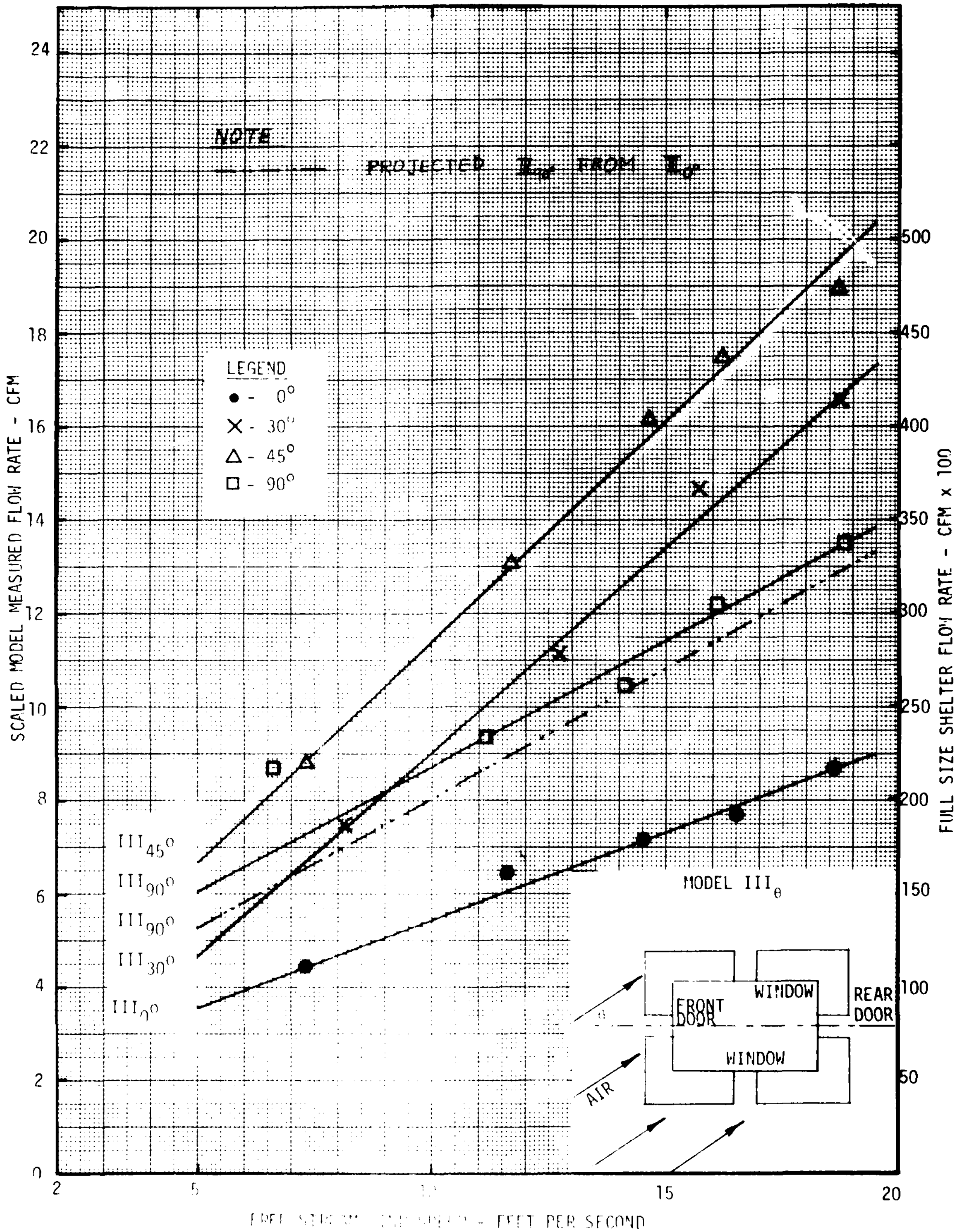

Figure 3.21 VENTILATION THROUGHPUT CFM VS. V_∞ FOR MODEL III

GARD, INC.

Table 3.2

VENTILATION THROUGHPUT CFM AT
VARIOUS WIND VELOCITIES AND ANGLES, MODEL I

I-0°					
WIND VELOCITY, FPS	7.7	11.3	14.3	16.5	19.1
TOTAL CFM - SCALED	3.5	4.3	5.5	5.8	6.2
- FULL SIZE	8750	10750	13750	14500	15500
I-15°					
WIND VELOCITY, FPS	7.8	11.6	14.5	16.4	18.8
TOTAL CFM - SCALED	3.5	5.0	6.2	6.9	7.2
- FULL SIZE	8750	12500	15500	17250	18000
I-30°					
WIND VELOCITY, FPS	7.1	11.2	14.2	16.4	19.1
TOTAL CFM - SCALED	3.3	4.8	5.6	6.5	7.5
- FULL SIZE	8250	12000	14000	16250	18750
I-45°					
WIND VELOCITY, FPS	6.8	11.0	14.0	16.0	18.8
TOTAL DFM - SCALED	3.7	4.8	5.9	6.9	7.2
- FULL SIZE	9250	12000	14750	17250	18000
I-90°					
VIRTUALLY NO FLOW AT ALL WIND VELOCITIES.					

Table 3.3

VENTILATION THROUGHPUT CFM AT
VARIOUS WIND VELOCITIES AND ANGLES, MODEL II

II-0^{o}					
WIND VELOCITY, FPS	7.3	11.5	13.7	15.9	19.0
TOTAL CFM - SCALED	3.9	5.2	6.9	7.1	8.2
- FULL SIZE	9750	13000	17250	17750	20500
II-15^{o}					
WIND VELOCITY, FPS	7.8	11.6	13.9	15.8	19.1
TOTAL CFM - SCALED	4.6	5.7	6.0	7.4	8.4
- FULL SIZE	11500	14250	15000	18500	21000
II-30^{o}					
WIND VELOCITY, FPS	7.4	11.5	14.4	16.2	18.7
TOTAL CFM - SCALED	3.9	5.4	6.3	7.4	7.8
- FULL SIZE	9750	13500	15750	18500	19500
II-45^{o}					
WIND VELOCITY, FPS	7.1	11.6	13.9	16.2	18.7
TOTAL CFM - SCALED	4.4	5.5	6.8	7.3	8.7
- FULL SIZE	11000	13750	17000	18250	21750
II-90^{o}					
WIND VELOCITY, FPS	7.3	12.0	14.2	16.3	19.2
TOTAL CFM - SCALED	6.4	8.7	10.5	10.8	12.0
- FULL SIZE	16000	21750	26250	27000	30000

Table 3.4

VENTILATION THROUGHPUT CFM AT
VARIOUS WIND VELOCITIES AND ANGLES, MODEL III

III-0°					
WIND VELOCITY, FPS	7.3	11.6	14.5	16.5	18.6
TOTAL CFM - SCALED	4.3	6.5	7.2	7.7	8.7
- FULL SIZE	10750	16250	18000	19250	21750
III-30°					
WIND VELOCITY, FPS	8.1	12.7	15.7	18.7	
TOTAL CFM - SCALED	7.5	11.1	14.7	16.6	
- FULL SIZE	18750	27750	36750	41500	
III-45°					
WIND VELOCITY, FPS	7.3	11.7	14.6	16.2	18.7
TOTAL CFM - SCALED	8.8	13.1	16.2	17.5	19.0
- FULL SIZE	22000	32750	40500	43750	47500
III-90°					
WIND VELOCITY, FPS	6.6	11.1	14.1	16.0	18.8
TOTAL CFM - SCALED	8.7	9.4	10.4	12.2	13.6
- FULL SIZE	21750	23500	26000	30500	34000

3.8 Discussion of Results

Several important observations and conclusions can be made from this study. These are discussed below.

1) At any given relative wind angle θ, the ventilation flow rate (q) through all three models varies linearly with wind speed (see Figures 3.19, 3.20 and 3.21).

2) For models I and II, the ventilation flow rate does not vary significantly with relative wind angle for values of θ not too large (as can be seen from the results for $0^\circ \leq \theta \leq 45^\circ$). Flows at non-zero values of θ, tend to be slightly larger than those at $\theta = 0^\circ$, because of the higher average pressure in the stagnation zone immediately upstream of the front door created by the sides of the berm. But this tendency is counteracted by the smaller door area normal to the wind at non-zero angles. (For model I, the total normal area decreases with wind angle. For model II, the opening area normal to the wind steadily increases as θ goes from 0° to 90°). For small values of θ, the former factor dominates and for larger values of θ the latter factor is dominant. A comparison of model I results for $\theta \leq 45^\circ$ (Figure 3.19) against those for 90° (and 80°) would reveal this. Although filming was not done, bubble flow through model I was observed at $\theta = 80^\circ$. A very small, but significant, through flow was noticed.

   For model III, throughput flow rate at non-zero values of θ is considerably greater than that for $\theta = 0^\circ$. This is what one would predict noting that both the average stagnation pressure and the total projected normal opening area are larger for winds at non-zero angles. At $\theta = 45^\circ$, for which the projected normal area is maximum, throughput flow rate for model III has its largest value.

3) Increasing the opening area on the windward side alone or on the leeward side alone does not augment the throughput flow rate very much. To realize maximum throughput flow rate, the total opening area must be more or less equally divided between the windward and leeward sides. A comparison of the results for models I, II and III clearly bears this out.

Model II has about 74% more total opening area than model I and model III has 43% more opening area than model II. For $\theta = 15^\circ$, 30° and 45°, throughput flow rate for model II is only about 20% larger than for model I, whereas for model III it is about 80% more than that for model II. Although model II has considerably larger area than model I on the windward side, it has the same area as model I on the leeward side. This severe flow restriction on the leeward side prevents the model II flow from going substantially higher than that for model I. Model III, on the other hand, has an even distribution of opening areas between the windward and leeward sides. It is also of interest to note that, model II has a much larger projected area of the inlet openings normal to the wind at $\theta = 45^\circ$; yet, the throughput flow rate is considerably smaller than for $\theta = 90^\circ$. This is due to the better distribution of opening areas between windward and leeward sides in the latter case. As would be expected, the highest flow rate for model III occurs at a relative wind angle of 45°.

4) For model I at 90° relative wind angle, there is practically zero flow through the openings (for this case both door openings are in planes parallel to the wind velocity). Model II, at the same wind angle, has some flow through the side openings induced by the suction at the rear window opening.

5) Most of the flow through model III at 90° relative wind angle, enters through the front window and exits through the rear window. The flow pattern at the side door openings is very complex. Through part of the side openings, flow is going out and through some other parts flow is coming in. The net flow is outwards and is calculated as the difference in volume flow rates through the front and rear windows.

   It may be noted that at $\theta = 90^\circ$, model III is essentially the same as it is at 0° with the only difference that the opening area normal to the wind is greater by a factor of 1.48. The projected flow rates obtained by multiplying those at 0° by 1.48 are shown by the chain line in Figure 3.21. The measured values are about 10% higher than the projected values. This is not surprising since the length of the main flow path (window-to-window distance) in this case is about 30% less than that for the 0° position (door-to-door distance).

6) Figures 3.22, 3.23, 3.24, and 3.25 show a comparison of inflow rates through the front door opening alone for models I, II and III for different wind speeds and angles. Several interesting observations can be made from these figures. At $\theta = 0^{\circ}$, flow rates through model III are larger than those through model II which in turn are slightly larger than flow rates through model I. This is to be expected because of the small, but non-zero, outflow through the side openings of models II and III. At $\theta = 15^{\circ}$, there is some inflow through the window of model II. The net flow through the window is still outwards. Therefore, inflow through the front door is still higher than that for model I. As θ is increased to 30°, the flow through model II window becomes unidirectional and inwards. Model II for this angle has a much larger inlet opening area although it has the same exit opening area as model I. The increased flow causes a pressure build-up upstream of the rear door inside the model. Consequently, the inlet flow through the front door opening sees a larger resistance and drops to a value less than that for model I, although the total throughput flow rate for model II is larger (see Figures 3.19 and 3.20). In the case of model III, this sort of a pressure build-up does not occur since the leeward side and windward side opening areas always match. However, as the cross stream from the windward side window becomes stronger, the pressure in the mixing zone of the two streams begins to rise. Consequently, the inlet flow through the front door sees an increasing resistance and drops to values slightly below those for model I (see results for $\theta = 45^{\circ}$).

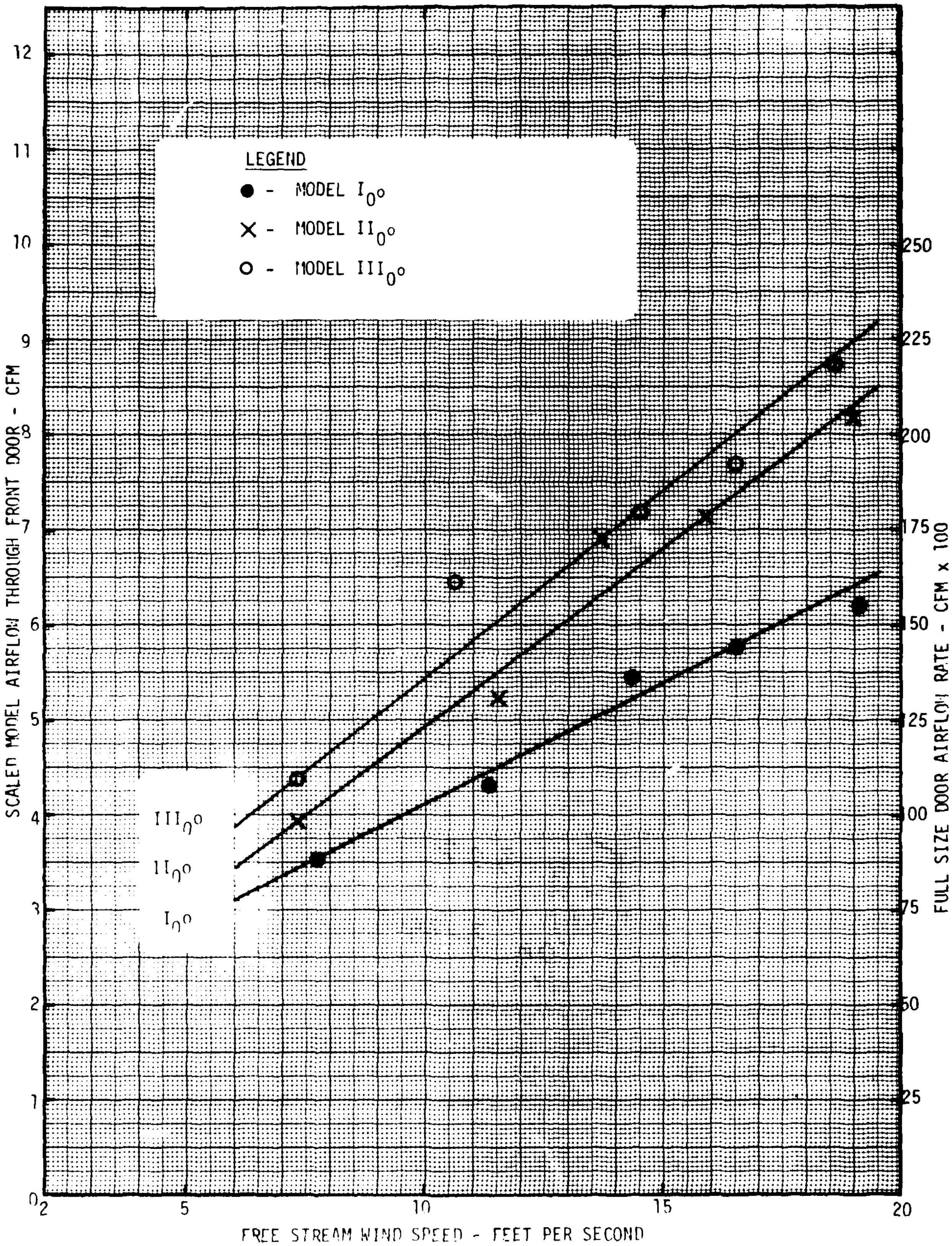

Figure 3.22 INFLOW RATES THROUGH THE FRONT DOOR AT 0^{0}

GARD, INC.

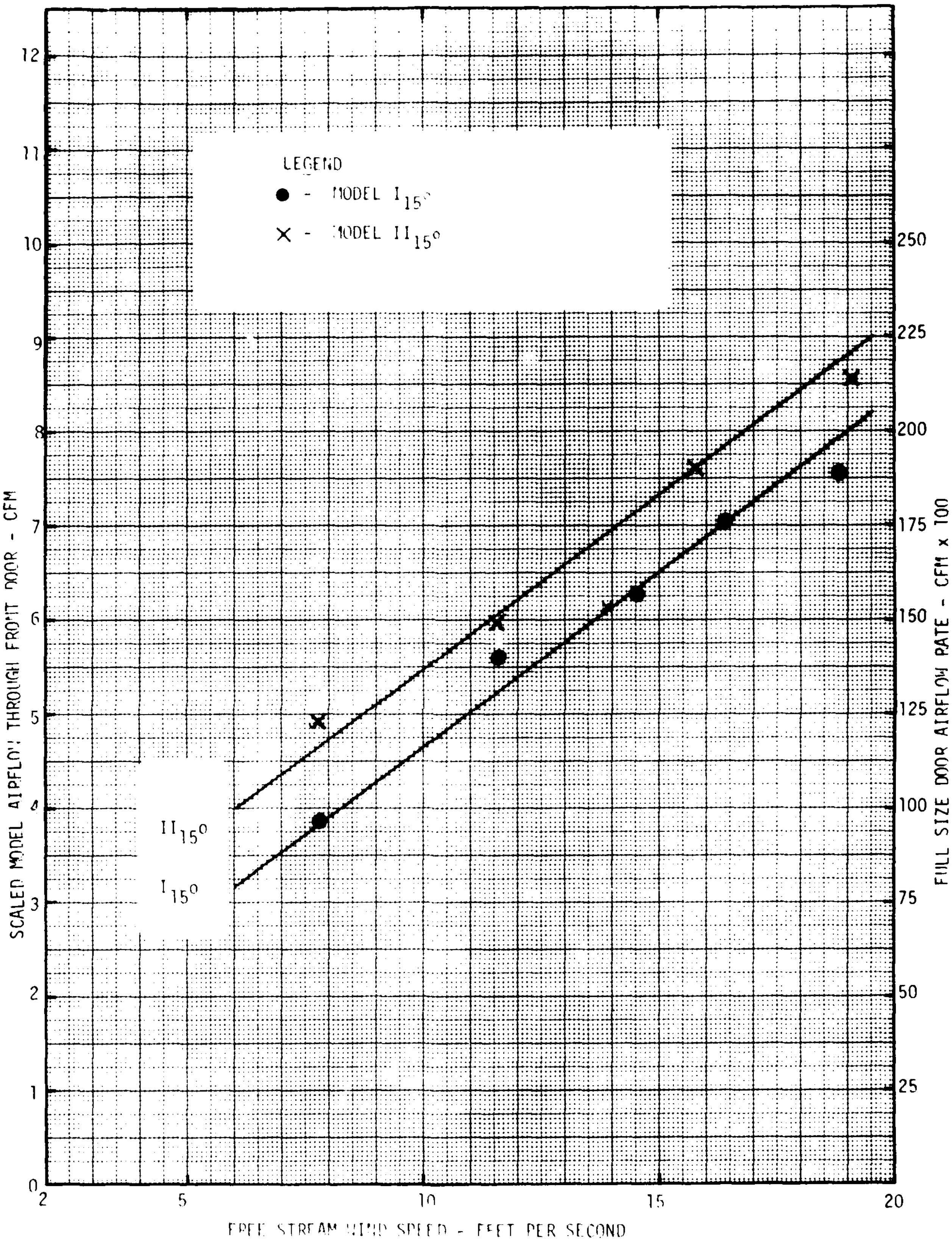

Figure 3.23 INFLOW RATES THROUGH THE FRONT DOOR AT 15°

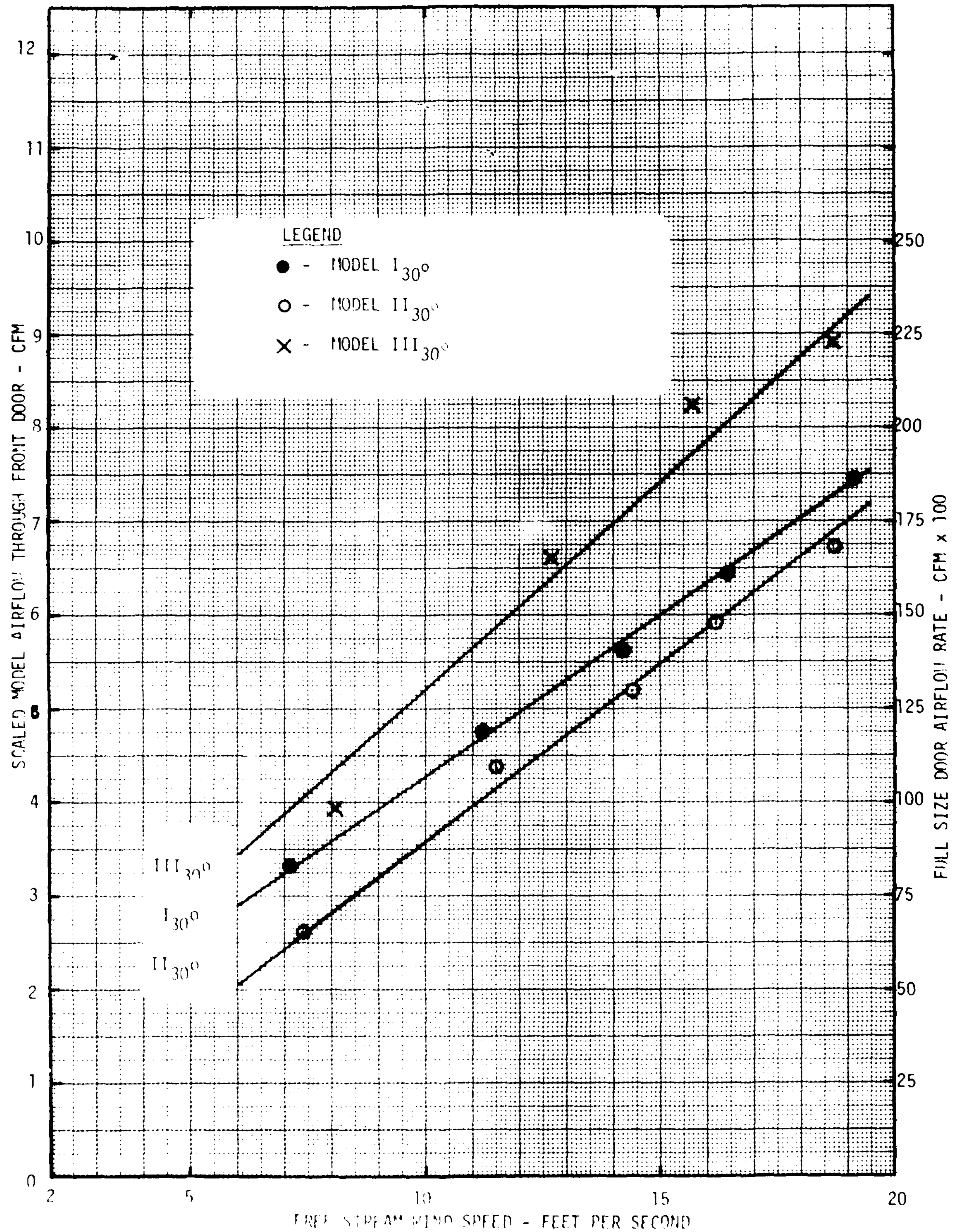

Figure 3.24 INFLOW RATES THROUGH THE FRONT DOOR AT 30°

GARD, INC.

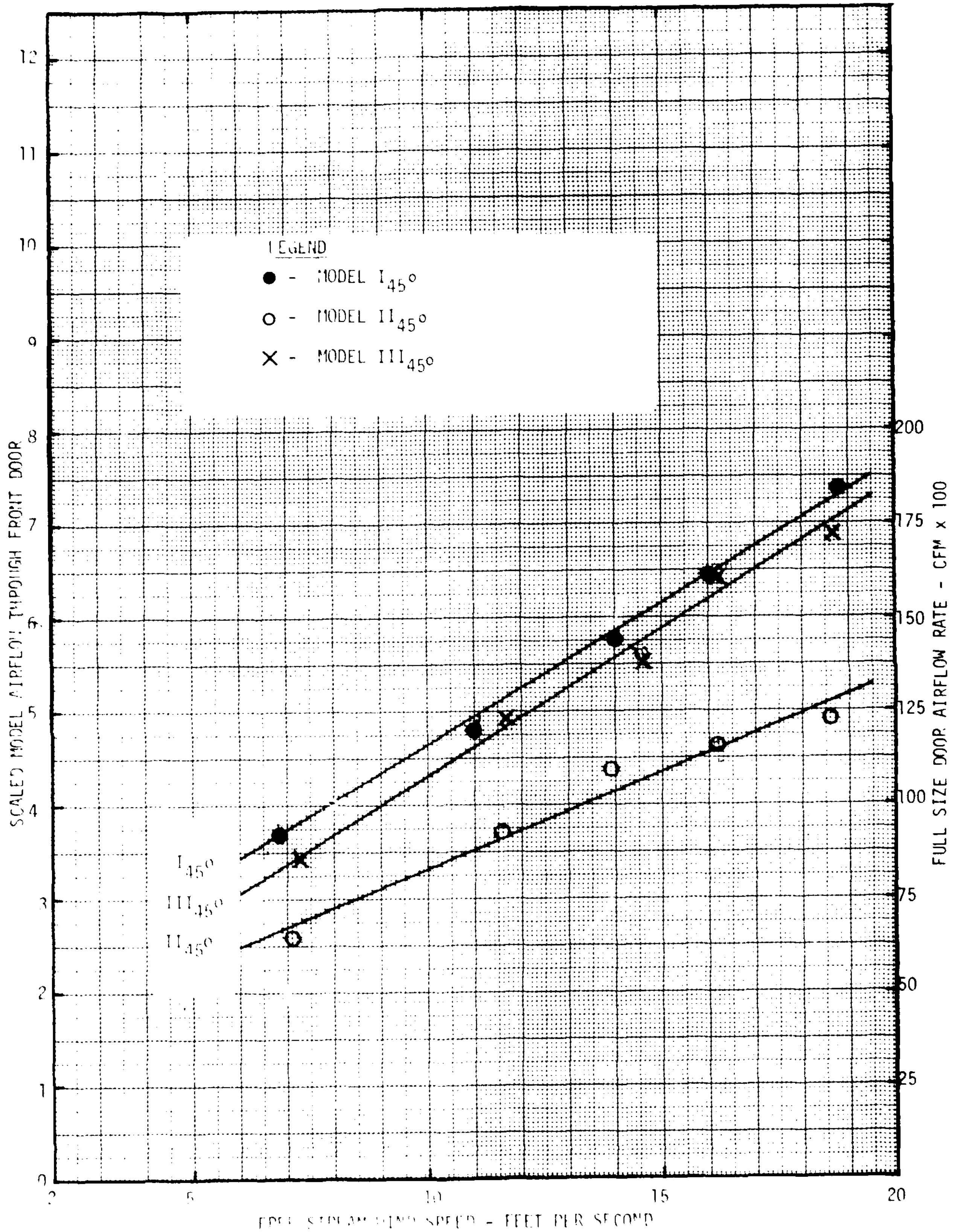

Figure 3.2? INFLOW RATES THROUGH THE FRONT DOOR AT 45°

GARD, INC.

Measurement of ventilation throughput in model buildings poses several difficulties. Due to practical considerations the maximum dimensions of the model and its openings are limited. Further, the flow patterns inside the model and in the neighborhood of the openings are so complex that measurement of flow through these openings using probes is undesirable. The method of flow tracing with neutrally buoyant bubbles and determining their velocity with motion photography developed by GARD and used in this study, is effective and relatively simple. Measurements are repeatable within $\pm$ 5%. However, there is one major drawback for this method (GARD is already in the process of finding correction factors to reduce errors from this source) which relates to the assumption that the average flow velocity obtained is a true average for the whole area of the opening. In reducing data from the films, for some of the runs, the average velocities of 15-20 bubbles were calculated from two different segments of the film. The maximum difference between the average velocities of the two sets was less than 10%. This shows that the average velocity obtained is the true average for the "through-flow area" of the opening. However, this need not be the average velocity for the whole area of the opening. A part of the opening area may be effectively blocked by recirculating vortices, so that the actual through-flow area of the opening could be significantly less than its full cross-sectional area.

An approximate value of the "through-flow area" for the front door opening of model I can be calculated in the following way. Let

$$A_c = \text{coefficient of area}$$

$$= \frac{\text{through-flow area of opening}}{\text{cross-sectional area of opening}}$$

Considering the entrance flow geometry, it appears reasonable to assume that the coefficient of area of the rear door opening ~ unity. Based on this and using the law of mass conservation, values of A_c for the front door opening can be calculated as

$$A_c = \frac{\text{average flow velocity through rear door}}{\text{average velocity for through-flow area of front door}}$$

$$= \frac{\text{average bubble flow velocity through rear door}}{\text{average bubble flow velocity through front door}}$$

Values of A_c as a function of wind speed and angle are shown in Figure 3.26. For a given wind speed and angle, the value of A_c for models II and III would be nearly the same as that for model I. Any difference in the values of A_c among the different models should arise from a change in the distribution of the pressure differentials across the front door, resulting from the air flow through the windows. This effect is likely to become significant only at larger values of θ when the momentum and mass flux through the window openings become large. Values of flow rate for the front door openings of models II and III plotted in Figures 3.22 through 3.25 were obtained by multiplying the product of the measured average velocity and the door area by the coefficient of area obtained for model I.

An important fact brought out by the present study relates to the non-linearities inherent in fluid dynamics problems of this sort and the need to exercise caution in interpolating/extrapolating experimental data. At $\theta = 30^\circ$ and 45°, flow through the side window of model II is inwards. Extrapolating, one finds that the flow through the window at $\theta = 15^\circ$ should be smaller, but, still inwards. In reality, the net flow through the model II window at $\theta = 15^\circ$ is outwards although there is a very small inflow through a section of this window.

Another illustration of the above facts can be seen by attempting to predict the throughput flow rate for model III at $\theta = 90^\circ$, from the results of models I and II. For model III at $\theta = 90^\circ$, one may be tempted to calculate the influx through the windward window opening by multiplying the throughput for model I at 0° by the area ratio of window to door. Adding to this the influx through the side door openings of model II at $\theta = -90^\circ$ (although not filmed, flow through model II for $\theta = -90^\circ$ was visually observed, a small but significant flow enters through the side doors and exits through the rear window), one might predict that for model III at $\theta = 90^\circ$, the efflux through the leeward window is more than the influx through the windward window and the net flow through the side door openings is inwards. This is incorrect based on visual observations and the measured values of throughput flow rate for model III at $\theta = 90^\circ$.

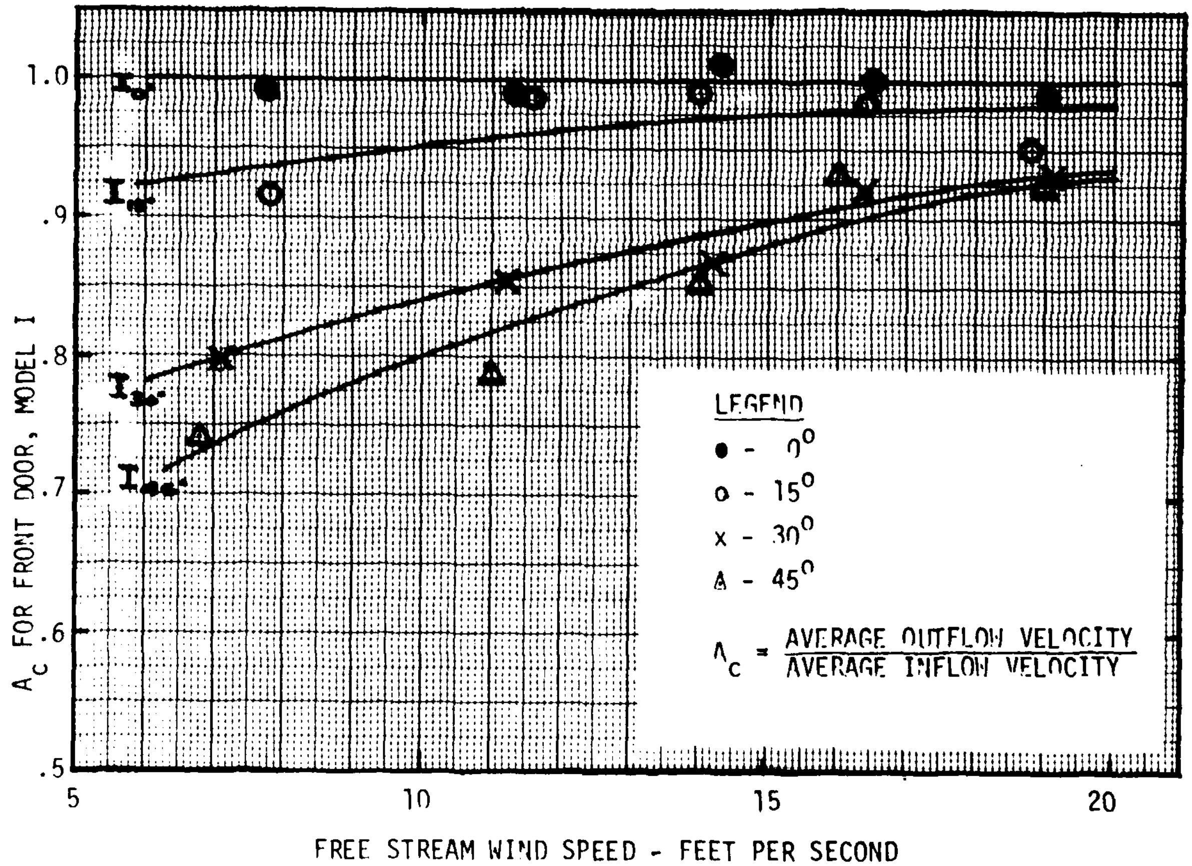

Figure 3.26 COEFFICIENT OF AREA, A_c, VS. V_∞

Based on the test results obtained from this program, it is clear that only an extended scaled model study yielding correlations of throughput flow with the dominant independent variables can provide the information required to make reasonably accurate predictions and meaningful recommendations with respect to ventilation in shelter buildings. This study must include all the dominant independent variables and extend over a wide enough range so that the results can be extrapolated or interpolated with confidence. The dominant variables for this study can be identified as wind speed and direction; height, width and length of the building; areas and locations of openings and internal resistances including those due to occupants. Since the number of independent variables is large and their interactions are non-linear, the test matrix will have to be selected judiciously to render the study sufficiently thorough and detailed while practical to perform.

References for Section 3

3.1 Schlichling, H., "Boundary-Layer Theory", McGraw-Hill Book Co., N.Y., 1968.

3.2 Hoerner, S. F., "Fluid-Dynamic Drag", Hoerner Fluid Dynamics, N.J., 1965.

3.3 "Wind Tunnel Studies at the BRS", Civil Engineering and Public Works Review, Vol. 60, No. 702, January, 1965.

3.4 Counihan, J., "An Improved Method of Simulating an Atmospheric Boundary Layer in a Wind Tunnel", Atmospheric Environment, Pergamon Press, Vol. 3, 197-214, 1969.

3.5 Chang-Keng, Liu., "An Experimental Study of Turbulent Boundary Layer on Rough Walls", Ph.D. Thesis, Stanford University, 1966.

3.6 Nagib, H. M., et al., "On Modeling of Atmospheric Surface Layers by the Counter-jet Technique", AAIA, 8th Aerodynamic Testing Conference, Bethesda, Maryland, July 8-10, 1974.

3.7 Davenport, A. G., "Rationale for Determining Design Wind Velocities", Journal of Structural Design, Proceedings of the American Society of Civil Engineers, 39-61, May, 1960.

The following articles, although of interest, have not been referenced in the text:

3.8 "The Feasibility of Using Models for Predetermining Natural Ventilation", Research Report No. 26, Texas Engineering Experiment Station, June, 1951.

3.9 "Natural Air Flow Around Building", Research Report No. 59, Texas Engineering Experiment Station, March, 1961.

3.10 Wannenburg, J. J. and Van Straaten, J. F., "Wind Tunnel Tests on Scale Model Buildings as a Means for Studying Ventilation and Allied Problems", J. Institution of Ventilating and Heating Engineers, 477-492, March, 1957.

3.11 Hadden, J. D., "The Use of Wind Tunnel Models for Determining the Wind Pressure on Building", Civil Engineering and Public Works Review, Vol. 55, No. 645, April, 1960.

3.12 Jensen, M., "The Model-Law For Phenomena in Natural Wind", INGENIREN, International Edition, Vol. 2, No. 4, November, 1958.

3.13 White, R. F., "Landscape Development and Natural Ventilation, Effect of Moving Air on Buildings and Adjacent Areas", Res. Report No. 45, Texas Engineering Experiment Station, March, 1954.

Section 4

NATURAL VENTILATION ADEQUACY ASSESSMENT TECHNIQUE

To accomplish the ultimate goal of this work unit, i.e., determine the adequacy of natural ventilation for upgraded shelters, the following approach was adopted as a means of performing the adequacy assessment calculations:

1) Determine experimentally the ventilation airflow characteristics of upgraded shelters as a function of such variables as ambient wind speed and direction, shelter configuration and opening pattern, internal flow impedance, etc.
2) Develop a mathematical model, based upon the results of (1) which can be combined with algorithms for performing shelter heat balances to determine resultant daily average shelter effective temperatures on the basis of historical weather.
3) Computerize the adequacy assessment methodology to enable parametric studies for various types of shelters and climatic zones to be done to determine if the 82^{o}F effective temperature and 90% adequacy criteria can be met for a range of occupant densities.

Step 1, as described in Section 3, was performed for a limited sample of simple shelter configurations and limited range of wind speeds and directions. Steps 2 and 3 are described in subsequent portions of this section along with other concepts that form the basis for the adequacy assessment technique.

4.1 Adequacy and Effective Temperature

"Effective temperature" (TEF) is an empirical thermal index which combines the effects of dry-bulb temperature, wet-bulb temperature and air movement to yield equal sensations of warmth or cold to a person. "Adequacy" may be defined as the percentage of time over some given time domain, that the daily average effective temperature of a shelter can be expected to be less than a prescribed limit. The relation between the two can perhaps be better seen through an example.

Let us assume that the shelter configuration, the hourly weather data and the density of occupants are known, and that the resulting average daily effective temperature (TEF) inside the shelter due to varying ambient weather can be plotted against time as shown in Figure 4.1. Also, let TEF_1, TEF_2 and

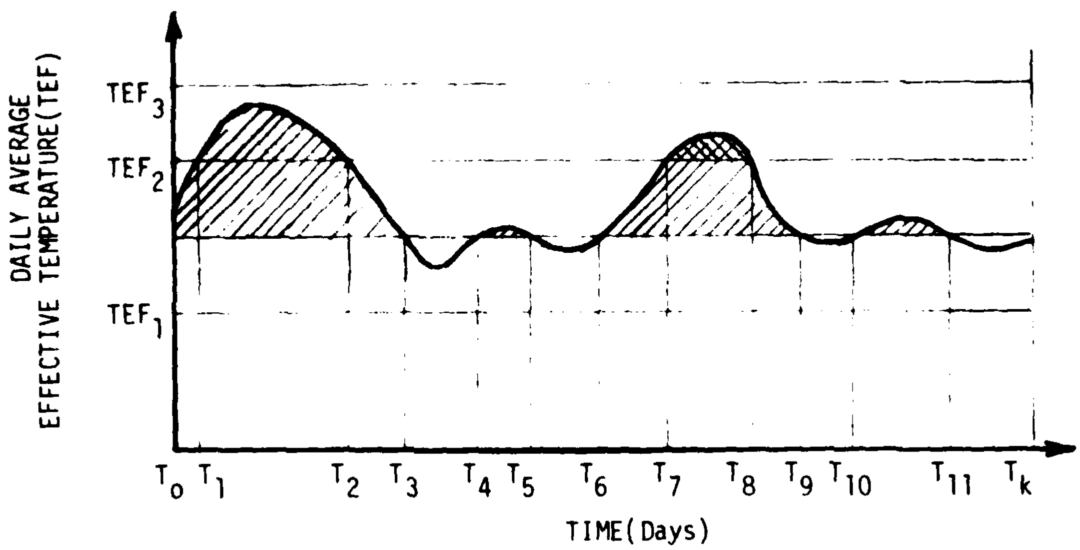

Figure 4.1 VARIATION OF SHELTER DAILY AVERAGE EFFECTIVE TEMPERATURE WITH TIME

GARD, INC.

TEF_3 be the prescribed limits for which it is desired to determine the percentage of time that the shelter was adequately ventilated. For each of these temperature limits, the adequacy (%) is the ratio of the number of days the daily average inside effective temperature TEF is less than the prescribed limit. The diagram indicates therefore that:

1) For TEF_1, the adequacy is zero, since the daily average effective temperature is higher than TEF_1 during the entire period from T_k to T_o.
2) For TEF_2, the adequacy, ADEQ, is equal to

$$ADEQ = \left[1 - \frac{(T_2 - T_1) + (T_8 - T_7)}{(T_k - T_o)}\right] \times 100 \qquad \text{(Eq. 4.1)}$$

3) For TEF_3, the adequacy is equal to 100% since the daily average effective temperatures are always lower than the prescribed limit.

Adequacy, then, may be calculated for a series of effective temperature limits. The result is a relationship like that depicted in Figure 4.2. There will always be effective temperature limits, which if set high enough (TEF_b) or low enough (TEF_a), will result in adequacies of 100% and 0% respectively. For $TEF_a < TEF < TEF_b$, the adequacy will range between zero and 100%. The shape of the curve and the temperature range over which this occurs will be a function of climatic zone, shelter characteristics, occupant densities, etc.

If the effects of various occupant densities and effective temperature limits on adequacy are also to be considered, a family of curves similar to those shown in Figure 4.3 will result. The curve labeled n_1 would represent the unoccupied condition while the curve labeled n_6 would represent the maximum occupant density, which for the purpose of this study is taken to be one person per 5 square feet or 0.2 person per sq. ft. The existance of a relationship like that depicted in Figure 4.3 is the basis of the adequacy assessment technique.

The effective temperature which results inside a shelter depends on many factors, including:

- ventilation air flow rate (L) through the shelter,
- dry-bulb temperature (DBT) and wet-bulb temperature (WBT) of ambient air,
- metabolic heat generation rate of occupants (Q_{occ}),
- heat transferred through the envelope of the structure,

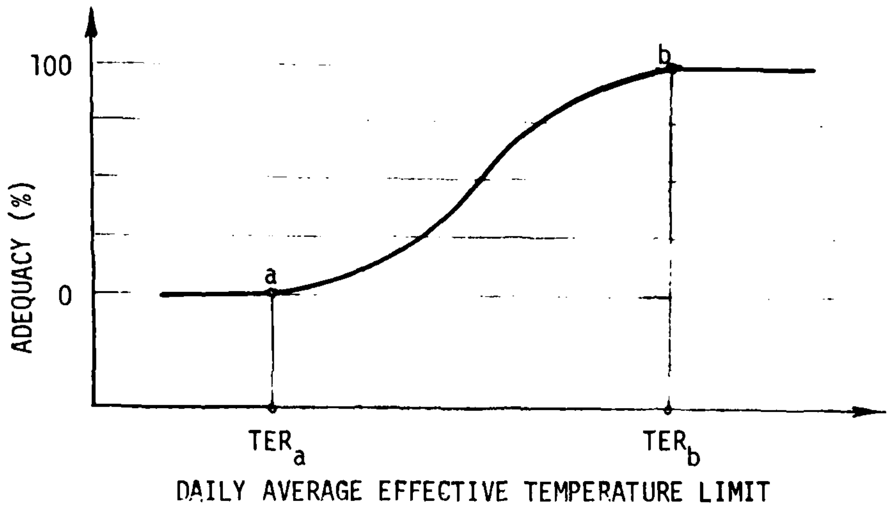

Figure 4.2 TYPICAL RELATIONSHIP BETWEEN ADEQUACY AND SHELTER DAILY AVERAGE EFFECTIVE TEMPERATURE LIMIT

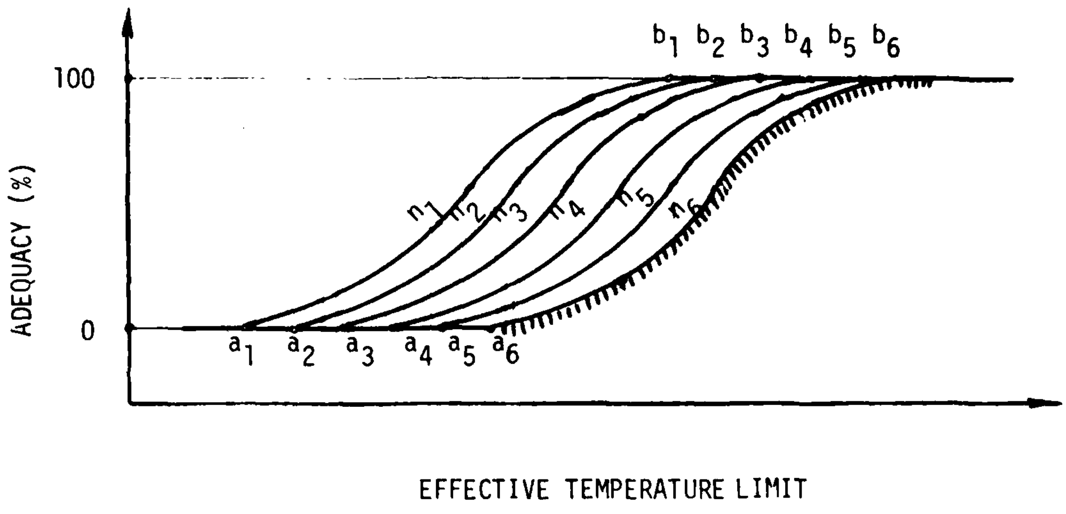

Figure 4.3 TYPICAL RELATIONSHIP BETWEEN OCCUPANT DENSITY AND EFFECTIVE TEMPERATURE LIMIT ON ADEQUACY

GARD, INC.

- additional heat loads like those from direct sun light, electric light bulbs, etc., and
- air flow pattern inside the shelter.

Little is known presently about the construction characteristics of upgraded shelters, and therefore heat transferred through shelter boundaries is assumed steady state and additional internal heat loads other than people, are being ignored. Further, it is assumed that air within the shelter is uniformly distributed such that no air stratification or temperature variation occurs. The shelter effective temperature is then a function of the following:

$$TEF = f(Q_{occ}, L, DBT, WBT) \qquad \text{(Eq. 4.2)}$$

4.2 Occupant Metabolic Heat

The metabolic heat produced by an individual depends on the sex, age and activity level. Average metabolic rates for sedentary activity levels as functions of age and sex for the most recent census of U.S. population are given in the 1978 ASHRAE Applications Handbook (Ref 4.1, Fig. 1, page 12.2). Table 4.1 below was developed using these data.

Table 4.1

Sedentary Metabolic Rates as a Function of Age and Sex

AGE	PERCENT OF POPULATION*		METABOLIC HEAT BTUH	
	MALE	FEMALE	MALE	FEMALE
75 and over	1.5	2.2	310	200
70 to 74	1.1	1.5	320	210
65 to 69	1.5	1.8	350	230
60 to 64	2	2.3	360	235
55 to 59	2.3	2.7	370	240
50 to 54	2.6	2.8	375	245
45 to 49	2.9	3.1	300	250
40 to 44	2.9	3	395	250
35 to 39	2.7	2.9	400	250
30 to 34	2.8	2.9	400	250
25 to 29	3.3	3.3	400	250
20 to 24	3.9	4.2	405	250
15 to 19	4.7	4.6	400	260
10 to 14	5.3	5	275	250
5 to 9	5	4.8	200	200
Under 5	4.3	4.1	150	150
Total	48.8	51.2	-	-

* "Social Indicators," 1973, U. S. Dept. of Commerce

Houghten (Ref. 4.2) derived polynomial expressions for metabolic heat generation that are convenient for computerized calculations and are as follows:

$$\begin{aligned} Q_{occ,\ total} &= a(TEF)^2 + b(TEF) + c \\ Q_{occ,\ sensible} &= A(TEF)^2 + B(TEF) + C \end{aligned} \qquad \text{(Eq. 4.3)}$$

where

1) $a = 0;\ b = -1.482;\ c = 514$, for $50^0 < TEF < 87^0F$
2) $a = -1.508;\ b = 259.7;\ c = -10795.2$, for $87^0 < TEF < 102^0F$
3) $a = 0;\ b = 0;\ c = 0$, for $TEF > 102^0F$
4) $A = -0.06875;\ B = 1.625;\ C = 523$, for $DBT > 50^0F$

and

$$Q_{occ,\ total} = Q_{occ,\ sensible} + Q_{occ,\ latent} \qquad \text{(Eq. 4.4)}$$

The applicability of these equations have been proved for only healthy male subjects in the age group 18-24 years. For this study an "average person" whose metabolic heat rate is the weighted average of that given in Table 4.1 has been created. Using the following relation:

$$Q_{average\ person} = \frac{(\%\ \text{of males}) \times (\text{BTUH male}) + (\%\ \text{of females}) \times (\text{BTUH female})}{100} = 281.32\ \text{BTUH} \qquad \text{(Eq. 4.5)}$$

This is 70% of the value given in the table, for males between 20-24 years. Using these equations and data from ASHRAE Handbook of Fundamentals (Ref. 4.3, page 8-6, Tables 2 and 3), the following equations were generated for calculating occupant metabolic heat:

$$\begin{aligned} Q_{occ,\ total} &= .413 \left[a(TEF)^2 + b(TEF) + c\right] \left[N + 1.091 \sum_{i=1}^{N} V_i^{0.6}\right] \\ Q_{occ,\ sensible} &= .413 \left[A(TEF)^2 + B(TEF) + C\right] \left[N + 1.091 \sum_{i=1}^{N} V_i^{0.6}\right] \end{aligned} \qquad \text{(Eq. 4.6)}$$

where N = number of occupants

V_i = air velocity felt by occupant - i

TEF = effective temperature of shelter air and can be calculated as

$$TEF = \frac{107.5(DBTS) - 45.2(WBTS)}{(DBTS) - (WBTS) + 62.3} \qquad \text{(Eq. 4.7)}$$

where DBTS = dry-bulb temperature of shelter air

WBTS = wet-bulb temperature of shelter air.

4.3 Shelter Heat Balance

A fallout shelter is a volume inclosed by boundaries into which sensible and latent heat loads and ventilating air are introduced and from which air is exhausted and energy is lost, see Figure 4.4. The following assumptions are made:

1) the air within the shelter is completely and instantaneously mixed,
2) the film heat transfer coefficients are constant for any one boundary surface,
3) the radiative energy transfer within the shelter can be neglected,
4) the condition of the air exhausted from the shelter is the condition of the shelter atmosphere,
5) the thermal and physical properties of the structural materials and of air are not temperature-dependent,
6) the incident solar radiation is absorbed on the outer surface of the boundaries and appears as conducted energy or is transmitted into the shelter and is considered an instantaneous load along with other internal loads, and
7) the thermal loads and the psychrometric states of the inlet and exhaust air are constant over short time intervals.

A heat balance of the shelter volume yields the following:

$$\begin{aligned}
\text{SENSIBLE HEAT GAIN} &= Q_{occ,\ sensible} + K \times F \times (DBT - DBTS) \\
\text{LATENT HEAT GAIN} &= Q_{occ,\ latent} \\
\text{SENSIBLE HEAT LOSS} &= 60 \times c_p \times \rho \times L \times (DBTS - DBT) \\
\text{LATENT HEAT LOSS} &= 0.625 \times 10^{-5} \times \rho \times L \times (WS - W)
\end{aligned} \qquad \text{(Eq. 4.8)}$$

Since the shelter must be in thermal equilbirium at the end of each time interval,

HEAT GAIN = HEAT LOSS

Therefore,

$$Q_{occ,\ sensible} = (60 \times c_p \times \rho \times L + K \times F)(DBTS - DBT)$$

$$\text{and } Q_{occ,\ latent} = 0.625 \times 10^{-5} \times \rho \times L\ (WS - W) \qquad \text{(Eq. 4.9)}$$

where ρ = density of leaving air
L = ventilation throughput
K = overall shelter heat transfer coefficient

GARD, INC.

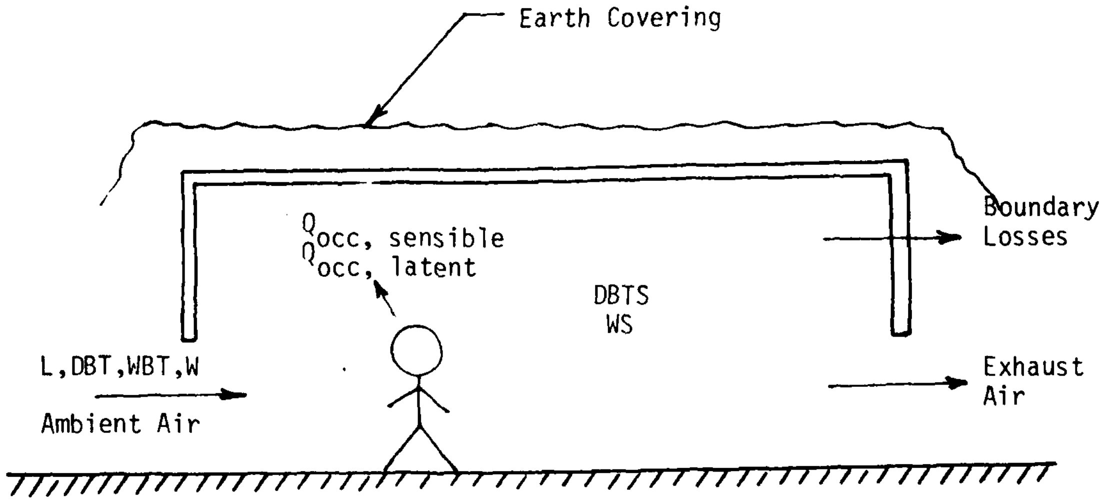

Figure 4.4 TYPICAL HEAT BALANCE REQUIRED FOR SHELTERS

GARD, INC.

F = total external surface area of shelter

WS = humidity ratio of shelter air

W = humidity ratio of outside air

c_p = specific heat of air

Using equations 4.3 through 4.9, one can obtain

$$DBTS = \frac{-(\bar{N} \times B + Z) \pm \sqrt{(\bar{N} \times B - Z)^2 - 4(\bar{N} \times A)\ Z(DBT) + \bar{N} \times C}}{2\ \bar{N} \times A} \quad \text{(Eq. 4.10)}$$

where $Z = 0.000355 \times (PB) \times L + K \times F$

$$\bar{N} = 0.413\ (N + 1.091 \sum_{i=1}^{N} V_i^{.6})$$

and PB = barometric pressure

Once the ventilation throughput rate, L, is established for each time interval, the resulting shelter effective temperature can be calculated for a range of occupant densities using the above equation.

4.4 Ventilation Air Throughput

Two different approaches can be taken in setting up the ventilation air throughput calculation model, i.e., (1) a global approach yielding a single general equation and (2) a differential approach yielding a system of equations, one for each of the openings. The former is preferred and results in a single relationship which can be solved once empirical constants have been determined by scaled model testing.

The variables that affect the ventilation air throughput rate can be identified as,

- building configuration,
- location of openings,
- wind speed and direction,
- area of openings,
- ratio of openings on windward and leeward sides, and
- shelter orientation.

Stack effect is ignored since it is likely to be important only in tall buildings or under no wind conditions.

The ventilation air flow rate (L) may be expressed as (see Appendix B for theoretical derivation):

$$L = m_{(sc,\theta,v)} \times S \times \Sigma Fe \times \sqrt{2gh} \qquad \text{(Eq. 4.11)}$$

where

$m_{(sc,\theta,v)}$ = shelter air resistance coefficient

S = specific area coefficient

ΣF_e = sum of all external wall opening areas

g = gravitational acceleration

h = "pressure head" difference between the windward and leeward sides of the shelter at a "standard" wind velocity and direction for a particular shelter configuration and is assumed to be 0.5 ft. of air

The specific area coefficient, S, is defined as,

$$S = \frac{1}{\sum_{j=2}^{2N} \left[\dfrac{2 - (\beta_{j,L}^2 + \beta_{j,R}^2)}{\alpha_j^2} \right]} \qquad \text{(Eq. 4.12)}$$

$$j = 2,4,6,\ldots,2N$$

$$\alpha_j = \frac{A_j}{\Sigma Fe}$$

A_j = area of j^{th} opening

$$\beta_{j,L} = \frac{A_j}{A_{j-1}}$$

$$\beta_{j,R} = \frac{A_j}{A_{j+1}}$$

where

N = Number of flow resistances between the windward and leeward sides.

The function $m_{(sc,\theta,v)}$ is a function of the shelter configuration (scheme) - sc, the relative wind angle between the wind and the shelter orientation - θ, and the wind velocity -v. The empirical function, m, can only be determined by means of scaled model testing due to its complex nature.

To accomplish this, equation, 4.11 was rearranged as follows.

$$m_{sc,\theta,v} = \frac{L}{S \times (\Sigma Fe) \times \sqrt{2g \times h}} \qquad \text{(Eq. 4.13)}$$

Scaled model testing as described in Section 3 was performed to determine the ventilation air throughput, L, as a function of the shelter scheme, sc, relative wind angle, θ, and wind velocity, v. Coefficients S and ΣFe were calculated from the shelter geometry. The pressure head difference, h, was assumed to be equivalent to 0.5 ft. air. The empirical function, m, was then calculated.

Experimental data was obtained for three shelter schemes at relative wind angles of 0^o, 15^o, 30^o, 45^o and 90^o and for wind velocities of 6-19 feet per second (4-13 mph). The resultant values of m were thus calculated and incorporated into the computerized adequacy assessment model.

4.5 Adequacy Assessment Technique

A computerized adequacy assessment technique was developed to allow quantitative determination of adequacy for a given shelter and occupant loading in a given climatic zone on the basis of historical weather. A computerized methodology also gives the capability of easily performing parametric analysis. A flowchart of the assessment methodology is shown in Figure 4.5. For a specified shelter scheme, shelter orientation, occupant density, and climatic zone, weather data is read periodically from a historical file and the shelter ventilation air throughput rate calculated. A total shelter heat balance is then performed and the resultant shelter effective temperature determined. The resultant daily average effective temperature is tabulated over the period of analysis and the resultant adequacy calculated. The process can be repeated for other densities, orientations and shelter schemes.

Historical weather data from the National Oceanic and Atmospheric Administration is used as a source of hourly data for:

1) dry-bulb temperature
2) wet-bulb temperature
3) wind velocity
4) wind direction
5) barometric pressure
6) cloud cover

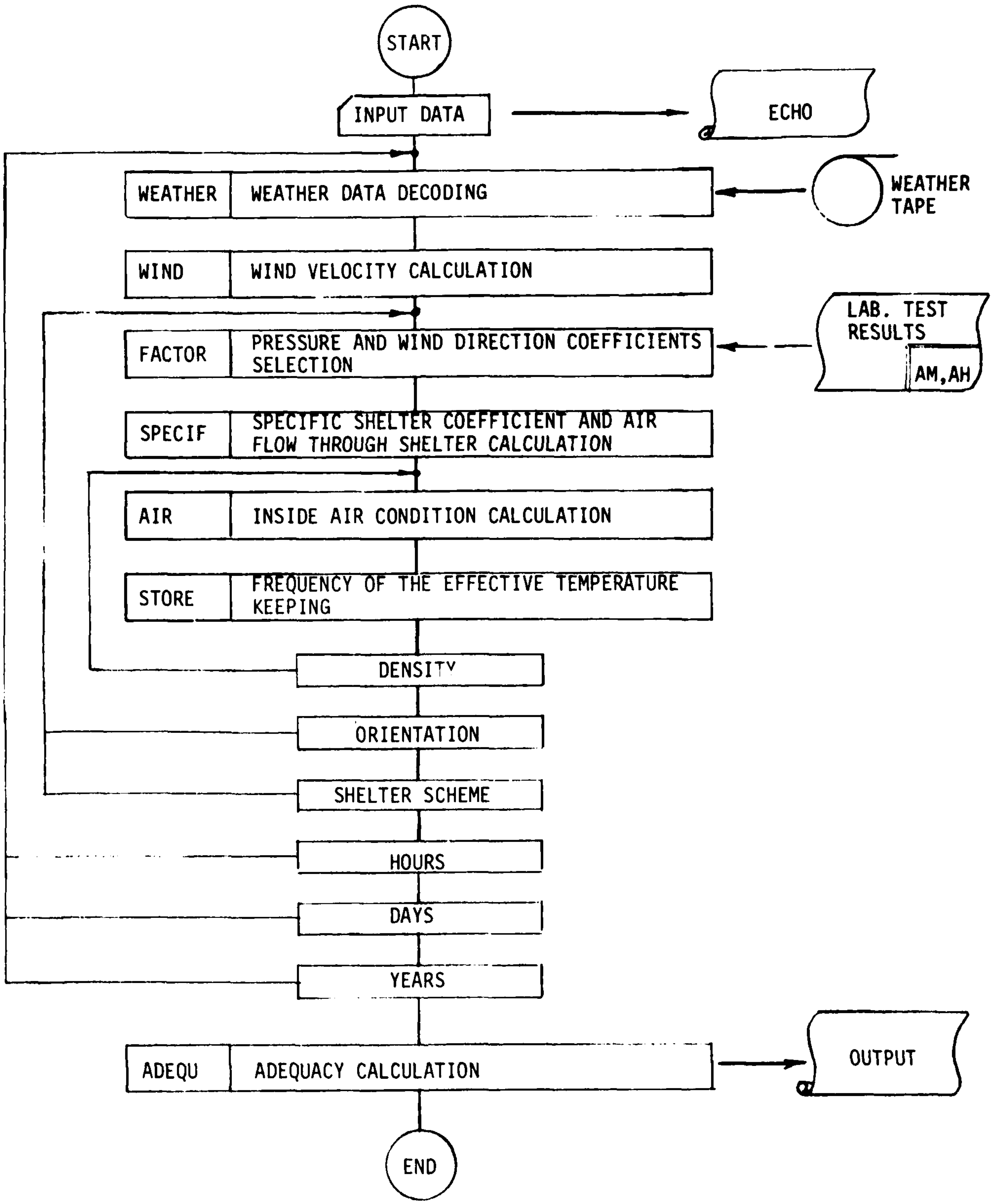

Figure 4.5 FLOWCHART OF NATURAL VENTILATION ASSESSMENT METHODOLOGY PROGRAM

As per FEMA's recommendation, the period of analysis was limited to the 10% hottest days of the year, which it was assumed fell within the period from May 1 through September 30th. Samples of program output reports are shown in Figures 4.6 to 4.10.

To demonstrate the methodology an analysis was performed for Model I described in Section 3, with a southern orientation and two different climatic zones represented by Atlanta, Georgia and Portland, Oregon. The results were as follows:

Table 4.2

OCCUPANT DENSITY AND VENTILATION RATES RESULTING IN 82°F DAILY AVERAGE EFFECTIVE TEMPERATURE AND 90% ADEQUACY FOR MODEL I

LOCATION	MAXIMUM NUMBER OF OCCUPANTS	MAXIMUM OCCUPANT DENSITY (SQ.FT./OCC)	RANGE OF CFM/OCCUPANT	
			MIN.	MAX.
ATLANTA	75	28	21	229
PORTLAND	420	5	4	35

As more extensive model testing is conducted for a wider range of independent variables and shelter characteristics, more confidence can be placed in the results obtained from the adequacy assessment technique.

GARD, INC.

```
                                                      I N P U T    D A T A
GEOGRAPHIC    PARAMETERS =    33.0        84.0       1035.0
YEARS  AND    MONTHS     =     1949     1950       1            5       10       1
DAYS   AND    HOURS      =        1       31       1            0       23       4
ORIENTATION   NUMBERS    =  1  0  0  0  1  0  0  0  1  0  0  0  1  0  0  0
PEOPLE  DENSITY          =      0.0      0.20      0.02
PERIOD OF SUN LOAD       =        30
MIN.DBT                  =      60.8
ELECTRIC HEAT            =       0.0

OPENING AND WALL AREAS
  P1        P2        P3        P4        P5        P6        P7        P8        B0        H
 42.0      42.0       0.0       0.0       0.0       0.0     584.0     774.0       0.0      14.6   SCHEME  1
  0.0       0.0       0.0       0.0       0.0       0.0       0.0       0.0       0.0       0.0   SCHEME  2
  0.0       0.0       0.0       0.0       0.0       0.0       0.0       0.0       0.0       0.0   SCHEME  3
  0.0       0.0       0.0       0.0       0.0       0.0       0.0       0.0       0.0       0.0   SCHEME  4
  0.0       0.0       0.0       0.0       0.0       0.0       0.0       0.0       0.0       0.0   SCHEME  5
  0.0       0.0       0.0       0.0       0.0       0.0       0.0       0.0       0.0       0.0   SCHEME  6
  0.0       0.0       0.0       0.0       0.0       0.0       0.0       0.0       0.0       0.0   SCHEME  7
  0.0       0.0       0.0       0.0       0.0       0.0       0.0       0.0       0.0       0.0   SCHEME  8
  0.0       0.0       0.0       0.0       0.0       0.0       0.0       0.0       0.0       0.0   SCHEME  9
 30.0      42.0      26.0       0.0       0.0       0.0     584.0     774.0       0.0      14.6   SCHEME 10
  0.0       0.0       0.0       0.0       0.0       0.0       0.0       0.0       0.0       0.0   SCHEME 11
 42.0      42.0      62.0      62.0       0.0       0.0     584.0     774.0       0.0      14.6   SCHEME 12
  0.0       0.0       0.0       0.0       0.0       0.0       0.0       0.0       0.0       0.0   SCHEME 13
  0.0       0.0       0.0       0.0       0.0       0.0       0.0       0.0       0.0       0.0   SCHEME 14
  0.0       0.0       0.0       0.0       0.0       0.0       0.0       0.0       0.0       0.0   SCHEME 15
  0.0       0.0       0.0       0.0       0.0       0.0       0.0       0.0       0.0       0.0   SCHEME 16
WEATHER    13874    1949      5          1       0   59.0     59.0   59  2904.0   5.0    68.0        2      10
WEATHER    13874    1949      5          1       4   60.0     59.0   59  2900.0   3.0    90.0        2      10
WEATHER    13874    1949      5          1       8   60.0     60.0   60  2905.0   8.0   135.0        2      10
WEATHER    13874    1949      5          1      12   68.0     65.0   64  2905.0   6.0    90.0        2      10
PERIOD  PREV.HOURS(M=   5,D=  1,H=   8)= 2888   CURR.HOURS= 2892   NEXT.HOURS(M=  5,D=  1,H= 16)= 2896   PERIOD=   4 HOURS
WEATHER    13874    1949      5          1      16   78.0     70.0   66  2898.0   9.0   180.0        2      10
PERIOD  PREV.HOURS(M=   5,D=  1,H=  12)= 2892   CURR.HOURS= 2896   NEXT.HOURS(M=  5,D=  1,H= 20)= 2900   PERIOD=   4 HOURS
WEATHER    13874    1949      5          1      20   61.0     60.0   59  2907.0   3.0   338.0        2      10
PERIOD  PREV.HOURS(M=   5,D=  1,H=  16)= 2896   CURR.HOURS= 2900   NEXT.HOURS(M=  5,D=  2,H=  0)= 2904   PERIOD=   4 HOURS
WEATHER    13874    1949      5          2       0   61.0     60.0   59  2903.0  10.0   112.0        2      10
PERIOD  PREV.HOURS(M=   5,D=  1,H=  20)= 2900   CURR.HOURS= 2904   NEXT.HOURS(M=  5,D=  2,H=  4)= 2908   PERIOD=   4 HOURS
WEATHER    13874    1949      5          2       4   59.0     58.0   58  2905.0   0.3     0.0        2       8
WEATHER    13874    1949      5          2       8   62.0     60.0   60  2909.0   0.3     0.0        2      10
PERIOD  PREV.HOURS(M=   5,D=  2,H=   4)= 2908   CURR.HOURS= 2912   NEXT.HOURS(M=  5,D=  2,H= 12)= 2916   PERIOD=   4 HOURS
WEATHER    13874    1949      5          2      12   74.0     65.0   60  2910.0   0.3     0.0        2      10
PERIOD  PREV.HOURS(M=   5,D=  2,H=   8)= 2912   CURR.HOURS= 2916   NEXT.HOURS(M=  5,D=  2,H= 16)= 2920   PERIOD=   4 HOURS
WEATHER    13874    1949      5          2      16   76.0     66.0   61  2908.0   3.0   225.0        2      10
PERIOD  PREV.HOURS(M=   5,D=  2,H=  12)= 2916   CURR.HOURS= 2920   NEXT.HOURS(M=  5,D=  2,H= 20)= 2924   PERIOD=   4 HOURS
```

Figure 4.6   SAMPLE OF ECHO OF INPUT DATA

EFFECTIVE TEMPERATURE C	22.20	22.75	23.31	23.86	24.42	24.97	25.53	26.08	26.64	27.19	27.75	28.30	28.86	29.41	29.97	30.52	31.08	31.63	32.19
TEMPERATURE F	72.	73.	74.	75.	76.	77.	78.	79.	80.	81.	82.	83.	84.	85.	86.	87.	88.	89.	90.
SHELTER SCHEME NO.10, SPECIFIC COEF.= 0.243, OPENING AREA= 98.00(SQ.FT), ORIENTATION=W ,DENSITY=0.09(PERS/SQ.FT)= 187.PEOPLE																			
NONADEQUACY %	34.13	31.32	27.81	24.55	20.50	16.76	12.83	9.09	6.35	3.90	1.71	0.80	0.16	0.05	0.0	0.0	0.0	0.0	0.0
QMIN CU.M/SEC	.0035	.0035	.0035	.0035	.0045	.0045	.0045	.0045	.0045	.0045	.0045	.0045	.0045	.0067	.0	.0	.0	.0	.0
CU.FT/MIN	7.5	7.5	7.5	7.5	9.5	9.5	9.5	9.5	9.5	9.5	9.5	9.5	9.5	14.3	0.0	0.0	0.0	0.0	0.0
QMAX CU.M/SEC	.0417	.0417	.0417	.0417	.0417	.0417	.0417	.0417	.0366	.0366	.0366	.0366	.0161	.0089	.0	.0	.0	.0	.0
CU.FT/MIN	88.7	88.7	88.7	88.7	88.7	88.7	88.7	88.7	78.0	78.0	78.0	78.0	34.3	19.0	0.0	0.0	0.0	0.0	0.0
SHELTER SCHEME NO.10, SPECIFIC COEF.= 0.243, OPENING AREA= 98.00(SQ.FT), ORIENTATION=W ,DENSITY=0.11(PERS/SQ.FT)= 234.PEOPLE																			
NONADEQUACY %	36.53	33.65	30.84	27.05	23.90	19.66	15.53	11.80	7.92	5.53	2.88	1.12	0.53	0.18	0.0	0.0	0.0	0.0	0.0
QMIN CU.M/SEC	.0028	.0028	.0028	.0028	.0028	.0028	.0036	.0036	.0036	.0036	.0036	.0036	.0036	.0036	.0	.0	.0	.0	.0
CU.FT/MIN	6.0	6.0	6.0	6.0	6.0	6.0	7.6	7.6	7.6	7.6	7.6	7.6	7.6	7.6	0.0	0.0	0.0	0.0	0.0
QMAX CU.M/SEC	.0333	.0333	.0333	.0333	.0333	.0333	.0333	.0333	.0293	.0293	.0293	.0293	.0171	.0071	.0	.0	.0	.0	.0
CU.FT/MIN	70.9	70.9	70.9	70.9	70.9	70.9	70.9	70.9	62.3	62.3	62.3	62.3	36.3	15.2	0.0	0.0	0.0	0.0	0.0
SHELTER SCHEME NO.10, SPECIFIC COEF.= 0.243, OPENING AREA= 98.00(SQ.FT), ORIENTATION=W ,DENSITY=0.13(PERS/SQ.FT)= 281.PEOPLE																			
NONADEQUACY %	37.90	36.05	32.85	29.76	25.96	22.60	18.33	14.34	10.41	7.10	4.36	2.01	0.87	0.43	0.21	0.0	0.0	0.0	0.0
QMIN CU.M/SEC	.0023	.0023	.0023	.0023	.0023	.0023	.0023	.0023	.0030	.0030	.0030	.0030	.0030	.0030	.0030	.0	.0	.0	.0
CU.FT/MIN	5.0	5.0	5.0	5.0	5.0	5.0	5.0	5.0	6.3	6.3	6.3	6.3	6.3	6.3	6.3	0.0	0.0	0.0	0.0
QMAX CU.M/SEC	.0277	.0277	.0277	.0277	.0277	.0277	.0277	.0277	.0244	.0244	.0244	.0244	.0142	.0059	.0059	.0	.0	.0	.0
CU.FT/MIN	59.0	59.0	59.0	59.0	59.0	59.0	59.0	59.0	51.9	51.9	51.9	51.9	30.2	12.7	12.7	0.0	0.0	0.0	0.0
SHELTER SCHEME NO.10, SPECIFIC COEF.= 0.243, OPENING AREA= 98.00(SQ.FT), ORIENTATION=W ,DENSITY=0.15(PERS/SQ.FT)= 328.PEOPLE																			
NONADEQUACY %	39.63	37.42	35.05	32.01	28.36	24.89	21.03	17.08	12.79	8.79	6.07	3.26	1.53	0.64	0.34	0.16	0.0	0.0	0.0
QMIN CU.M/SEC	.0020	.0020	.0020	.0020	.0020	.0020	.0020	.0020	.0020	.0026	.0026	.0026	.0026	.0026	.0026	.0026	.0	.0	.0
CU.FT/MIN	4.3	4.3	4.3	4.3	4.3	4.3	4.3	4.3	4.3	5.4	5.4	5.4	5.4	5.4	5.4	5.4	0.0	0.0	0.0
QMAX CU.M/SEC	.0238	.0238	.0238	.0238	.0238	.0238	.0238	.0238	.0238	.0210	.0210	.0210	.0122	.0092	.0051	.0026	.0	.0	.0
CU.FT/MIN	50.7	50.7	50.7	50.7	50.7	50.7	50.7	50.7	50.7	44.6	44.6	44.6	26.0	19.6	10.9	5.4	0.0	0.0	0.0
SHELTER SCHEME NO.10, SPECIFIC COEF.= 0.243, OPENING AREA= 98.00(SQ.FT), ORIENTATION=W ,DENSITY=0.18(PERS/SQ.FT)= 375.PEOPLE																			
NONADEQUACY %	40.87	38.93	36.69	34.29	30.78	27.03	23.56	19.50	15.39	11.19	7.67	4.79	2.42	1.14	0.59	0.30	0.07	0.02	0.02
QMIN CU.M/SEC	.0022	.0022	.0022	.0022	.0022	.0022	.0022	.0022	.0022	.0022	.0022	.0022	.0022	.0022	.0022	.0022	.0022	.0	.0
CU.FT/MIN	4.8	4.8	4.8	4.8	4.8	4.8	4.8	4.8	4.8	4.8	4.8	4.8	4.8	4.8	4.8	4.8	4.8	0.0	0.0
QMAX CU.M/SEC	.0208	.0208	.0208	.0208	.0208	.0208	.0208	.0208	.0208	.0183	.0183	.0183	.0183	.0081	.0045	.0034	.0022	.0	.0
CU.FT/MIN	44.4	44.4	44.4	44.4	44.4	44.4	44.4	44.4	44.4	39.0	39.0	39.0	39.0	17.1	9.5	7.1	4.8	0.0	0.0
SHELTER SCHEME NO.10, SPECIFIC COEF.= 0.243, OPENING AREA= 98.00(SQ.FT), ORIENTATION=W ,DENSITY=0.20(PERS/SQ.FT)= 422.PEOPLE																			
NONADEQUACY %	41.87	40.02	38.33	35.71	32.83	29.16	25.82	21.85	17.67	13.33	9.29	6.19	3.61	1.94	1.05	0.55	0.27	0.05	0.02
QMIN CU.M/SEC	.0020	.0020	.0020	.0020	.0020	.0020	.0020	.0020	.0020	.0020	.0020	.0020	.0020	.0020	.0020	.0020	.0020	.0020	.0
CU.FT/MIN	4.2	4.2	4.2	4.2	4.2	4.2	4.2	4.2	4.2	4.2	4.2	4.2	4.2	4.2	4.2	4.2	4.2	4.2	0.0
QMAX CU.M/SEC	.0185	.0185	.0185	.0185	.0185	.0185	.0185	.0185	.0185	.0163	.0163	.0163	.0163	.0095	.0040	.0040	.0020	.0020	.0
CU.FT/MIN	39.4	39.4	39.4	39.4	39.4	39.4	39.4	39.4	39.4	34.6	34.6	34.6	34.6	20.2	8.4	8.4	4.2	4.2	0.0
SHELTER SCHEME NO.10, SPECIFIC COEF.= 0.243, OPENING AREA= 98.00(SQ.FT), ORIENTATION=N ,DENSITY=0.0 (PERS/SQ.FT)= 0.PEOPLE																			
NONADEQUACY %	20.78	17.17	14.61	11.53	9.00	6.37	4.61	2.88	1.53	0.50	0.21	0.11	0.0	0.0	0.0	0.0	0.0	0.0	0.0
QMIN CU.M/SEC	.0	.0	.0	.0	.0	.0	.0	.0	.0	.0	.0	.0	.0	.0	.0	.0	.0	.0	.0
CU.FT/MIN	0.0	0.0	0.0	0.0	0.0	0.0	0.0	0.0	0.0	0.0	0.0	0.0	0.0	0.0	0.0	0.0	0.0	0.0	0.0
QMAX CU.M/SEC	.0	.0	.0	.0	.0	.0	.0	.0	.0	.0	.0	.0	.0	.0	.0	.0	.0	.0	.0
CU.FT/MIN	0.0	0.0	0.0	0.0	0.0	0.0	0.0	0.0	0.0	0.0	0.0	0.0	0.0	0.0	0.0	0.0	0.0	0.0	0.0
SHELTER SCHEME NO.10, SPECIFIC COEF.= 0.243, OPENING AREA= 98.00(SQ.FT), ORIENTATION=N ,DENSITY=0.02(PERS/SQ.FT)= 47.PEOPLE																			
NONADEQUACY %	24.79	20.89	17.56	14.52	11.14	8.20	6.03	4.02	2.33	0.89	0.34	0.11	0.0	0.0	0.0	0.0	0.0	0.0	0.0
QMIN CU.M/SEC	.0182	.0182	.0182	.0182	.0182	.0182	.0182	.0182	.0182	.0182	.0182	.0449	.0	.0	.0	.0	.0	.0	.0
CU.FT/MIN	38.7	38.7	38.7	38.7	38.7	38.7	38.7	38.7	38.7	38.7	38.7	95.6	0.0	0.0	0.0	0.0	0.0	0.0	0.0
QMAX CU.M/SEC	.1695	.1695	.1695	.1695	.1695	.1695	.1298	.1298	.1133	.1133	.1133	.1133	.0	.0	.0	.0	.0	.0	.0
CU.FT/MIN	360.6	360.6	360.6	360.6	360.6	360.6	276.2	276.2	241.1	241.1	241.1	241.1	0.0	0.0	0.0	0.0	0.0	0.0	0.0
SHELTER SCHEME NO.10, SPECIFIC COEF.= 0.243, OPENING AREA= 98.00(SQ.FT), ORIENTATION=N ,DENSITY=0.04(PERS/SQ.FT)= 94.PEOPLE																			
NONADEQUACY %	28.76	25.05	21.35	17.67	14.20	10.55	7.72	5.37	3.47	1.58	0.55	0.21	0.0	0.0	0.0	0.0	0.0	0.0	0.0
QMIN CU.M/SEC	.0090	.0090	.0090	.0090	.0090	.0090	.0090	.0090	.0090	.0090	.0090	.0090	.0	.0	.0	.0	.0	.0	.0
CU.FT/MIN	19.1	19.1	19.1	19.1	19.1	19.1	19.1	19.1	19.1	19.1	19.1	19.1	0.0	0.0	0.0	0.0	0.0	0.0	0.0
QMAX CU.M/SEC	.0838	.0838	.0838	.0838	.0838	.0838	.0642	.0642	.0642	.0560	.0560	.0560	.0	.0	.0	.0	.0	.0	.0
CU.FT/MIN	178.4	178.4	178.4	178.4	178.4	178.4	136.6	136.6	136.6	119.3	119.3	119.3	0.0	0.0	0.0	0.0	0.0	0.0	0.0

QMIN AND QMAX ARE GIVEN PER ONE OCCUPANT

Figure 4.7 SAMPLE OF DETAILED RESULTS

MAXIMUM NUMBER OF PEOPLE IN THE SHELTERS

WITH 82 F EFFECTIVE TEMPERATURE AND 90% ADEQUACY WEATHER CONDITIONS

NO. OF SCHEME	O R I E N T A T I O N															
	S	SSW	SW	WSW	W	WNW	NW	NNW	N	NNE	NE	ENE	E	ESE	SE	SSE
1	35	0	0	0	220	0	0	0	35	0	0	0	220	0	0	0
2	0	0	0	0	0	0	0	0	0	0	0	0	0	0	0	0
3	0	0	0	0	0	0	0	0	0	0	0	0	0	0	0	0
4	0	0	0	0	0	0	0	0	0	0	0	0	0	0	0	0
5	0	0	0	0	0	0	0	0	0	0	0	0	0	0	0	0
6	0	0	0	0	0	0	0	0	0	0	0	0	0	0	0	0
7	0	0	0	0	0	0	0	0	0	0	0	0	0	0	0	0
8	0	0	0	0	0	0	0	0	0	0	0	0	0	0	0	0
9	0	0	0	0	0	0	0	0	0	0	0	0	0	0	0	0
10	421	0	0	0	421	0	0	0	421	0	0	0	421	0	0	0
11	0	0	0	0	0	0	0	0	0	0	0	0	0	0	0	0
12	421	0	0	0	421	0	0	0	421	0	0	0	421	0	0	0
13	0	0	0	0	0	0	0	0	0	0	0	0	0	0	0	0
14	0	0	0	0	0	0	0	0	0	0	0	0	0	0	0	0
15	0	0	0	0	0	0	0	0	0	0	0	0	0	0	0	0
16	0	0	0	0	0	0	0	0	0	0	0	0	0	0	0	0

Figure 4.8 SAMPLE OF SUMMARY OF MAXIMUM OCCUPANT DENSITIES

MINIMUM AIR FLOW PER PERSON IN THE SHELTERS
WITH 82 F EFFECTIVE TEMPERATURE AND 80% ADEQUACY WEATHER CONDITIONS

NO. OF SCHEME	S	SSW	SW	WSW	W	WNW	NW	NNW	N	NNE	NE	ENE	E	ESE	SE	SSE
	ORIENTATION															
1	29.1	0.0	0.0	0.0	6.6	0.0	0.0	0.0	29.1	0.0	0.0	0.0	6.6	0.0	0.0	0.0
2	0.0	0.0	0.0	0.0	0.0	0.0	0.0	0.0	0.0	0.0	0.0	0.0	0.0	0.0	0.0	0.0
3	0.0	0.0	0.0	0.0	0.0	0.0	0.0	0.0	0.0	0.0	0.0	0.0	0.0	0.0	0.0	0.0
4	0.0	0.0	0.0	0.0	0.0	0.0	0.0	0.0	0.0	0.0	0.0	0.0	0.0	0.0	0.0	0.0
5	0.0	0.0	0.0	0.0	0.0	0.0	0.0	0.0	0.0	0.0	0.0	0.0	0.0	0.0	0.0	0.0
6	0.0	0.0	0.0	0.0	0.0	0.0	0.0	0.0	0.0	0.0	0.0	0.0	0.0	0.0	0.0	0.0
7	0.0	0.0	0.0	0.0	0.0	0.0	0.0	0.0	0.0	0.0	0.0	0.0	0.0	0.0	0.0	0.0
8	0.0	0.0	0.0	0.0	0.0	0.0	0.0	0.0	0.0	0.0	0.0	0.0	0.0	0.0	0.0	0.0
9	0.0	0.0	0.0	0.0	0.0	0.0	0.0	0.0	0.0	0.0	0.0	0.0	0.0	0.0	0.0	0.0
10	4.2	0.0	0.0	0.0	4.2	0.0	0.0	0.0	4.2	0.0	0.0	0.0	4.2	0.0	0.0	0.0
11	0.0	0.0	0.0	0.0	0.0	0.0	0.0	0.0	0.0	0.0	0.0	0.0	0.0	0.0	0.0	0.0
12	7.4	0.0	0.0	0.0	7.4	0.0	0.0	0.0	7.4	0.0	0.0	0.0	7.4	0.0	0.0	0.0
13	0.0	0.0	0.0	0.0	0.0	0.0	0.0	0.0	0.0	0.0	0.0	0.0	0.0	0.0	0.0	0.0
14	0.0	0.0	0.0	0.0	0.0	0.0	0.0	0.0	0.0	0.0	0.0	0.0	0.0	0.0	0.0	0.0
15	0.0	0.0	0.0	0.0	0.0	0.0	0.0	0.0	0.0	0.0	0.0	0.0	0.0	0.0	0.0	0.0
16	0.0	0.0	0.0	0.0	0.0	0.0	0.0	0.0	0.0	0.0	0.0	0.0	0.0	0.0	0.0	0.0

Figure 4.9 SAMPLE OF SUMMARY OF MAXIMUM AIRFLOW PER OCCUPANT

MAXIMUM AIR FLOW PER PERSON IN THE SHELTERS

WITH 82 F EFFECTIVE TEMPERATURE AND 80% ADEQUACY WEATHER CONDITIONS

NO. OF SCHEME	S	SSW	SW	WSW	W	WNW	NW	NNW	N	NNE	NE	ENE	E	ESE	SE	SSE
	ORIENTATION															
1	200.5	0.0	0.0	0.0	55.5	0.0	0.0	0.0	200.5	0.0	0.0	0.0	55.5	0.0	0.0	0.0
2	0.0	0.0	0.0	0.0	0.0	0.0	0.0	0.0	0.0	0.0	0.0	0.0	0.0	0.0	0.0	0.0
3	0.0	0.0	0.0	0.0	0.0	0.0	0.0	0.0	0.0	0.0	0.0	0.0	0.0	0.0	0.0	0.0
4	0.0	0.0	0.0	0.0	0.0	0.0	0.0	0.0	0.0	0.0	0.0	0.0	0.0	0.0	0.0	0.0
5	0.0	0.0	0.0	0.0	0.0	0.0	0.0	0.0	0.0	0.0	0.0	0.0	0.0	0.0	0.0	0.0
6	0.0	0.0	0.0	0.0	0.0	0.0	0.0	0.0	0.0	0.0	0.0	0.0	0.0	0.0	0.0	0.0
7	0.0	0.0	0.0	0.0	0.0	0.0	0.0	0.0	0.0	0.0	0.0	0.0	0.0	0.0	0.0	0.0
8	0.0	0.0	0.0	0.0	0.0	0.0	0.0	0.0	0.0	0.0	0.0	0.0	0.0	0.0	0.0	0.0
9	0.0	0.0	0.0	0.0	0.0	0.0	0.0	0.0	0.0	0.0	0.0	0.0	0.0	0.0	0.0	0.0
10	39.4	0.0	0.0	0.0	34.6	0.0	0.0	0.0	26.3	0.0	0.0	0.0	26.3	0.0	0.0	0.0
11	0.0	0.0	0.0	0.0	0.0	0.0	0.0	0.0	0.0	0.0	0.0	0.0	0.0	0.0	0.0	0.0
12	79.5	0.0	0.0	0.0	79.5	0.0	0.0	0.0	79.5	0.0	0.0	0.0	79.5	0.0	0.0	0.0
13	0.0	0.0	0.0	0.0	0.0	0.0	0.0	0.0	0.0	0.0	0.0	0.0	0.0	0.0	0.0	0.0
14	0.0	0.0	0.0	0.0	0.0	0.0	0.0	0.0	0.0	0.0	0.0	0.0	0.0	0.0	0.0	0.0
15	0.0	0.0	0.0	0.0	0.0	0.0	0.0	0.0	0.0	0.0	0.0	0.0	0.0	0.0	0.0	0.0
16	0.0	0.0	0.0	0.0	0.0	0.0	0.0	0.0	0.0	0.0	0.0	0.0	0.0	0.0	0.0	0.0

Figure 4.10 SAMPLE OF SUMMARY OF MINIMUM AIRFLOW PER OCCUPANT

References for Section 4

4.1 ASHRAE Applications Handbook, Chapter 12, "Environmental Control For Survival", 1978.

4.2 Houghten, F. C., "Heat and Moisture Losses From The Human Body and Their Relation To Air Conditioning Problems", ASHVE, Transactions, Vol. 35, 1929.

4.3 ASHRAE Handbook of Fundamentals, Chapter 8, "Physiological Principles, Comfort and Health", 1977.

Section 5

CONCLUSIONS AND RECOMMENDATIONS

During this experimental and analytical program, the following was achieved:

1) a specially designed low speed wind tunnel suitable for scaled model testing of buildings was constructed and photographic measurement techniques developed which utilized flow tracing of neutrally buoyant bubbles through models
2) The scaled model testing of three upgraded shelter configurations was completed establishing the ventilation air throughput rate as a function of wind speed and direction.
3) An analytical flow model was developed based upon the experimental results and was incorporated into a computerized natural ventilation adequacy assessment technique.

It is understood that the air throughput rate is a complex function of many independent variables including such dominant ones as wind speed and direction; height, width and length of the building; areas and locations of openings and internal resistances. Certain of these have been carefully controlled over a range of consideration and the resulting data is summarized in Table 5.1. These projections are made based upon an assumed occupant density of 10 sq. ft. per person and wind speeds in excess of 5 mph (7.3 FPS). Extrapolation of the results to wind speeds lower than 5 mph is not adviseable due to the non-linearity that may exist in this range and the presence of other dominant effects not yet considered.

The results summarized in Table 5.1 are very encouraging in the light of data reported by FEMA (Ref. 5.1) where the per capita rate of ventilation required to maintain an effective temperature of 82°F in an occupied space with 90% adequacy during a normal year is shown to range from 7.5 to 40 CFM per person depending upon climatic area in the U.S. All but the southeast portion of the U.S. can be satisfied with a rate as low as 20 CFM per person. Before these results can be accepted with confidence however, the effects of other factors, such as:

1) internal flow resistances including partition walls and occupants,
2) areas and locations of openings in walls,
3) wider selection of wind approach angles, and

4) wind speeds less than 5 mph

should be studied so that their effects can be factored into the overall results. The existing test apparatus provides the capability to test these parameters in great enough detail and range to allow accurate predictions and meaningful recommendations to be made with respect to ventilation of shelter buildings.

The test results also indicated an interesting effect that bermed openings have on the flow characteristics of upgraded shelters, i.e., larger shelter throughput rates are experienced when the wind approaches the openings at angles other than normal to the opening (see results for models I, II and III at 45^0). This effect should be studied in greater depth and recommendations developed as to how the berm should be configured in the neighborhood of doors and windows to give best overall shelter throughput rates.

In conclusion, this study had indicated that for upgraded shelters, ventilation rates due to wind forces are sizeable, even at low wind speeds, and with the proper opening area and location can very probably be relied upon to meet the 82^0F effective temperature and 90% adequacy criteria. Further research is necessary however, before the natural ventilation characteristics of upgraded shelters are fully understood.

AD-A087 676   GARD INC   NILES ILL   F/G 20/4
ADEQUACY OF WIND VENTILATION IN UPGRADED SHELTERS.(U)
MAY 80   R H HENNINGER, R J TSAL   DCPA01-78-C-0319
UNCLASSIFIED   GARD-A1-11 (1713)   NL

2 2

END
DATE
FILMED
9 80
DTIC

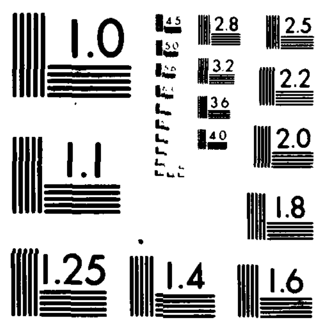

MICROCOPY RESOLUTION TEST CHART
NATIONAL BUREAU OF STANDARDS 1963 A

TABLE 5.1

ESTIMATED VENTILATION FLOWS RATES ACHIEVEABLE WITH NATURAL VENTILATION BASED ON SCALED MODEL TESTS FOR WIND SPEEDS IN EXCESS OF 5 mph AND OCCUPANT DENSITY OF 10 SQ. FT. PER PERSON

SHELTER	FLOOR AREA (SQ.FT.)	OPENING CONFIGURATION	TOTAL OPENING AREA (SQ.FT.)	VENTILATION RATE (CFM/OCC)		
				0^{o}	45^{o}	90^{o}
I	2120	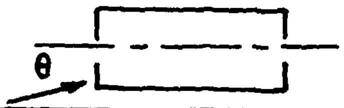	84	41	44	0
II	2120	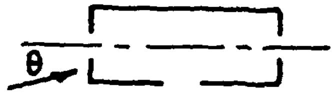	146	46	52	75
III	2120	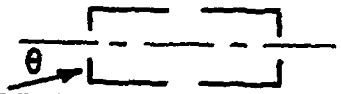	208	50	103	102

REFERENCES FOR SECTION 5

5.1 ASHRAE Applications Handbook, Chapter 12, "Environmental Control For Survival", Figure 13, pg. 12.13, 1978.

APPENDIX A

SUMMARY OF MATHEMATICAL MODELS TAKEN FROM REFERENCES IN SECTION 2

SOURCE, YEAR	WIND PROFILE	WIND DIRECTION	WIND (W) AND/OR THERMO (T) FORCES	COMMENTS
ASHRAE Ref. 2.1, 1977	$P_{STATIC} = K \times P_v$ k = 0.5 to 0.9 -windward k = 0.3 to 0.6 -leeward		$Q_W = EAV$ $Q_T = 9.4 \times A\sqrt{h(t_i - t_o)}$ $P_T = 0.52(NPL)\left(\frac{1}{T_o} - \frac{1}{T_i}\right)$ $NPL = \frac{H}{1+\left[\left(\frac{A_1}{A_2}\right)^2\left(\frac{T_o}{T_i}\right)\right]}$	V - Wind Velocity
Randall Ref. 2.6, 1977		$Q = f(\theta)$	$Q_T = 60\sqrt{\frac{M(\Delta T)}{2R\,T_{INSIDE}}}$	Θ = Angle of Wind M= Distance T =Temperature Difference
Emswiler Ref.2.7, 1930		$\Delta p_W = f(V,\theta)$ is the table function		4-floor building
Bailey Ref.2.8, 1943	$\frac{V_H}{V_{10}} = K\left\{1 + 2.81\log(H + 4.7)\right\}$ $K = 0.2337$			
Dick, Thomas Ref.2.10, 1950			$Q_W = A + BW + (C + DW)(n + 1.4m)$ $Q_T = (C + Dn)\sqrt{\Delta T}$ FOR $\frac{V^2}{\Delta T} < 14$	28 homes
Macksimov Ref.2.13, 1955	$P_{STATIC} = K\frac{V^2\gamma}{2g}$ $K = 0.6$ for windward $K = -0.3$ for leeward		$G_{WT} = \mu F\sqrt{2g\gamma c(V_T^2 - V_K^2)}$	

SOURCE, YEAR	WIND PROFILE	WIND DIRECTION	WIND (W) AND/OR THERMO (T) FORCES	COMMENTS
Bahnfleth Mosley, Harris Ref. 2.15, 1957			$Q_{WT} = A + BV + C(\Delta T)$	2 research houses
Haddon Ref. 2.17, 1960	$\frac{M}{M_1} = \left(\frac{Z}{Z_1}\right)^{\frac{n}{2-n}}$ $n = 0.2$			M/M1 - window areas ratio Z/Z1 - height ratio
Tamura, Wilson Ref. 2.19, 1963			$Q_{WT} = f(V, \Delta T) +$ $Q_{WT} \neq AV_{\Delta T=0} + B(\Delta T)_{W=0}$	2 houses, Low summer wind velocity.
Konstantinova Ref. 2.20, 1969	P = f (Wind High) -draw function for suburban area		$P_W = A_1 C_W + A_2 G_W^2$ $Q_W = \frac{-S + \sqrt{S^2 + 4pT'}}{2T'}$ $T' = B\left(\frac{1}{F_o^2 \gamma_o^2} + \frac{1}{F_i^2 \gamma_i^2}\right) + 2\varphi$ $P_T = \Delta\gamma \times \Delta L\ ;\ P_{FAN} = D_0 + D_1 G + D_2 G^2$ $Q_T = \frac{-D + \sqrt{D^2 + 4pNF^2\gamma^2}}{2NF\gamma}$ $N = \frac{B}{F^2\gamma^2} + \varphi$ $\varphi = \frac{\Sigma \zeta}{2g \cdot 3600^2 F^2 \gamma}$	
Laschober, Healy Ref. 2.21, 1964		$V_L = V \times \cos\alpha$	$Q_{WT} = A + BV_L + C(\Delta T)$	α = angle between wind direction and normal to the wall.

SOURCE, YEAR	WIND PROFILE	WIND DIRECTION	WIND (W) AND/OR THERMO (T) FORCES	COMMENTS
King Ref. 2.24, 1959			$Q_W = EAV$	Underground Shelters
Baturin Ref. 2.25, 1965		$V = f(\theta)$ Table Functions	$\sum \mu_i F_i \sqrt{P_i(L) - P_x(L)} = \frac{2a\sqrt{(P_i - P_o)^3}}{3(\gamma_o - \gamma_i)}$	Industrial Buildings
Howard Ref. 2.28, 1966			$Q_{WT} = f($wind velocity, chimney openings$)$	
Lokmanhekim, Rathmann, Baschiere Ref. 2.29, 1967			$Q_W = (1 + \beta) EAV$	B = coefficient which describes inlet/outlet opening area ratio
Henninger Ref. 2.33, 1968		$\frac{Q}{AV} = C_\perp (S_\perp)^m + [C_\parallel \times (S_\parallel)^n - C_\perp (S)^m] \cdot \sin\theta$	$Q_W = (1 + \beta) EAV$	
Elkins, Hensman Ref. 2.39, 1971			$Q_W = (A - B \cdot \theta) V$	2 houses
Sander Ref. 2.42, 1974	V = f (wind velocity profile with ground effect)		$Q_W = EA(\Delta P)^x$ $Q_T = f($stack effect, air handling system$)$	Computer Program
Hittman Ref. 2.44, 1975			$Q_{WT} = A + BV + C(\Delta T)$	

SOURCE, YEAR	WIND PROFILE	WIND DIRECTION	WIND (W) AND/OR THERMO (T) FORCES	COMMENTS
Sepsy, Jones, McBride, Blancett Ref. 2.50, 1977		$SF = 0.75 + 0.25(2(\theta-\theta$	$Q_{WT} = \beta_0 C_T \sqrt{4\Delta P_T + \sqrt{2} \times \Delta p_W} + \beta_1(\text{open door factor})V + \beta_2(\text{exhaust fan factor}) + \beta_3(\text{combustion, factor}) + \sum_i (B_i C_i + M_i)$ $\Delta p_T = A p h\left(\frac{1}{T_o} - \frac{1}{T_i}\right)$ $\Delta p_W = \frac{\beta}{T_o} + V^2$	SF = Shape Factor 9 residences
Shaw, Tamura Ref. 2.51, 1977	$V_z = K Z^{0.23}$		$Q_W = c(\Delta p)^n$ $Q_{WT} = Q_L\left(1 + 0.24\frac{Q_S}{Q_L}\right)^{3.3}$ $Q_L = MAX(Q_{W,O}; Q_{O,\Delta T}),\ Q_S = MIN(Q_{W,O}; Q_{O,\Delta T})$	Z = height above ground Tall Buildings
Malik Ref. 2.52, 1977			$Q_{WT} = A + BV\lvert\cos(\theta - \theta_o)\rvert + C\Delta T + DG + EB + FK$	G = gas consumption B = time the basement door is open F = the same of front door For townhouse
Konrad, Larsen Ref. 2.54, 1978	$V_z = f(V_{STATION})$	$V = f(\theta)$	$G_{WT_j} = S_r(R_j)^{-n_j}\left[p + \frac{P}{R}\left(\frac{C_j V^2}{2T_o} + g h_j\left(\frac{1}{T_i} - \frac{1}{T_o}\right)\right) - p_1\right]^{-n_j} + f($	Computer Program for small residential buildings
Shaw Ref. 2.61, 1979	$V = KZ^{0.43}$	$\alpha_o = \beta_{o1}^{0.65} + \frac{W}{L}\beta_{o2}^{0.65}$ $\alpha_{SH} = 1.15\exp(-0.85\frac{h}{H})$	$Q_W = C_j A_j (\Delta p_j)^{0.65}$ $Q_W = 0.036\, C_W A_1 H^{0.56} V^{1.3}$	Z = height above ground α_o = direction angle α_{Sh} = Shielding A = Area

SOURCE, YEAR	WIND PROFILE	WIND DIRECTION	WIND (W) AND/OR THERMO (T) FORCES	COMMENTS
Tamura Ref. 2.62, 1979	$V_{HOUSE} = \alpha V_{STATION}$ α = FROM 0.56 TO 0.65		$Q_W = C_W A_W (\Delta p)^n$ $A_W = \frac{A_W}{3}\left(\frac{a}{f}\right)$	a= length of front wall f= length of side wall
Hayakawa, Togari, Hioki Ref. 2.55, 1978			$Q_{WT} = 0.22\,\Delta p^{-n} + f$(stack effect) + f(air handling system)	Computer Program. Large Buildings, Open Windows
Reeves, McBride, Sepsy Ref. 2.59, 1979			$Q_{WT} = \beta C_T \left(A(\Delta p)_T + B(\Delta p)_W\right)^{0.5}$	

APPENDIX B

VENTILATION THROUGHPUT CALCULATION MODEL

Appendix B

VENTILATION THROUGHPUT CALCULATION MODEL

Figure B.1 illustrates the application of Bernoulli's equation to the air flow through a shelter. A_j is the flow area and V_j the flow velocity at Section j of the air stream that eventually passes through the shelter. Applying Bernoulli's equation between Sections 1 and 2, we obtain,

$$\frac{P_j - P_{j+1}}{\gamma} - H = \frac{V_{j+1}^2 - V_j^2}{2g} = h_j$$

where, p_j and P_{j+1} are the static pressures

γ the air density

and H the irrecoverable pressure head loss.

Using mass conservation,

$$V_j A_j = V_{j+1} A_{j+1}$$

Therefore, $h_j = \frac{V_{j+1}^2}{2g}\left[1 - \left(\frac{A_{j+1}}{A_j}\right)^2\right]$

and $$L_j = L_{j+1} = A_{j+1}V_{j+1} = A_{j+1}\sqrt{\frac{2gh_j}{1 - \left(\frac{A_{j+1}}{A_j}\right)^2}} \qquad \text{(Eq. B.1)}$$

Denoting the smaller of the two flow areas A_j by A_s and the larger area by A_ℓ, one gets

$$L = A_s\sqrt{\frac{2gh_x}{1 - \left(\frac{A_s}{A_\ell}\right)^2}} = C_x\sqrt{2gh_x} \qquad \text{(Eq. B.2)}$$

Here, h_x is the velocity head difference between the two sections, and

$$C_x = A_s\sqrt{\frac{1}{1 - \left(\frac{A_s}{A_\ell}\right)^2}} = \frac{A_s \times A_\ell}{\sqrt{A_\ell^2 - A_s^2}} \qquad \text{(Eq. B.3)}$$

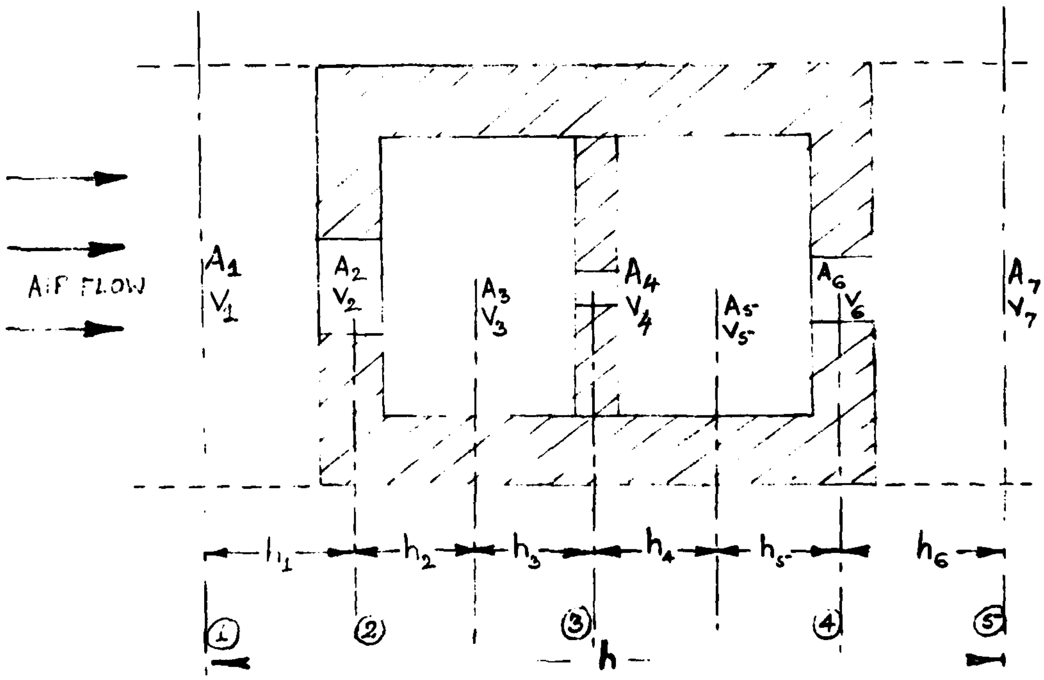
AIR FLOW
A1
V1
A2
V2
A3
V3
A4
V4
A5
V5
A6
V6
A7
V7
h1
h2
h3
h4
h5
h6
1
2
3
4
5
h

Figure B.1

Referring to Figure B.1 for flow between sections 1 and 2,

$$C_1 = \frac{A_2 \times A_1}{\sqrt{A_1^2 - A_2^2}} \qquad \text{and} \qquad L_1 = L = C_1\sqrt{2gh_1}$$

If h is the velocity head difference between sections 1 and 7,

$$h = \frac{V_7^2 - V_1^2}{2g} = \frac{V_7^2 - V_6^2}{2g} + \frac{V_6^2 - V_5^2}{2g} + \frac{V_5^2 - V_4^2}{2g} + \frac{V_4^2 - V_3^2}{2g} + \frac{V_3^2 - V_2^2}{2g} + \frac{V_2^2 - V_1^2}{2g}$$

i.e., $h = h_6 + h_5 + h_4 + h_3 + h_2 + h_1$.

From continuity,

$$C_1\sqrt{h_1} = C_2\sqrt{h_2} = C_3\sqrt{h_3} = C_4\sqrt{h_4} = C_5\sqrt{h_5} = C_6\sqrt{h_6}$$

$$h_2 = h_1\left(\frac{C_1}{C_2}\right)^2 \; ; \quad h_3 = h_1\left(\frac{C_1}{C_3}\right)^2 \; ; \quad h_4 = h_1\left(\frac{C_1}{C_4}\right)^2 \; ; \quad h_5 = h_1\left(\frac{C_1}{C_5}\right)^2 \; ;$$

and $h_6 = h_1\left(\frac{C_1}{C_6}\right)^2$

we get, $h = h_1\left[\left(\frac{C_1}{C_1}\right)^2 + \left(\frac{C_1}{C_2}\right)^2 + \left(\frac{C_1}{C_3}\right)^2 + \left(\frac{C_1}{C_4}\right)^2 + \left(\frac{C_1}{C_5}\right)^2 + \left(\frac{C_1}{C_6}\right)^2\right]$

In general, $h = h_x C_x^2 \sum_{i=1}^{2N} \frac{1}{C_i^2}$ (Eq. B.4)

$$h_x = \frac{h}{C_x^2} \times \frac{1}{\sum_{i=1}^{2N} \frac{1}{C_i^2}}$$

where N = number of flow resistances, 3 in Figure 4.4,

$$L = L_x = C_x\sqrt{2gh_x} = \frac{\sqrt{2gh}}{\sqrt{\sum_{i=1}^{2N} \frac{1}{C_i^2}}}$$

GARD, INC.

i.e., $$L = \frac{\sqrt{2gh}}{\sqrt{\sum_{i=1}^{2N} \frac{1}{C_i^2}}} \qquad \text{(Eq. B.5)}$$

We shall now show that the specific area coefficient S, defined by Equation 4. , can be expressed in terms of the orifice coefficient C_j as,

$$S \times \Sigma Fe = \frac{1}{\sum_{i=1}^{2N} \frac{1}{C_i^2}} \quad , i = 1,2,\ldots,2N$$

From 4. ,

$$S = \frac{1}{\sqrt{\sum_{j=2}^{2N} \left[\frac{2 - (\beta_{j,L}^2 + \beta_{j,R}^2)}{\alpha_j^2} \right]}} \quad , j = 2,4,\ldots,2N$$

$$\alpha_j = \frac{A_j}{\Sigma Fe} \quad , \text{ Referring to Figure B.1,}$$

$$\alpha_2 = \frac{A_2}{\Sigma Fe} \quad , \therefore \; A_2 = \alpha_2 \, \Sigma Fe \qquad \text{(Eq. B.6)}$$

$$\alpha_4 = \frac{A_4}{\Sigma Fe} \quad , \therefore \; A_4 = \alpha_4 \, \Sigma Fe \qquad \text{(Eq. B.7)}$$

and $$\alpha_6 = \frac{A_6}{\Sigma Fe} \quad , \therefore \; A_6 = \alpha_6 \, \Sigma Fe \qquad \text{(Eq. B.8)}$$

Also $A_6 = \Sigma Fe - A_2 = \Sigma Fe(1 - \alpha_2)$

$$\therefore \; \alpha_6 = 1 - \alpha_2 \qquad \text{(Eq. B.9)}$$

We also had,

$$\beta_{j,L} = \frac{A_j}{A_{j-1}} \quad \text{and} \quad \beta_{j,R} = \frac{A_j}{A_{j+1}} \quad , \quad j = 2,4,\ldots,2N$$

$$\beta_{2,L} = \frac{A_2}{A_1} = \frac{\Sigma Fe\alpha_2}{A_1} \quad ; \quad \therefore \quad A_1 = \Sigma Fe \times \frac{\alpha_2}{\beta_{2,L}} \qquad \text{(Eq. B.10)}$$

$$\beta_{2,R} = \frac{A_2}{A_3} = \frac{\alpha_2 \Sigma Fe}{A_3} \quad ; \quad A_3 = \Sigma Fe \times \frac{\alpha_2}{\beta_{2,R}} \qquad \text{(Eq. B.11)}$$

$$\beta_{4,L} = \frac{A_4}{A_3} = \frac{\alpha_4 \Sigma Fe}{\left(\frac{\alpha_2 \Sigma Fe}{\beta_{2,R}}\right)} = \beta_{2,R} \times \frac{\alpha_4}{\alpha_2} \; ; \; \beta_{4,L} = \beta_{2,R} \times \frac{\alpha_4}{\alpha_2} \qquad \text{(Eq. B.12)}$$

$$\beta_{4,R} = \frac{A_4}{A_5} = \frac{\alpha_4 \Sigma Fe}{A_5} \quad ; \quad A_5 = \frac{\Sigma Fe \times \alpha_4}{\beta_{4,R}} \qquad \text{(Eq. B.13)}$$

$$\beta_{6,L} = \frac{A_6}{A_5} = \frac{\alpha_6 \Sigma Fe}{\left(\frac{\alpha_4 \Sigma Fe}{\beta_{4,R}}\right)} = \beta_{4,R} \times \frac{\alpha_6}{\alpha_4} = \beta_{4,R} \left(\frac{1 - \alpha_2}{\alpha_4}\right) \qquad \text{(Eq. B.14)}$$

$$\beta_{6,R} = \frac{A_6}{A_7} = \frac{(1 - \alpha_2)\Sigma Fe}{A_7} \quad ; \quad A_7 = \frac{(1 - \alpha_2)\Sigma Fe}{\beta_{6,R}} \qquad \text{(Eq. B.15)}$$

From equation B.3,

$$C_x = \frac{A_s \times A_\ell}{\sqrt{A_\ell^2 - A_s^2}}$$

$$C_1^2 = \frac{A_1^2 \, A_2^2}{A_1^2 - A_2^2}$$

GARD, INC.

Substituting for A_1 and A_2 from (B.10) and (B.6),

$$\frac{1}{C_1^2} = \frac{\left(\frac{\alpha_2 \Sigma Fe}{\beta_{2,L}}\right)^2 - (\alpha_2 Fe)^2}{\left(\frac{\alpha_2 \Sigma Fe}{\beta_{2,L}}\right)^2 (\alpha_2 Fe)^2} = \frac{1 - \beta_{2,L}^2}{(\alpha_2 Fe)^2} \qquad \text{(Eq. B.16)}$$

Similarly,

$$\frac{1}{C_2^2} = \frac{A_3^2 - A_2^2}{A_2^2\ A_3^2} = \frac{\left(\frac{\alpha_2 \Sigma Fe}{\beta_{2,R}}\right)^2 - (\alpha_2 \Sigma Fe)^2}{\left(\frac{\alpha_2 \Sigma Fe}{\beta_{2,R}}\right)^2 (\alpha_2 \Sigma Fe)^2} = \frac{1 - \beta_{2,R}^2}{(\alpha_2 Fe)^2} \qquad \text{(Eq. B.17)}$$

$$\frac{1}{C_3^2} = \frac{A_3^2 - A_4^2}{A_3^2\ A_4^2} = \frac{\left(\frac{\alpha_2 \Sigma Fe}{\beta_{2,R}}\right)^2 - (\alpha_4 \Sigma Fe)^2}{\left(\frac{\alpha_2 \Sigma Fe}{\beta_{2,R}}\right)^2 (\alpha_4 \Sigma Fe)^2} = \frac{1 - \left(\beta_{2,R}\ \frac{\alpha_4}{\alpha_2}\right)^2}{(\alpha_4 \Sigma Fe)^2} = \frac{1 - \beta_{4,L}^2}{(\alpha_4 \Sigma Fe)^2}$$

(Eq. B.18)

$$\frac{1}{C_4^2} = \frac{A_5^2 - A_4^2}{A_4^2\ A_5^2} = \frac{\left(\frac{\alpha_4 \Sigma Fe}{\beta_{4,R}}\right)^2 - (\alpha_4 \Sigma Fe)^2}{\left(\frac{\alpha_4 \Sigma Fe}{\beta_{4,R}}\right)^2 (\alpha_4 \Sigma Fe)^2} = \frac{1 - \beta_{4,R}^2}{(\alpha_4 \Sigma Fe)^2} \qquad \text{(Eq. B.19)}$$

$$\frac{1}{C_5^2} = \frac{A_5^2 - A_6^2}{A_5^2\ A_6^2} = \frac{\left(\frac{\alpha_4 \Sigma Fe}{\beta_{4,R}}\right)^2 - \left[(1 - \alpha_2)\Sigma Fe\right]^2}{\left(\frac{\alpha_4 \Sigma Fe}{\beta_{4,R}}\right)^2 \left[(1 - \alpha_2)\Sigma Fe\right]^2}$$

$$= \frac{1 - \left[\frac{(1 - \alpha_2)\Sigma Fe}{\alpha_4 \Sigma Fe} \times \beta_{4,R}\right]^2}{\left[(1 - \alpha_2)\Sigma Fe\right]^2} = \frac{1 - \beta_{6,L}^2}{(\alpha_6 \Sigma Fe)^2} \qquad \text{(Eq. B.20)}$$

and

$$\frac{1}{C_6^2} = \frac{A_7^2 - A_6^2}{A_6^2\, A_7^2} = \frac{\left[\frac{(1-\alpha_2)\Sigma Fe}{\beta_{6,R}}\right]^2 - \left[(1-\alpha_2)\Sigma Fe\right]^2}{\left[\frac{(1-\alpha_2)\Sigma Fe}{\beta_{6,R}}\right]^2 \left[(1-\alpha_2)\Sigma Fe\right]^2}$$

$$= \frac{1-\beta_{6,R}^2}{\left[(1-\alpha_2)\Sigma Fe\right]^2} = \frac{1-\beta_{6,R}^2}{(\alpha_6 \Sigma Fe)^2} \qquad \text{(Eq. B.21)}$$

$$\therefore \quad \sum_{i=1}^{2N} \frac{1}{C_i^2} = \frac{1-\beta_{2,L}^2}{(\alpha_2\Sigma Fe)^2} + \frac{1-\beta_{2,R}^2}{(\alpha_2\Sigma Fe)^2} + \frac{1-\beta_{2,L}^2}{(\alpha_4\Sigma Fe)^2} + \frac{1-\beta_{4,R}^2}{(\alpha_4\Sigma Fe)^2}$$

$$+ \frac{1-\beta_{6,L}^2}{(\alpha_6\Sigma Fe)^2} + \frac{1-\beta_{6,R}^2}{(\alpha_6\Sigma Fe)^2}$$

i.e., $$\sum_{i=1}^{2N} \frac{1}{C_i^2} = \frac{1}{(\Sigma Fe)^2} \left[\frac{2-(\beta_{2,L}^2+\beta_{2,R}^2)}{\alpha_2^2} + \frac{2-(\beta_{4,L}^2+\beta_{4,R}^2)}{\alpha_4^2} + \frac{2-(\beta_{6,L}^2+\beta_{6,R}^2)}{\alpha_{6,}^2} \right]$$

$i = 1,2,\ldots,2N$

$$= \frac{1}{(\Sigma Fe)^2} \sum_{j=2}^{2N} \frac{2-(\beta_{j,L}^2+\beta_{j,R}^2)}{\alpha_j^2}$$

$, \; j = 2,4,\ldots,2N$

Substituting this in Equation B.5,

$$L = \frac{\sqrt{2gh}}{\sqrt{\frac{1}{(\Sigma Fe)^2} \times \sum_{j=2}^{2N} \frac{2-(\beta_{j,L}^2 + \beta_{j,R}^2)}{\alpha_j^2}}}$$

$$\text{i.e. } L = \frac{1}{\sqrt{\sum_{j=2}^{2N} \frac{2-(\beta_{j,L}^2 + \beta_{j,R}^2)}{\alpha_j^2}}} \times \Sigma Fe, \sqrt{2gh}$$

$$\text{i.e. } L = S \times \Sigma Fe \times \sqrt{2gh} \qquad \text{(Eq. B.22)}$$

The equation derived above is based on a simple one dimensional flow model. In order to account for deviations of the real flow from this simple model and its dependence on such variables as shelter orientation, wind angle, shelter geometry, presence of earth berm, etc., the theoretical equation is modified by incorporating the empirical function $m(v, \theta, s_c)$.

$$L = m \times S \times \Sigma Fe \times \sqrt{2gh} \qquad \text{(Eq. B.23 or 4.2)}$$

GARD, INC., NILES, ILLINOIS

Adequacy of Wind Ventilation in Upgraded Shelters
GARD Final Report AI-11 (1713)
FEMA Contract No. DCPA01-78-C-0319, FEMA Work Unit 1214B
By Henninger, R.H., Krishnakumar, C.K., Tsal, R.J.
June 1980 (UNCLASSIFIED) pp 117

Experimental and analytical investigations were conducted for the purpose of evaluating the adequacy of natural ventilation in upgraded shelters. A unique low-speed wind tunnel which used photographic measurement techniques for flow tracing of neutrally bouyant bubbles through openings was utilized to conduct scaled model tests of three shelter models to determine the ventilation air throughput CFM as a function of wind speed, relative wind approach angle and opening pattern. The results indicate that sizeable ventilation rates are achieveable at low wind speeds and based upon data reported by ASHRAE would result in adequate ventilation rates to meet the 82^{o}F effective temperature and 90% adequacy criteria for but all the southeast portion of the U.S. Further research is required however, to determine the effects of internal flow resistances, air stratification, areas and locations of openings, etc., before the ventilation throughput characteristics of upgraded shelters are understood.

GARD, INC., NILES, ILLINOIS

Adequacy of Wind Ventilation in Upgraded Shelters
GARD Final Report AI-11 (1713)
FEMA Contract No. DCPA01-78-C-0319, FEMA Work Unit 1214B
By Henninger, R.H., Krishnakumar, C.K., Tsal, R.J.
June 1980 (UNCLASSIFIED) pp 117

Experimental and analytical investigations were conducted for the purpose of evaluating the adequacy of natural ventilation in upgraded shelters. A unique low-speed wind tunnel which used photographic measurement techniques for flow tracing of neutrally bouyant bubbles through openings was utilized to conduct scaled model tests of three shelter models to determine the ventilation air throughput CFM as a function of wind speed, relative wind approach angle and opening pattern. The results indicate that sizeable ventilation rates are achieveable at low wind speeds and based upon data reported by ASHRAE would result in adequate ventilation rates to meet the 82^{o}F effective temperature and 90% adequacy criteria for but all the southeast portion of the U.S. Further research is required however, to determine the effects of internal flow resistances, air stratification, areas and locations of openings, etc., before the ventilation throughput characteristics of upgraded shelters are understood.

GARD, INC., NILES, ILLINOIS

Adequacy of Wind Ventilation in Upgraded Shelters
GARD Final Report AI-11 (1713)
FEMA Contract No. DCPA01-78-C-0319, FEMA Work Unit 1214B
By Henninger, R.H., Krishnakumar, C.K., Tsal, R.J.
June 1980 (UNCLASSIFIED) pp 117

Experimental and analytical investigations were conducted for the purpose of evaluating the adequacy of natural ventilation in upgraded shelters. A unique low-speed wind tunnel which used photographic measurement techniques for flow tracing of neutrally bouyant bubbles through openings was utilized to conduct scaled model tests of three shelter models to determine the ventilation air throughput CFM as a function of wind speed, relative wind approach angle and opening pattern. The results indicate that sizeable ventilation rates are achieveable at low wind speeds and based upon data reported by ASHRAE would result in adequate ventilation rates to meet the 82^{o}F effective temperature and 90% adequacy criteria for but all the southeast portion of the U.S. Further research is required however, to determine the effects of internal flow resistances, air stratification, areas and locations of openings, etc., before the ventilation throughput characteristics of upgraded shelters are understood.

GARD, INC., NILES, ILLINOIS

Adequacy of Wind Ventilation in Upgraded Shelters
GARD Final Report AI-11 (1713)
FEMA Contract No. DCPA01-78-C-0319, FEMA Work Unit 1214B
By Henninger, R.H., Krishnakumar, C.K., Tsal, R.J.
June 1980 (UNCLASSIFIED) pp 117

Experimental and analytical investigations were conducted for the purpose of evaluating the adequacy of natural ventilation in upgraded shelters. A unique low-speed wind tunnel which used photographic measurement techniques for flow tracing of neutrally bouyant bubbles through openings was utilized to conduct scaled model tests of three shelter models to determine the ventilation air throughput CFM as a function of wind speed, relative wind approach angle and opening pattern. The results indicate that sizeable ventilation rates are achieveable at low wind speeds and based upon data reported by ASHRAE would result in adequate ventilation rates to meet the 82^{o}F effective temperature and 90% adequacy criteria for but all the southeast portion of the U.S. Further research is required however, to determine the effects of internal flow resistances, air stratification, areas and locations of openings, etc., before the ventilation throughput characteristics of upgraded shelters are understood.

DISTRIBUTION LIST

Addresses	Number of Copies
Federal Emergency Management Agency Mitigation and Research ATTN: Administrative Officer Washington, D.C. 20472	60
Assistant Secretary of the Army (R&D) ATTN: Assistant for Research Washington, D.C. 20301	1
Chief of Naval Research Washington, D.C. 20306	1
Defense Technical Information Center Cameron Station Alexandria, Virginia 22314	12
Oak Ridge National Laboratory ATTN: Librarian P.O. Box X Oak Ridge, Tennessee 37830	1
Mr. Phillip M. Smith Associate Director, Natural Resources & Commercial Services Office of Science and Technology Policy Executive Office Bldg, Washington, D.C. 20500	1
Los Alamos Scientific Laboratory ATTN: Document Library Los Alamos, N.M. 87544	1
The RAND Corporation ATTN: Document Library 1700 Main Street Santa Monica, CA 90401	1

Ballistic Research Laboratory 1
ATTN: Librarian
Aberdeen Proving Ground, MD 21005

Mr. James Beck 1
SRI International
333 Ravenswood Avenue
Menlo Park, CA 94025

Dr. William Chenault 1
Human Science Research Inc.
Westgate Industrial Park
7710 Old Springhouse Rd.
McLean, CA 22102

University of Florida 1
Civil Defense Technical Services Center
College of Engineering
Department of Engineering
Gainesville, Florida 32601

Dr. Leo Schmidt 1
Institute for Defense Analyses
400 Army-Navy Drive
Arlington, VA 22202

Mr. Bert Greenglass 1
Director, Office of Administration
Program Planning and Control
Department of Housing and Urban Development
Washington, D.C. 20410

Mr. Jack C. Greene 1
Greenwood
Route 4 - Box 85A
Bakerville, NC 28705

Richard K. Laurino 1
Center for Planning and Research, Inc.
2483 E. Bayshore Rd.
Palo Alto, CA 94303

Nuclear Engineering Department 1
Duncan Annex
Purdue University
West Lafayette, IN 47907

Sandia National Laboratory 1
Box 5800
Albuquerque, New Mexico 87185

Director, Army Materials and Mechanics Research Center 1
ATTN: Technical Library
Watertown, Massachusetts 02170

Commanding Officer 1
U.S. Army Combat Development Command
Institute of Nuclear Studies
Fort Bliss, Texas 79916

Director, U. S. Army Engineer Waterways Experiment Station 1
ATTN: Document Library
Post Office Box 631
Vicksburg, Mississippi 39180

Mr. Donald A. Bettge 1
Mitigation and Research
Federal Emergency Management Agency
1725 I Street
Washington, D.C. 20472

Dr. Lewis V. Spencer 1
Radiation Theory Section 4.3
National Bureau of Standards
Washington, D.C. 20234

Mr. Antole Longinow 1
IIT Research Institute
10 West 35th Street
Chicago, Illinois 60616

Mr. Chuck Wilton 1
Scientific Service Inc.
517 E. Bayshore
Redwood City, California 94063

Mr. Samuel Kramer, Chief 1
Office of Federal Building Technology
Center for Building Technology
National Bureau of Standards
Washington, D.C. 20234

Dr. Clarence R. Mehl 1
Division 1112
Sandia National Laboratory
Box 5800
Albuquerque, New Mexico 87185

Director, Defense Nuclear Agency 1
ATTN: Mr. Tom Kennedy
Washington, D.C. 20305

Director, Defense Nuclear Agency ATTN: Technical Library Washington, D.C. 20305	1
Emergency Technology Division Oak Ridge National Laboratory Post Office Box X Oak Ridge, Tennissee 37830 ATTN: Librarian	1
Technology & Management Consultants 1850 N. Whitley Avenue Suite 916 Hollywood, CA 90028	1
Defense Logistics Agency Civil Preparedness Office Richmond, VA 23297	1
H.L. Murphy Associates Box 1727 San Mateo, CA 94401	1
Department of Energy Headquarters Library, G-49 Washington, D.C. 20545	1
Disaster Research Center Ohio State University 404B West 17th Avenue Columbus, Ohio 43210	1
Dr. Charles Fritz National Academy of Sciences 2101 Constitution Avenue Washington, D.C. 20418	1
Dr. Leon Goure Advanced International Studies, Inc. Suite 1122 East-West Towers 4330 East-West Highway Washington, D.C. 20014	1
Agbabian Associates 250 North Nash Street El Segunda, CA 90245	1
Bell Telephone Laboratories Whippany Road Whippany, NJ 07981 ATTN: Mr. E. Wilt Mr. R. May Mr. J. Foss	1

Mr. Edward L. Hill 1
Research Triangle Institute
Post Office Box 12194
Research Triangle Park,
North Caroling 27709

Commanding Officer 1
U.S. Naval Civil Engineering Laboratory
ATTN: Document Library
Port Hueneme, California 93041

AFWL/Civil Engineering Division 1
ATTN: Technical Library
Kirtland Air Force Base
Albuquerque, New Mexico 87117

Director, U.S. Army Engineer Waterways 1
Experiment Station
Post Office Box 631
Vicksburg, Mississippi 39180

Dikewood Industries, Inc. 1
1009 Bradbury Drive, S.E.
University Research Park
Albuquerque, New Mexico 87106

Department of Energy 1
Assistant Director for Field Ops.
Dept. of Military Application
Washington, D.C. 20545
ATTN: Civil Eff. Br.
Mr. L.J. Deal
Dr. Rudolf J. Engelmann

GARD, Inc. 1
7449 North Natchez Avenue
Niles, Illinois 60648

Director 1
Ballistic Research Laboratory
ATTN: Document Library
Aberdeen Proving Ground, Maryland 21005

Civil Engineering Center/AF/PRECET 1
ATTN: Technical Library
Wright-Patterson Air Force Base
Dayton, Ohio 45433

Mr. Ken Kaplan 1
Management Science Association
P.O. Box 239
Los Altos, CA 94022

Science Applications, Inc. 1
1710 Goodridge Drive
P.O. Box 1303
McLean, VA 22102

DATE

ILMED

8